CALIFORNIA INSTITUTE OF TECHNOLOGY

EARTHQUAKE ENGINEERING RESEARCH LABORATORY

# GRAVITY EFFECTS ON THE EARTHQUAKE RESPONSE OF YIELDING STRUCTURES

by

Raúl Husid

A report on research conducted under a grant from the National Science Foundation

Pasadena, California

June 1967

# GRAVITY EFFECTS ON THE EARTHQUAKE RESPONSE OF YIELDING STRUCTURES

Thesis by

Raúl Husid

In Partial Fulfillment of the Requirements

For the Degree of

Doctor of Philosophy

California Institute of Technology

Pasadena, California

1967

(Submitted May 22, 1967)

# ACKNOWLEDGMENTS

The author desires to express his sincere gratitude to his research advisors Professors G. W. Housner, P. C. Jennings and D. E. Hudson for their guidance, encouragement and assistance in the preparation of this work. Professors T. K. Caughey and J. N. Franklin provided helpful suggestions and their cooperation is appreciated also.

The author, on leave of absence from the Faculty of Engineering, University of Chile, since September 1963, wishes to thank the Organization of American States, the University of Chile, the California Institute of Technology, and the National Science Foundation for giving him the necessary assistance to complete this thesis.

During his stay in this country the author is very grateful for the help given to him by Dr. H. F. Bohnenblust, Dean of Graduate Studies, Dr. H. Lurie, Associate Dean of Graduate Studies and Dr. F. C. Lindvall, Chairman of the Division of Engineering and Applied Science at Caltech.

The author is especially indebted to his family who, in one way or another, made it possible for this work to become a reality. The encouragement and help of T. Wise is indeed sincerely appreciated.

The author is further thankful to Professor Arturo Arias, his former advisor and close associate, and Dean E. d'Etigny, both from the Faculty of Engineering, University of Chile, for making possible his leave of absence, and for repeated extensions of this leave.

During his studies and research the author got assistance in experimental work from Mr. Rafael Ronderos and in miscellaneous subjects from Mrs. Alice Gear, Secretary of the C.E. Department. To both of them thanks and appreciation. To Mrs. Alrae Tingley goes my sincere appreciation for typing this thesis.

# ABSTRACT

The effect of gravity on the earthquake response of one degree of freedom yielding structures is studied by subjecting them to earthquake-like excitation. Interest is centered on the time required for yielding to progress to the point of collapse. The results show that the effect of gravity is to increase significantly the development of permanent set over that occurring when gravity is ignored. Because the gravity effect increases as the deflection grows, the permanent set increases rapidly just prior to failure.

A statistical study of the time to failure for elasto-plastic structures indicates that the average time to failure is inversely proportional to the square of the ratio of the earthquake strength to the lateral yield level of the structure, implying that an earthquake of short duration would have to possess significantly higher accelerations than a longer earthquake in order to cause failure of a given structure.

It was found that for the range of periods considered the average time to collapse for the yielding structures was independent of period. For the bilinear hysteretic structure the results show a large increase in the time of failure when the second slope increases from zero.

Calculations made with simultaneous vertical and horizontal excitation, and with recorded strong earthquake accelerograms, indicate that the thesis results, obtained from artificial earthquakes, should be applicable for strong earthquake excitation.

Comparison of the results with those of a one-dimensional random walk indicates that on the average a yielding structure will collapse after the input of a certain amount of energy.

TABLE OF CONTENTS

# LIST OF FIGURES

# I. INTRODUCTION

The response of structures to earthquake motions is usually studied under the assumption that the structure is able to resist strong shaking without failure. In general, this approach implies relatively small displacements, and therefore the influences of gravity upon the response can be disregarded. However, when interest is focused on the possibility of failure and collapse under the action of strong earthquake motions, gravity effects become important because the weight becomes the predominant force when the displacements approach the failure range.

When a structure is designed so that yielding will occur during an earthquake, this admits the possibility of permanent displacements and eventual collapse; therefore it is of primary interest to know how near to failure the yielding structure is. This makes it necessary to take gravity into account when studying the response.

It is the purpose of this thesis to study the influences of gravity on the possibility of collapse and failure of structures during earthquakes by examining the failure of simple yielding structures under earthquake excitation.

## Analytical Approach

For many problems in the dynamics of structures, a linear model does not give an accurate representation of the situation and it is necessary to consider nonlinear behavior if a realistic representation of the phenomenon is to be found. For some nonlinear problems

it is possible to show that the nonlinear terms do not change the character of the response much from the linear solution, and methods have been developed to find approximately equivalent linear systems[1,2] for which the solutions may be rapidly obtained.

Analytical methods also have been developed to obtain approximate solutions for nonlinear dynamic problems in which the nonlinearity is small in a certain sense. These methods include the method of slowly varying parameters[3]; the method of equivalent linearization[4]; and perturbation techniques[5,6].

For systems with a few degrees of freedom, the use of analogue computer techniques can often provide an adequate solution for linear and nonlinear vibration problems. Analogue computer techniques also can be adapted to relatively simple systems when analytical techniques will not provide a closed-form solution. However, if the significance of the nonlinearity is increased and at the same time the number of degrees of freedom is raised, the possibility of solving nonlinear vibration problems by analogies disappears for practical purposes. The only tool that is available for those problems that do not as yet allow analytical solutions, and for which the use of analogues is not practical, is the high-speed digital computer.

## Linear Analysis

Because of the nature of the excitation, analogue and digital computers have been used extensively in earthquake engineering research. However, digital computations of earthquake response of structures are not done routinely in practice because of the

computer time and expense, and also because the values of stiffnesses, type and amount of damping and various structural details usually are not well known.

For cases where detailed calculations are not practical, the concept of a response spectrum has found wide use in the analysis and design of earthquake-resistant structures[7,8,9,10,11,12]. The spectrum is the maximum response to an earthquake of a linear one-degree of freedom oscillator plotted as a function of the viscous damping and the period of the oscillator. Response spectra are most commonly made of the velocity, displacement and acceleration, but spectra of other quantities, such as shear and moment are useful for design and analysis of particular structures.

Particularly useful for design are the average velocity spectra and average acceleration spectra, which have been constructed using the 8 components of the four strongest earthquakes recorded in America up to 1959[12]. These average spectra are used to estimate the maximum velocities of a one-degree of freedom structure in response to earthquakes of a specified strength.

Because of the simple relations existing between spectra, the maximum displacements and accelerations in response to earthquake motion can be approximated from the velocity spectrum results[10,11] and other response values also can be approximated. Spectrum techniques can be applied also in the design of multistory structures when modal techniques are applicable[12,13,14,15,16].

Yielding Effects

R. W. Clough[17] reviewed the dynamic effects of earthquakes on structures and compared the theoretical results with those obtained when using the lateral force provisions recommended for the Uniform Building Code by the Structural Engineers Association of California (SEAOC). It was shown that it is necessary to use a yielding model for the structure if an agreement between the theory and the performance of buildings subjected to earthquakes is expected.

It is not practicable to design structures to resist all possible earthquakes elastically and the current philosophy of earthquake-resistant design is to insure that a well-designed structure remains elastic only for moderate earthquake shaking. For great earthquakes it is expected that the structural members will experience relatively large amounts of yielding, but that collapse will not occur. Thus, some yielding is expected in well-designed structures when subjected to strong earthquakes such as El Centro, 1940, Chile, 1960 or Alaska, 1964.

The elasto-plastic and bilinear hysteretic models are the most common yielding relations that have been used for the purpose of describing observed behavior of structures subjected to earthquake-type excitation. T. K. Caughey[3,4] and W. D. Iwan[18,19] have provided important contributions to the better understanding of the dynamics of these yielding models. Using the elasto-plastic and other yielding models, several authors[20,21,22,23,24] have investigated the yielding one degree of freedom structure subjected to earthquake

motions recorded by the United States Coast and Geodetic Survey and to artificial excitations.

The first computations of the response of a multidegree of freedom elastoplastic structure to earthquake excitations were done by G. V. Berg[25]. Figure 1.1 is taken from his results and shows that an appreciable permanent deformation developed after a relatively short period of time (10 seconds). It is noted that Berg's results were obtained neglecting gravity effects. Studies by other authors indicate similar results[26,27,28,29].

Gravity Effects

Gravity effects in the response to earthquakes are negligible for all practical purposes if the structure remains linear. However, for structures which permit excursions into the plastic range when subjected to typical earthquakes, gravity effects can be of primary importance[30]. If, during a strong earthquake, a structure begins to yield and drift as shown in Figure 1.1, it is apparent that if the drift continues to grow, the structure will eventually collapse due to the effects of gravity. Therefore, although relatively insignificant for small deflections, gravity must eventually become the dominant force if collapse occurs.

Probably the first examination of the effects of gravity on earthquake response was that by Arthur C. Ruge[31] who discussed the gravity effect in the determination of earthquake stresses in elastic structures with the aid of models, and made estimations of the changes in period and deflection of a simple vertical cantilever

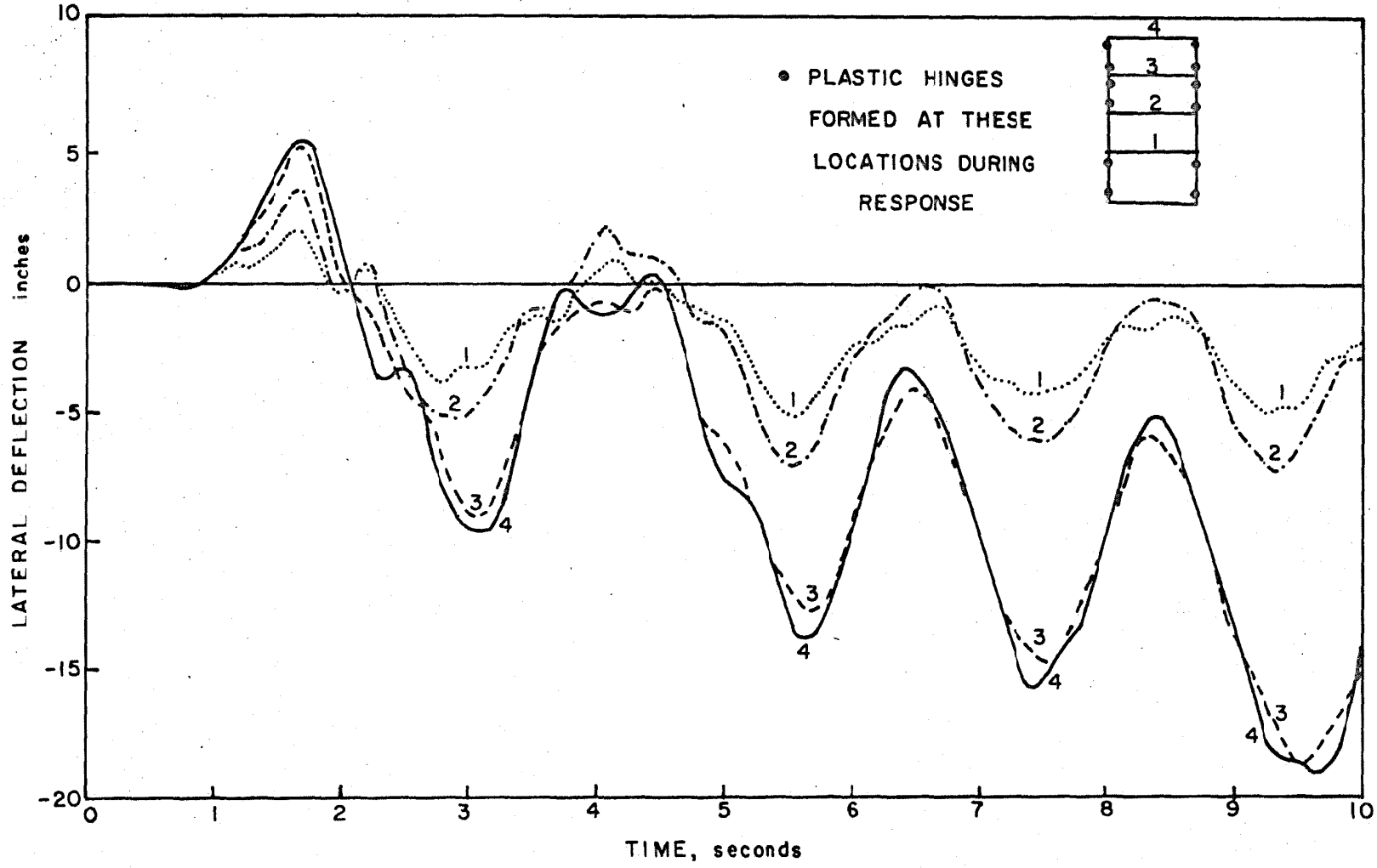


Figure 1.1. Response of Four-Story Elastic-Plastic Frame, El Centro 1940 (N.S.) (Ref. 25).

loaded at the end with a weight.

L. S. Jacobsen[31] also considered gravity effects when he analyzed the behavior of a single mass nonlinear structure by the phase-plane-delta method. A phase-plane solution for large deformations of the structure subjected to a horizontal symmetrical ground displacement pulse was presented and an appreciable permanent set was obtained. These two references are the only studies where gravity was considered explicitly in the computation of the yielding response of structures.

Examples of Gravity Effects

In a broad sense every structure that has collapsed during an earthquake is an example of the effect of gravity, but to understand how gravity affects earthquake response, it is informative to examine structures where failure, though near, has not yet occurred.

During the great Alaskan earthquake of 1964, a simple garage structure was severely damaged as can be seen in the foreground in Figure 1.2. In essence, the structure consisted of a heavy wooden roof supported by the steel pipe columns shown in the figure. After the earthquake the heads of the columns were displaced horizontally by 10-5/8 inches and the angle they made with the vertical was about $6.3^{\circ}$ (0.11 radians). It is clear that the garage suffered large deformations in the yielding range and it appears that gravity was in this case on the border of producing collapse.

Recently[33], in the vicinity of Matsushiro, Japan, it was reported that several houses inclined about four degrees in the

Figure 1.2. Garage Structure after the 1964 Alaskan Earthquake.

direction of the street faced by each house. The final inclination resulted from consecutive increments produced by several earthquakes. It appears that in this case, the effects of three successive earthquakes were similar to that expected from one long earthquake. Presumably, further shaking would eventually cause collapse of the houses.

Organization of the Thesis

In section II of the thesis a simple model is selected for studying the influence of gravity on the response and failure of yielding structures. A selection of the important parameters is made and artificial earthquakes[33] are selected as appropriate excitations for the major part of this study.

Section III of this study presents numerical calculations of response and failure for selected values of important parameters for the one-story structure when artificial earthquakes are used as excitations. This section is closed with a discussion of the general trends in the digital response.

In section IV, sample calculations for real earthquakes are presented and a comparison is made with the results obtained in the previous section. An investigation is made of the influence that the change from an elastoplastic to a positive bilinear hysteretic yielding model has on the time for collapse, using the artificial earthquakes as excitations. Exploratory computations were made to see if the introduction of the vertical component of earthquake motion has an appreciable effect upon the time for failure for an elastoplastic

structure.

Section V introduces a problem that has the same general characteristics of the one under study and that is solvable, i.e., a random walk with bias. An analysis of this random walk problem is carried out and an exact expression for the continuous probability distribution is obtained. The mean and variance of the position as functions of time are presented. In the same section upper bounds for the displacement of the structure subjected to earthquake-like excitation are obtained and a discussion of the suitability of such bounds are included.

The thesis is concluded with a general discussion of the results obtained.

# II. RESPONSE OF SIMPLE YIELDING STRUCTURES

## A. Formulation and Analysis

The analysis of the behavior of linear structures[31] when subjected to earthquake excitation in the past has been focused on the amplitudes of vibration rather than on the failure of the system. Since a linear structure can fail only by buckling and since most structures are not near the buckling range, it is natural to omit consideration of gravity in this type of analysis.

As a matter of analytical convenience it has been customary to use simplified, linearly damped models such as the one shown in Figure 2.1 to represent structures and these simple structures have been analyzed for their responses to different excitations[35,36,7.8]. For the system shown in Figure 2.1 the equation of motion is given by:

$$m\ddot{x} + c\dot{x} + Kx = G(t) \qquad (2.1)$$

in which $m$ is the mass of the structure, $K$ is the stiffness (constant) and $c$ is the constant for the dashpot considered in the model.

The model given in Figure 2.1 is not able to reconcile theory with the observed behavior of structures subjected to strong earthquakes, and about a decade ago a realistic modification of the model was initiated. A nonlinear yielding restoring force-deflection relation was introduced to represent more nearly a real structure. The most commonly used models were the elastoplastic and the bilinear hysteretic relations. Figure 2.2 shows these nonlinear restoring forces; and the corresponding equation of motion is:

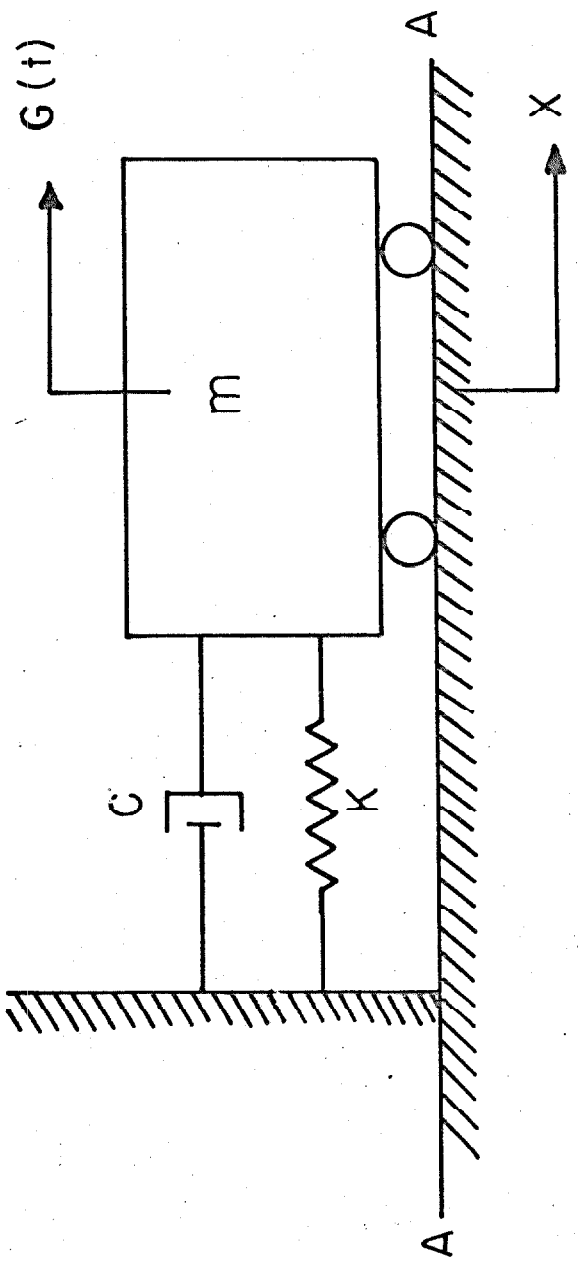


Figure 2.1. Linear Model

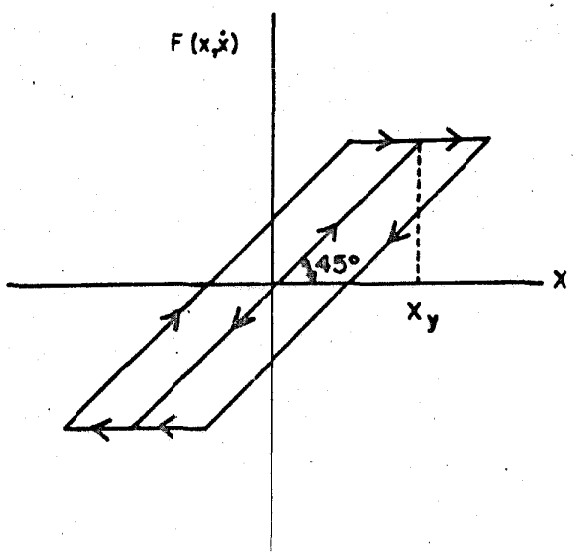


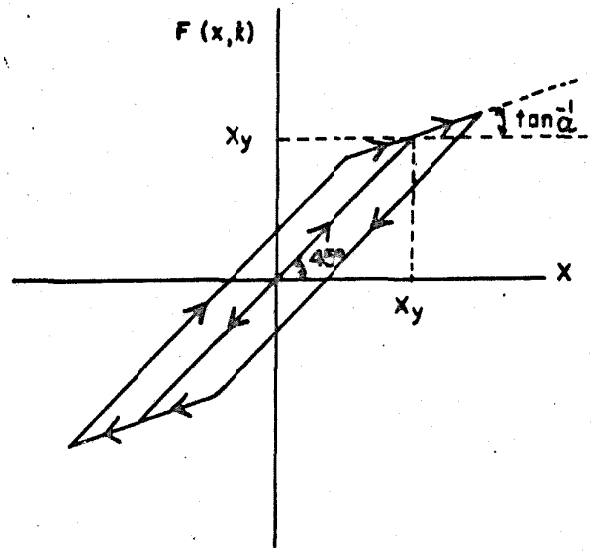


Figure 2.2. Nonlinear Restoring Forces.

$$m\ddot{x} + c\dot{x} + KF(x,\dot{x}) = G(t) \qquad (2.2)$$

In these nonlinear relations $x_y$ represents the displacement at which yielding begins.

Ryo Tanabashi[20] was one of the first to study the nonlinear vibrations of structures subjected to destructive earthquakes. Using the elastoplastic relation for the restoring force characteristic, he concluded that slight modifications in the restoring force curve had little influence on the dynamic behavior of the structure. Subsequently, different models of yielding, other than those shown in Figure 2.2, have been used by different authors[37,38].

In a real structure, the development of yielding depends in a complicated manner on the axial load and the horizontal component of the shear force and bending moment, as well as the geometry of the cross section. It is possible to study these effects by approximating the interaction between these forces to determine the point at which yielding begins[39], but in this thesis this is not done. Rather, the yielding characteristics are simplified by considering the yield point to be a function of the bending deformation only, and effort is concentrated upon the basic mechanism of earthquake response and collapse of the yielding structure.

When a strong earthquake causes large deformations in a yielding structure, it is possible that the structure will not return to the original vertical position when the motion ceases, thus permanent deformations can appear. These residual displacements are

attributed to the nonlinear character of the structure and are called permanent set.

Knowledge of the influence of gravity upon the development of permanent set is important, since the yielding structure will collapse if the permanent set reaches values near the displacement that produces failure statically. Structures represented by models like that shown in Figure 2.1 ignore gravity, as is seen in Equations 2.1 and 2.2.

A model of a simple structure that considers the effect of gravity is shown in Figure 2.3(a). The girder is considered to be infinitely rigid with a total mass 2m. The columns are also assumed to be infinitely rigid but without mass. The connections between columns and the girder and between columns and the foundation are represented by nonlinear springs that operate in torsion to generate corresponding nonlinear restoring moments. Together with the four equal springs are included four equal linear viscous dashpots. Figure 2.3(b) shows the model in a deflected position.

When gravity is neglected, i.e., when the structure can be represented by Figure 2.1, then the mass 2m moves only along a horizontal line. The inclusion of gravity replaces the horizontal trajectory by a curve (it is understood that there is only planar motion) and for the special case of the simple model of Figure 2.3, this curve is a circular arc, as is seen in Figure 2.3(b).

In essence, when gravity is not neglected, the change of height of the mass of the structure modifies the equation of motion for the

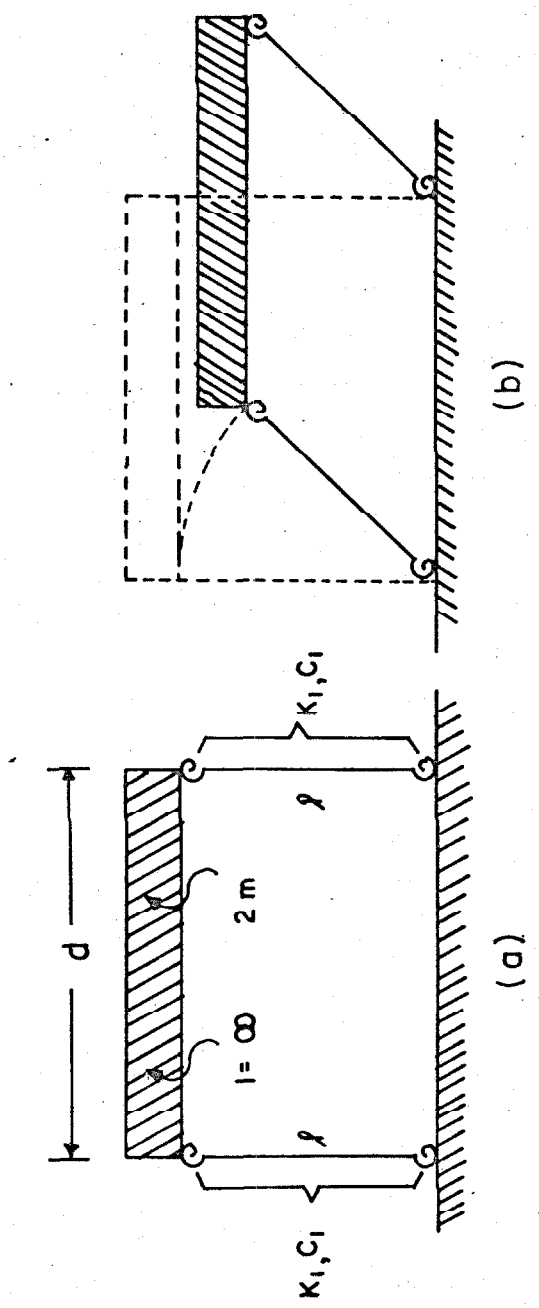


Figure 2.3. Simple Structure Model that Considers Gravity.

system under consideration. The reason for selecting a circular path is to eliminate the complicated relation between vertical and horizontal motions that exists if the elastic curves of the bending columns are considered. Fortunately, for most practical cases the important features of the deflection path can be approximated very closely by a circular arc. The equation of motion for free oscillations of the undamped structure of Figure 2.3 can be written with the help of the free body diagrams shown in Figure 2.4.

Figure 2.5 shows the convenience of the model selected through the direct relationship between $\omega$, the vertical displacement of the mass, and $\phi$, the angle of rotation of the columns. From the geometry of Figure 2.5 it follows that:

$$\omega = \ell(1 - \cos \phi) \tag{2.3}$$

in which $\ell$ is the height of the structure, $\omega$ is the vertical displacement of the mass, and $\phi$ is the angle that the columns make with the vertical.

The system shown in Figure 2.4 is in equilibrium when the D'Alambert forces are included, which leads to the following equations:

$$2M - H_1 \ell \cos \phi - V_1 \ell \sin \phi = 0 \tag{2.4}$$

$$2M - H_2 \ell \cos \phi - V_2 \ell \sin \phi = 0 \tag{2.5}$$

$$2m\ddot{z} + H_1 + H_2 = 0 \tag{2.6}$$

$$2m\ddot{\omega} - 2mg + V_1 + V_2 = 0 \tag{2.7}$$

$$2M + (V_1 - V_2)d/2 = 0 \tag{2.8}$$

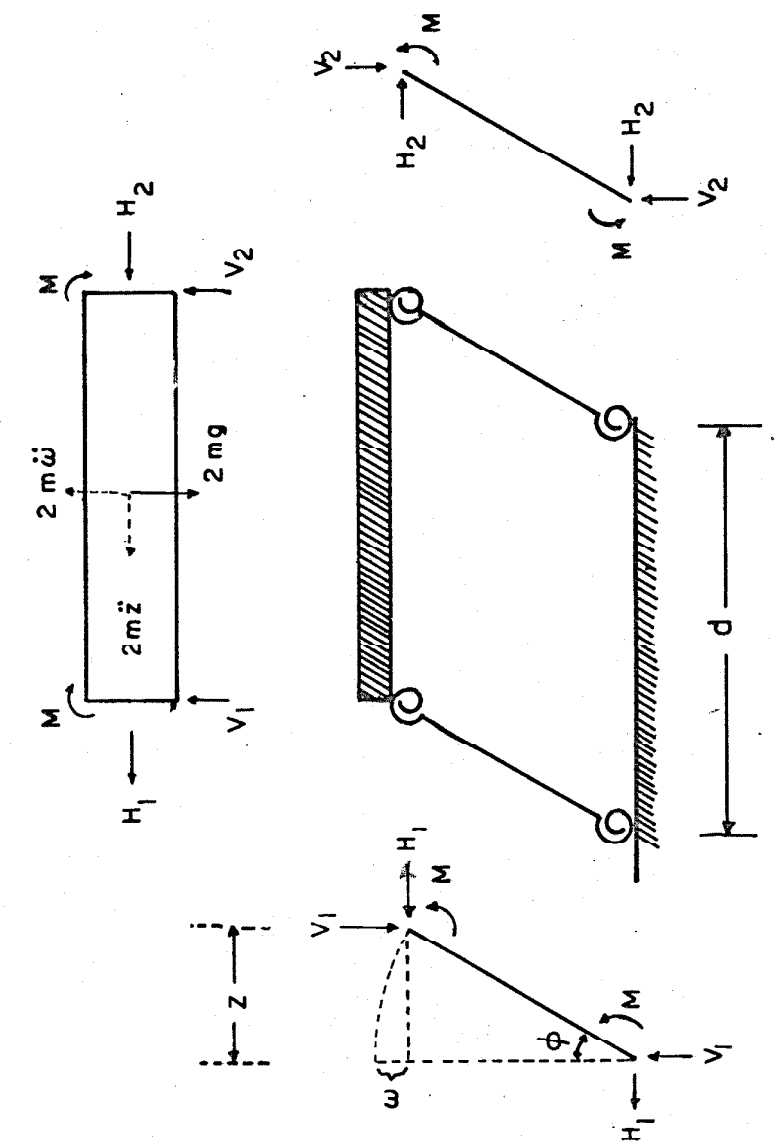


Figure 2.4. Free Body Diagrams for Model Selected.

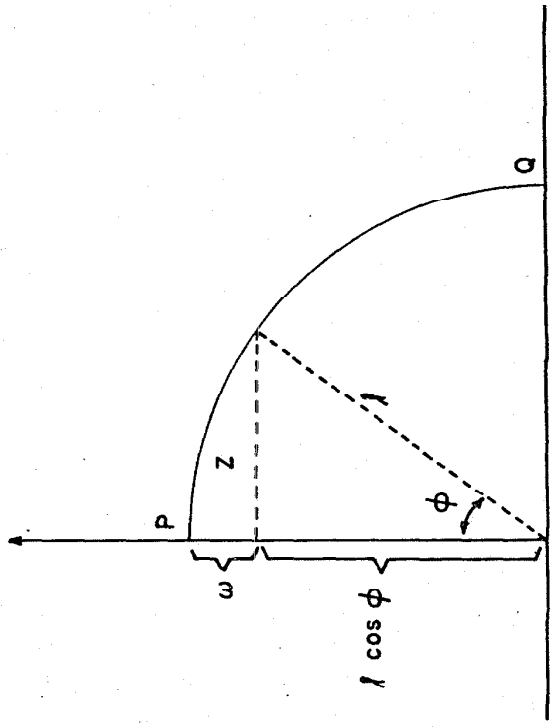


Figure 2.5. Circular Trajectories of the Columns of the Frame.

in which d is the length of the girder. It is interesting to note that Equation 2.8 depends on the length of the girder and is needed only if the individual forces $V_1$, $V_2$, $H_1$ and $H_2$ are required. For the purposes of this study this information is not necessary.

The geometry of the structure gives,

$$z = \ell \sin \phi \tag{2.9}$$

New force parameters H and V are defined as follows:

$$\begin{aligned} H_1 + H_2 &= 2H \\ V_1 + V_2 &= 2V \end{aligned} \tag{2.10}$$

The introduction of H and V and the use of Equations 2.4 through 2.7 will give an equivalent system of equations in which interest is focused on the evaluation of the angle as a function of time. Simplifying the equivalent system, and recalling that $M = K_1 F(\phi, \dot{\phi}) = \frac{K}{2} F(\phi, \dot{\phi})$ produces:

$$\ddot{\phi} + \frac{K}{m\ell^2} F(\phi, \dot{\phi}) - \frac{g}{\ell} \sin \phi = 0 \tag{2.11}$$

in which $F(\phi, \dot{\phi})$ is a nonlinear function of the type described in Figure 2.2. If the structure has linear damping and is subjected to a base excitation $\ddot{u}(t)$, the equation of motion becomes

$$\ddot{\phi} + \frac{2c_1}{m\ell^2} + \frac{K}{m\ell^2} F(\phi, \dot{\phi}) - \frac{g}{\ell} \sin \phi + \frac{\ddot{u}(t)}{\ell} \cos \phi = 0 \tag{2.12}$$

The initial conditions for earthquake excitation are assumed to be

$$\phi(0) = 0$$
$$\dot{\phi}(0) = 0 \qquad (2.13)$$

In Equations 2.11 and 2.12, the influence of gravity is represented by the term $(-\frac{g}{\ell}\sin\phi)$.

Assuming that the deformations are small and that the structure remains elastic, equation 2.11 for free oscillations can be simplified because under these conditions:

$$\sin\phi \approx \phi$$
$$F(\phi, \dot{\phi}) \approx \phi \qquad (2.14)$$

From 2.11 and 2.14 it is found that:

$$\ddot{\phi} + \left(\frac{K}{m\ell^2} - \frac{g}{\ell}\right)\phi = 0 \qquad (2.15)$$

The period change produced by gravity is given by

$$T = \frac{T_o}{\sqrt{1 - \frac{gT_o^2}{4\pi^2\ell}}} \qquad (2.16)$$

in which $T_o$ is the period when gravity is not considered.

From the last relation it is seen that the effect of gravity in the linear range is to increase the natural period of vibrations. For most structures $g/\ell$ is much less than $K/m\ell^2$ because equality of these two terms implies that the structure will fail by

elastic buckling.

The effect of gravity in the fundamental period of vibration of multistory structures is also negligible in general. That this is the case can be seen from examination of the linear structure shown in Figure 2.6. It is assumed that the mass and story height are constant throughout the structure and that the deflection of the first mode can be approximated by a straight line. To determine the effects of gravity on the fundamental period it is necessary to find the work done by gravity during the vibration. The gravity effect can then be approximated by the application of Rayleigh's principle[40]

$$(K.E.)_{max} = U_{max} - W_{max} \tag{2.17}$$

in which K.E. is the kinetic energy of vibration, U is the strain energy stored in bending of the columns, and W is the work done by gravity.

For this calculation the interfloor displacement can be approximated sufficiently well by

$$v = \frac{A}{2}\left(1 - \cos\frac{\pi x}{\ell}\right) \tag{2.18}$$

in which $\ell$ is the story height, A is the amplitude of interfloor deflection and x varies from 0 to $\ell$.

Defining $\Delta\ell$ as the change in interfloor height during the vibration it is easily shown for the deflected shape given by Equation 2.8 that

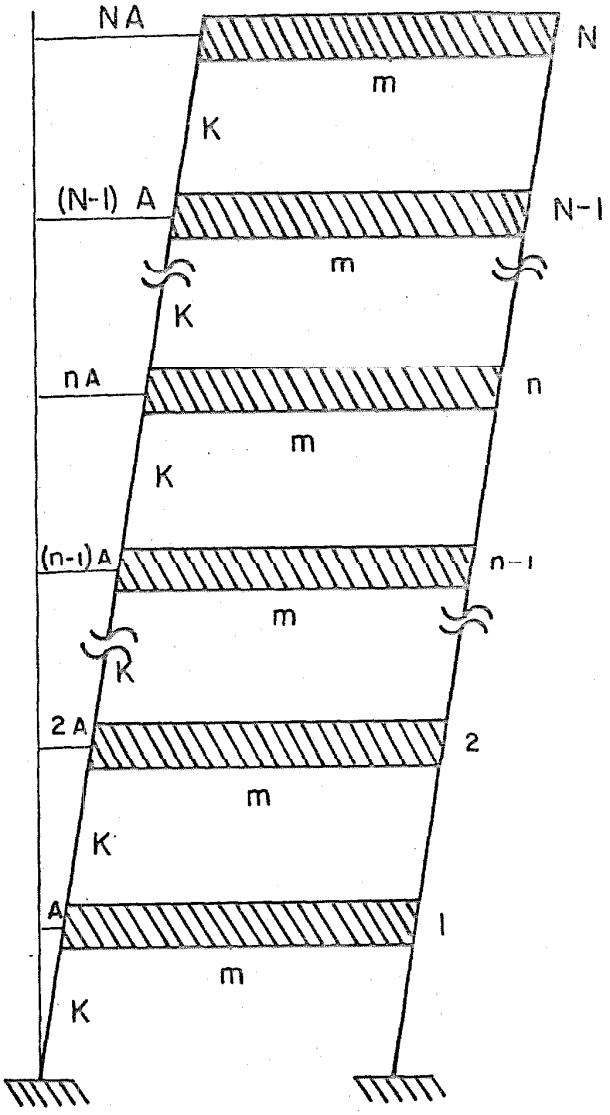


Figure 2.6. Building Model.

$$\Delta \ell = \frac{\pi^2 A^2}{16 \ell} \tag{2.19}$$

Because the mass and interfloor displacement are constant throughout the structure the work done by gravity is

$$W = mg\Delta\ell[\, N + N\text{-}1 + N\text{-}2 + \ldots + \,] \tag{2.20}$$

This series can be summed and using Equation 2.19 it is found that:

$$W_{max} = \frac{mg\pi^2 A^2}{32 \ell} \; N(N+1) \tag{2.21}$$

The interfloor displacement is A, so the velocity of the $n^{th}$ floor is

$$\dot{v}_n = n\left(\frac{2\pi}{T}\right) A \sin\left(\frac{2\pi}{T}\right) t \tag{2.22}$$

in which T is the fundamental period of the structure.

The maximum kinetic energy of the structure then becomes

$$(K.E.)_{max} = \frac{m}{2} \sum_{n=1}^{N} n^2 A^2 \left(\frac{2\pi}{T}\right)^2 \tag{2.23}$$

Equation 2.23 can be simplified to yield

$$(K.E)_{max} = \frac{1}{12}\, mA^2 \left(\frac{2\pi}{T}\right)^2 N(N+1)(2N+1) \tag{2.24}$$

Substituting Equation 2.24 and 2.21 in Equation 2.17 yields:

$$\frac{1}{T^2} = \frac{U_{max}}{\frac{1}{3}\pi^2 mA^2 N(N+1)(2N+1)} - \frac{3g}{32\ell(2N+1)} \tag{2.25}$$

But the first quotient in the right side of Equation 2.25 is $1/T_o^2$, in which $T_o$ is the fundamental period of the structure if gravity is not considered. Using $T_o$, and solving for $T$ produces

$$T = \frac{T_o}{\sqrt{1 - \frac{3gT_o^2}{32\ell(2N+1)}}} \qquad (2.26)$$

Comparing Equation 2.26 for $N = 1$ with Equation 2.16 shows a difference in constants: 32 compared with $4\pi^2$. This difference arises because a circular path was assumed in the derivation of Equation 2.16 whereas a trigonometric path was used to obtain Equation 2.26.

For moderately tall buildings, the magnitude of the gravity effect implied by Equation 2.26 can be estimated by letting $\ell = 10$ ft, $g = 32$ ft/sec$^2$, and $T_o = 0.08N$[41]. For these values, Equation 2.26 becomes

$$T = \frac{T_o}{\sqrt{1 - \frac{N^2}{520(2N+1)}}} \qquad (2.27)$$

From Equation 2.27 it is seen that for most multistory structures the gravity effects are negligible, for example, if $N = 20$ the increase in period is about one per cent.

For extremely tall structures, Housner and Brady[42] found that a good estimation of the fundamental period of American buildings was obtained when a linear relationship between period and $\sqrt{N}$

is assumed. An approximate period relation of this type for extremely tall structures would be $T_o = \sqrt{N/7.8}$ for $N \geq 20$, with this, Equation 2.26 can be used to estimate the effect of gravity in the period of oscillation for very tall buildings. Taking $\ell = 10$ ft, $g = 32.2$ ft/sec$^2$ and $T_o = \sqrt{N/7.8}$ produces

$$T = \frac{T_o}{\sqrt{1 - \frac{1}{52(1 + \frac{1}{2N})}}} \tag{2.28}$$

It is clear that for $N > 20$, the influence of gravity on $T_o$ is of the same order of magnitude as for $N = 20$, i.e., about one per cent.

B. Examination of the important parameters

Equation 2.12 describes the response of a one story elasto-plastic structure subjected to earthquake excitation, including the effect of gravity. Before doing any numerical work with Equation 2.12, it is advantageous to transform the equation to dimensionless form. The equation of motion for the system under consideration was shown to be:

$$\ddot{\phi} + \frac{2c_1\dot{\phi}}{m\ell^2} + \frac{K}{m\ell^2} F(\phi, \dot{\phi}) - \frac{g}{\ell} \sin\phi + \frac{\ddot{u}}{\ell} \cos\phi = 0 \tag{2.12}$$

The concept of critical damping can be introduced into this equation in the same way as is done for a linear structure. To obtain an expression for the critical damping relation 2.12 is linearized by

requiring $\phi$ to be sufficiently small. From the resulting equation it is found that

$$\frac{c_{1c}}{m\ell^2} = \sqrt{\frac{K}{m\ell^2} - \frac{g}{\ell}} \tag{2.29}$$

The natural frequency of small, linear vibrations is given by

$$\omega_o = \sqrt{\frac{K}{m\ell^2} - \frac{g}{\ell}} \tag{2.30}$$

From 2.12 and Equations 2.29 and 2.30 follows:

$$\ddot{\phi} + 2\left(\frac{c_1}{c_{1c}}\right)\omega_o\dot{\phi} - \frac{g}{\ell}\sin\phi + \frac{K}{m\ell^2}F(\phi,\dot{\phi}) + \frac{\ddot{u}}{\ell}\cos\phi = 0 \tag{2.31}$$

Defining $a_y$ as the acceleration that will statically produce yielding in the four equal springs of the structure under consideration, and writing the equilibrium equation for lateral yielding gives

$$2K_1\phi_y = mg\ell\phi_y + m\ell a_y \tag{2.32}$$

where:

$\phi_y$ is the yielding level for the springs and

$2K_1 = K$

Algebraic transformations of 2.32 gives:

$$\phi_y = \lambda\frac{a_y}{g} \tag{2.33}$$

where

$$\lambda = \frac{g}{\ell \omega_o^2} = \frac{1}{\frac{K}{mg\ell} - 1} \tag{2.34}$$

Replacing $\ddot{u} = \overline{\ddot{u}}\,\sigma(\tau)$ in 2.31, where $\overline{\ddot{u}}$ is the r.m.s. value for the input, and introducing also the notation:

$$\frac{c_1}{c_{1c}} = n$$

$$\omega_o t = \tau \tag{2.35}$$

the following equation is obtained

$$\frac{d^2\phi}{d\tau^2} + 2n\frac{d\phi}{d\tau} + F(\phi,\dot{\phi}) + \frac{g}{\ell\omega_o^2}\left\{F(\phi,\dot{\phi}) - \sin\phi + \frac{\overline{\ddot{u}}}{g}\sigma(\tau)\cos\phi\right\} = 0 \tag{2.36}$$

where the gravity effect is represented by the term $(-\frac{g}{\ell\omega_o^2}\sin\phi)$. Note that $F(\phi,\dot{\phi})$ is not defined unless the yielding level $\phi_y$ is given.

Equation 2.36 is a convenient dimensionless form of the equation of motion of the simple yielding structure studied in the thesis. For convenience, a resumé of the dimensionless parameters used in the equation is given below

| | |
|---|---|
| $\tau = \omega_o t$ , time | $n = \frac{c_1}{c_{1c}}$ , damping |
| $\frac{\overline{\ddot{u}}}{g}$ , acceleration | $\lambda = \frac{g}{\ell\omega_o^2}$ , length |
| $\frac{a_y}{g}$ , yield level | $\phi$ , displacement |

It is informative to give typical values of the selected dimensionless parameters for real structures. Table 1 gives the approximate values for $\overline{\ddot{u}}$ for the four strongest earthquakes recorded in America until 1959.[23]

TABLE 1
R. M. S. Acceleration. Real Earthquakes

| Earthquake | Date | $\overline{\ddot{u}}$ [ft/sec$^2$] |
|---|---|---|
| El Centro | 1940 | 2.01 |
| El Centro | 1934 | 1.35 |
| Olympia | 1949 | 1.76 |
| Taft | 1952 | 1.44 |

Using 2.33 and selected values of $\lambda$ and $a_y/g$, corresponding angles of yielding, in radians, are obtained and are given in Table 2. Because $\lambda$ is a measure of how close the structure is to elastic buckling, representative values of $\lambda$ are less than unity.

TABLE 2

Angles of yielding

$\phi_y$

| $\lambda = g/\ell\omega_o^2$ | $\frac{a_y}{g} = 0.03$ | $\frac{a_y}{g} = 0.05$ | $\frac{a_y}{g} = 0.10$ | $\frac{a_y}{g} = 0.20$ | $\frac{a_y}{g} = 0.30$ |
|---|---|---|---|---|---|
| 0.021 | 0.00063 | 0.00105 | 0.00210 | 0.00420 | 0.00630 |
| 0.100 | 0.00300 | 0.00500 | 0.01000 | 0.02000 | 0.03000 |
| 0.484 | 0.01450 | 0.02420 | 0.04840 | 0.09680 | 0.14500 |

It is noted that for typical values of $a_y/g$ and $\lambda$, $\phi_y$ is small, generally less than 0.10 rad.

Angle of static failure

It is possible to determine the angle for which static collapse of an elasto-plastic structure will occur. The maximum angle for which the structure is statically stable is defined by:

$$K\phi_y = mg\ell \sin |\phi_s| \tag{2.37}$$

in which $\phi_s$ represents the angle of static failure. After some algebra and using relation 2.33, it follows that

$$\sin |\phi_s| = \phi_y + \frac{a_y}{g} \tag{2.38}$$

For typical values of the parameters, the right-hand member of 2.38 is smaller than unity and if $\phi_s$ is such that $\sin \phi_s \approx \phi_s$, which is generally true for real structures, then

$$|\phi_s| \approx \phi_y + \frac{a_y}{g} \tag{2.39}$$

or

$$\frac{\phi_s}{\phi_y} \approx 1 + \frac{1}{\lambda} \tag{2.40}$$

Relation 2.39 was used to estimate the angles of static failure given in Table 3 for the same values of $\lambda$ and $a_y/g$ that were considered for Table 2.

The angle $\phi_s$ divides the static range of $\phi$ into stable and unstable portions and it is expected that it will indicate also the approximate ranges of stable and unstable motions in the dynamic case.

TABLE 3

Angles of Collapse

$\phi_s$

| $\lambda$ | $\frac{a_y}{g} = 0.03$ | $\frac{a_y}{g} = 0.05$ | $\frac{a_y}{g} = 0.10$ | $\frac{a_y}{g} = 0.20$ | $\frac{a_y}{g} = 0.30$ |
|---|---|---|---|---|---|
| 0.021 | 0.03063 | 0.05105 | 0.10210 | 0.20420 | 0.30630 |
| 0.100 | 0.03300 | 0.05500 | 0.11000 | 0.22000 | 0.33000 |
| 0.484 | 0.04450 | 0.07420 | 0.14840 | 0.29680 | 0.44500 |

For typical values of $a_y/g$, Table 3 shows that the angle for which collapse will occur statically is rather small.

Selection of the excitation

Unfortunately, very few strong earthquakes have been recorded in the past. Among recent destructive earthquakes throughout the world, such as Mexico (1957), Morocco (1960), Chile (1960), Iran (1962), Skopje (1963), Alaska (1964), and Perú (1966), due to the small number of instruments available, a recording of the ground motion was obtained only for Perú (1966).

When real earthquakes are used to study the statistics of response and failure of structures it is difficult to interpret the results obtained. Recorded earthquakes have durations, maximum accelerations, intensities etc. that vary widely and it is inappropriate to consider recorded earthquakes as samples from a single ensemble. When artificially generated earthquakes are considered as excitation for structures, it becomes possible to make more meaningful statistical studies of response and collapse, because artificial earthquakes can be constructed with specified duration and intensities.

A simple statistical model for earthquake accelerograms has been derived[23] and artificial earthquakes have been generated on a digital computer. The generation process began with an approximate white noise, i.e., a process with a power spectral density constant over the range of interest. The white noise was formed on the digital computer from a sequence of uncorrelated Gaussian numbers with a mean of zero and a variance of unity. The white noise was then passed through a linear filter, producing artificial earthquakes which are sections of a stationary Gaussian random process. The properties of the linear filter were determined from the average undamped velocity spectrum described in Reference 12.

Eight 30 second accelerograms are available[34], and these artificial earthquakes, plus selected real earthquake motions, are the excitations selected for use in this study.

# III. DIGITAL RESPONSE STUDY

## A. Selection of Parameters

In a digital response calculation such as this, where many parameters may influence the response, it is necessary to try to select a limited number of cases that will provide adequate information about the phenomenon, and yet at the same time cover a range of structures that occur in practice. The selection of the important parameters is guided by the equation of motion of the model selected for this study:

$$\frac{d^2\phi}{d\tau^2} + 2n\frac{d\phi}{d\tau} + F(\phi,\dot{\phi}) + \frac{g}{\ell\omega_o^2}\left\{F(\phi,\dot{\phi}) - \sin\phi + \frac{\ddot{\bar{u}}}{g}\sigma(\tau)\cos\phi\right\} = 0 \quad (2.36)$$

It is seen from this equation that the parameters of the problem include the fraction of critical damping, the frequency or period of the structure, the yield level $\phi_y$ (implicit in $F(\phi,\dot{\phi})$), the height $\ell$ of the structure and the intensity and form of the earthquake excitation. Each of these parameters will be discussed in turn.

### Excitation

When a statistical study is undertaken using earthquake-like excitation, it is convenient to utilize many samples from an ensemble of earthquakes. Since real earthquakes do not belong precisely to an ensemble, but have characteristics which suggest their classification in different ensembles, i.e., different duration, intensity, magnitude, distance between the site of recording and the epicenter, quality of the soil at the site where the accelerogram was obtained, depth of

the hypocenter, etc., and considering that the number of accelerograms recorded is quite small[9], it was thought preferable to do the basic part of this investigation using an ensemble of well defined pseudo-earthquakes[34].

The first problem that appears is how to characterize the excitation with the minimum number of parameters, when the interest is focused on the time elapsed between the beginning of the earthquake and structural collapse, if it occurs. For the artificial earthquakes, which are samples of a simple random process, it can be shown that the r.m.s. acceleration is a suitable parameter for measuring their severity[23]. In addition it is clear that the duration of the earthquake has an important role in the collapse of elasto-plastic structures. In particular, too short a duration does not make clear the relative safety of the structure as a function of time. Ideally, each calculation should be carried to failure, if failure can occur, so one can make an estimate of the nearness to collapse at the end of shorter excitations. The strong phases of recorded U.S. earthquakes have not exceeded 25 sec and even in a great earthquake it is thought that the duration of the strong portions of the shaking would not exceed one minute. Therefore, 60 sec was chosen as the basic duration for the artificial earthquake excitation. Eight 30 seconds-duration accelerograms of artificial earthquakes are available for the principal part of the digital response calculations. They are reproduced on computer cards using a step size, $\Delta t = 0.025$ sec. Two of the articifial earthquakes are shown in Figures 3.1 and 3.2. As mentioned in Chapter II, these are

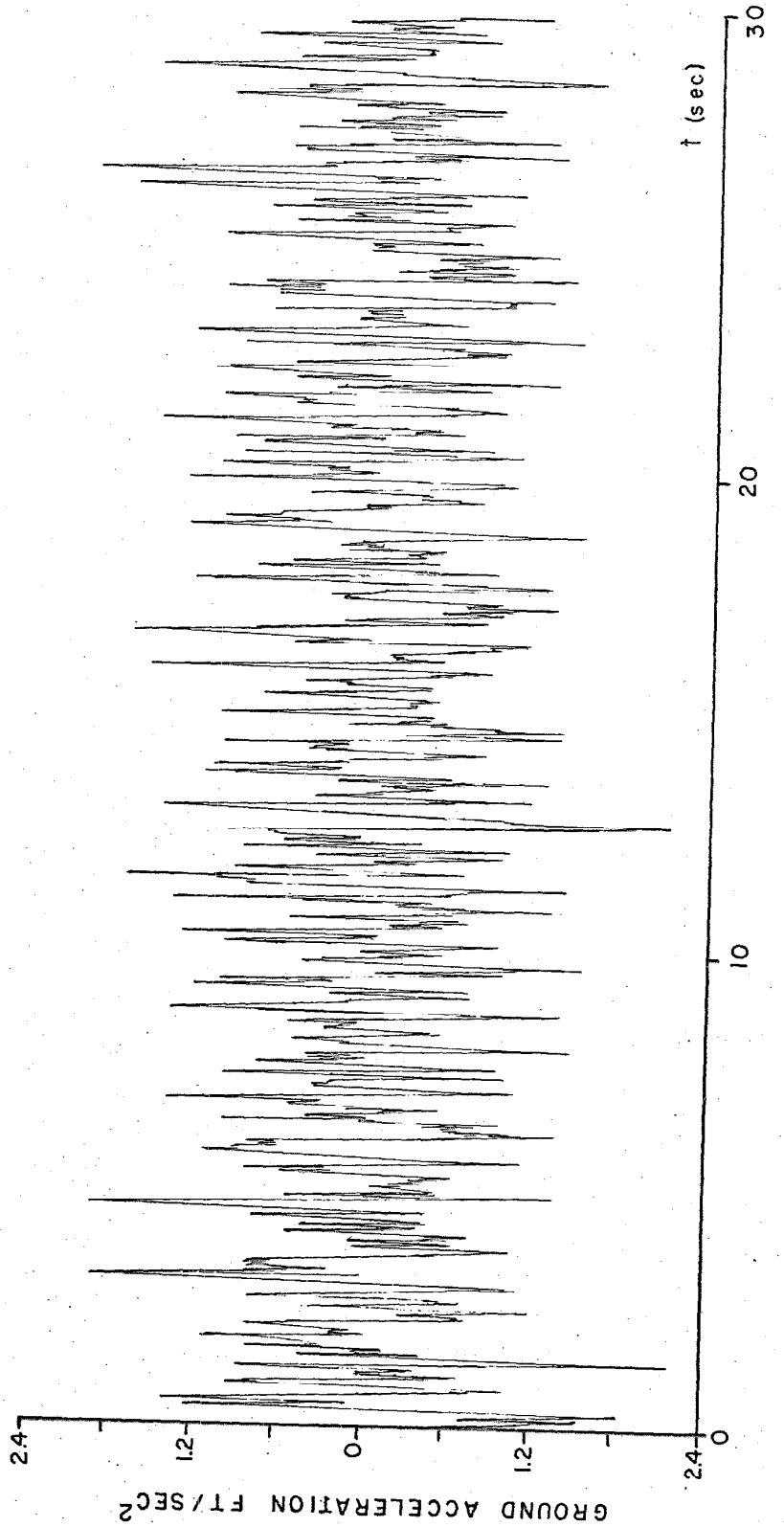


Figure 3.1. Accelerogram for Artificial Earthquake No. 2.

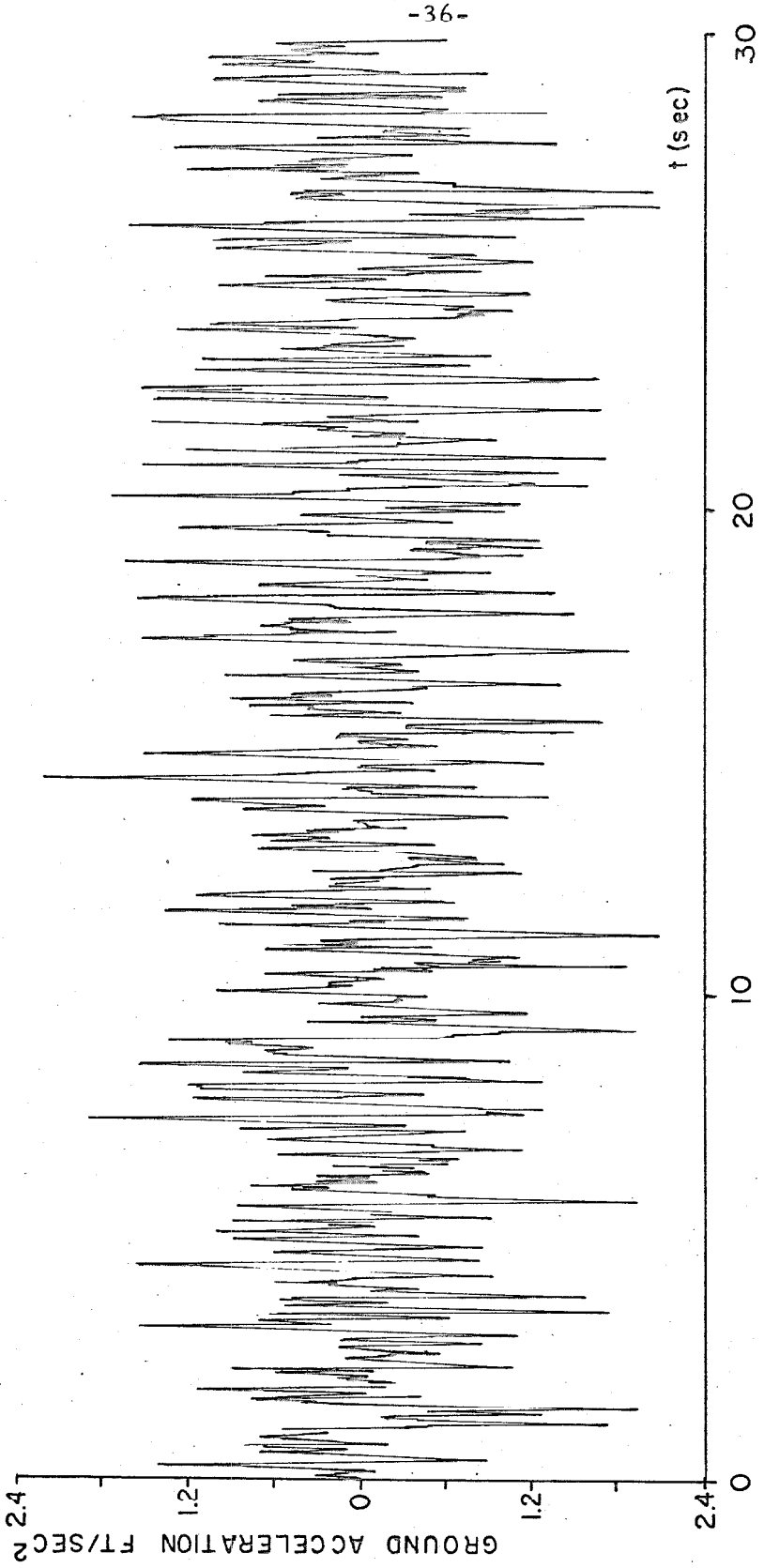


Figure 3.2. Accelerogram for Artificial Earthquake No. 3.

generated on a digital computer by passing an approximate white noise through a filter selected to give spectral properties similar to those of recorded accelerograms.

For most of the computations of the response and failure of one degree of freedom yielding structures, four 60 sec long artificial earthquakes were used. These were constructed from the 30 sec earthquakes by joining pairs. The pairs were formed arbitrarily by joining artificial earthquakes 1 and 2, 3 and 4, 5 and 6, and 7 and 8.

In view of the fact that this study is based mainly on the response of structures to artificial earthquakes, it is appropriate to give some detailed information about them.

The r.m.s. acceleration for each of the 8 artificial earthquakes was computed as a function of time, in order to see how quickly a stationary value is approached and to verify that the r.m.s. acceleration obtained for each earthquake was representative of the ensemble. Figures 3.3, 3.4 and 3.5 show the r.m.s. acceleration for three artificial earthquakes as a function of time. It is seen that the r.m.s. approaches its stationary value rapidly, generally being within ± 10% by the end of 5 seconds. In table IV, the r.m.s. accelerations and zero crossings are given together with other characteristics of the 8 artificial earthquakes[23]. From the above, it is concluded that the r.m.s. acceleration is a suitable measure of the severity of the artificial earthquakes.

The ensemble of pseudo-earthquakes, whose principal characteristics are given in table IV, have an average r.m.s.

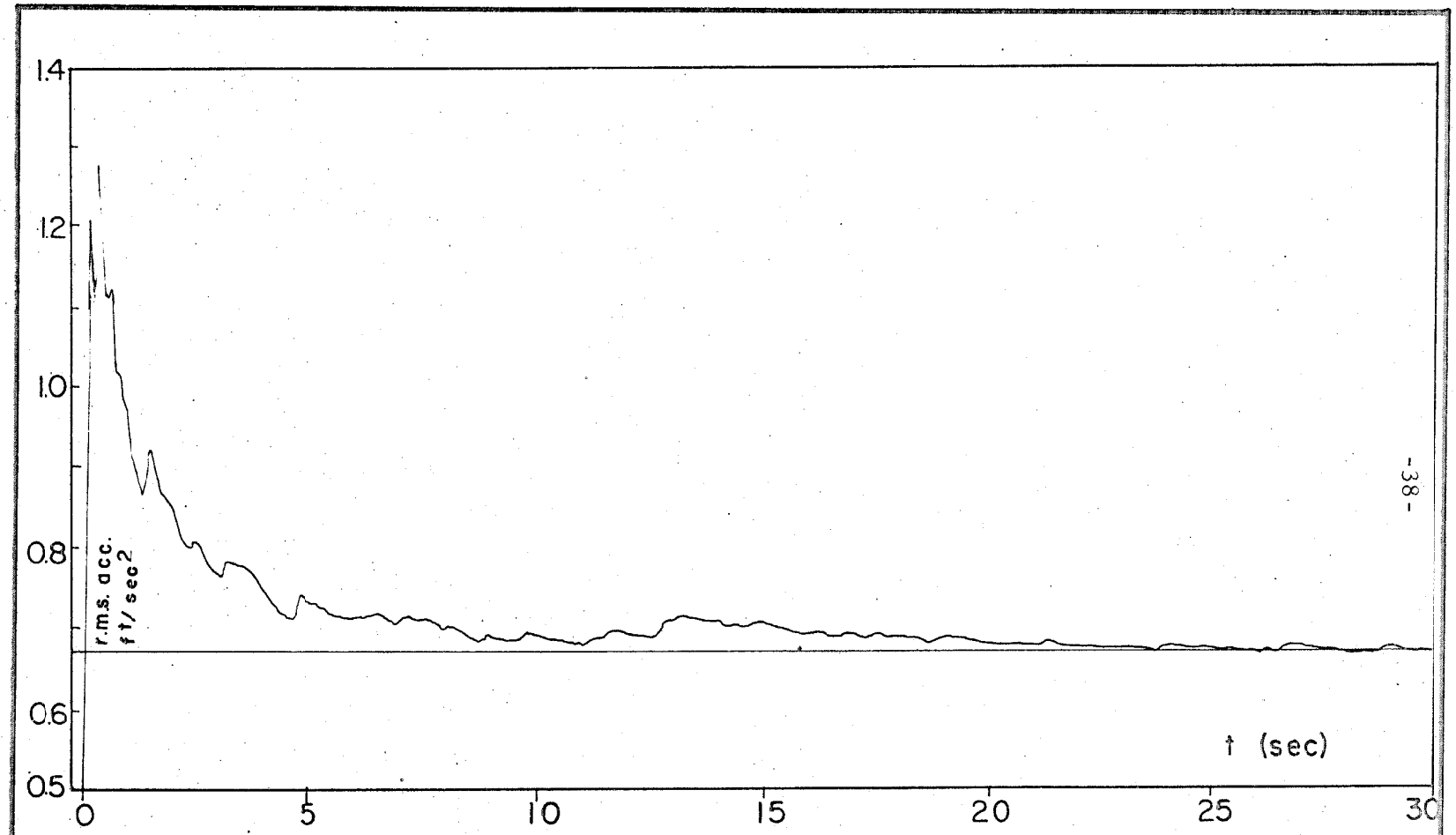




Figure 3.3. R.M.S. Acceleration for Artificial Earthquake No. 1.

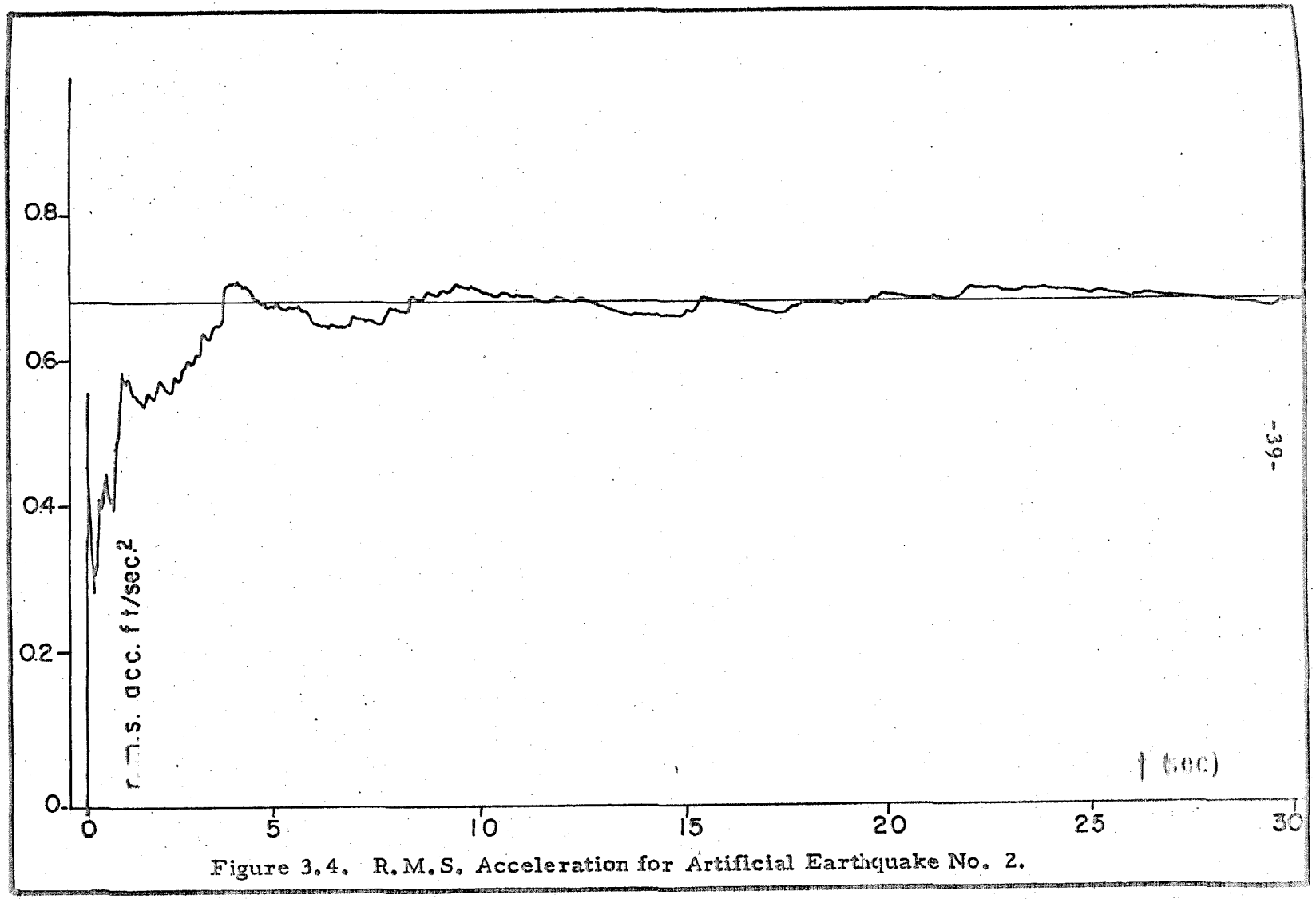


Figure 3.4. R.M.S. Acceleration for Artificial Earthquake No. 2.

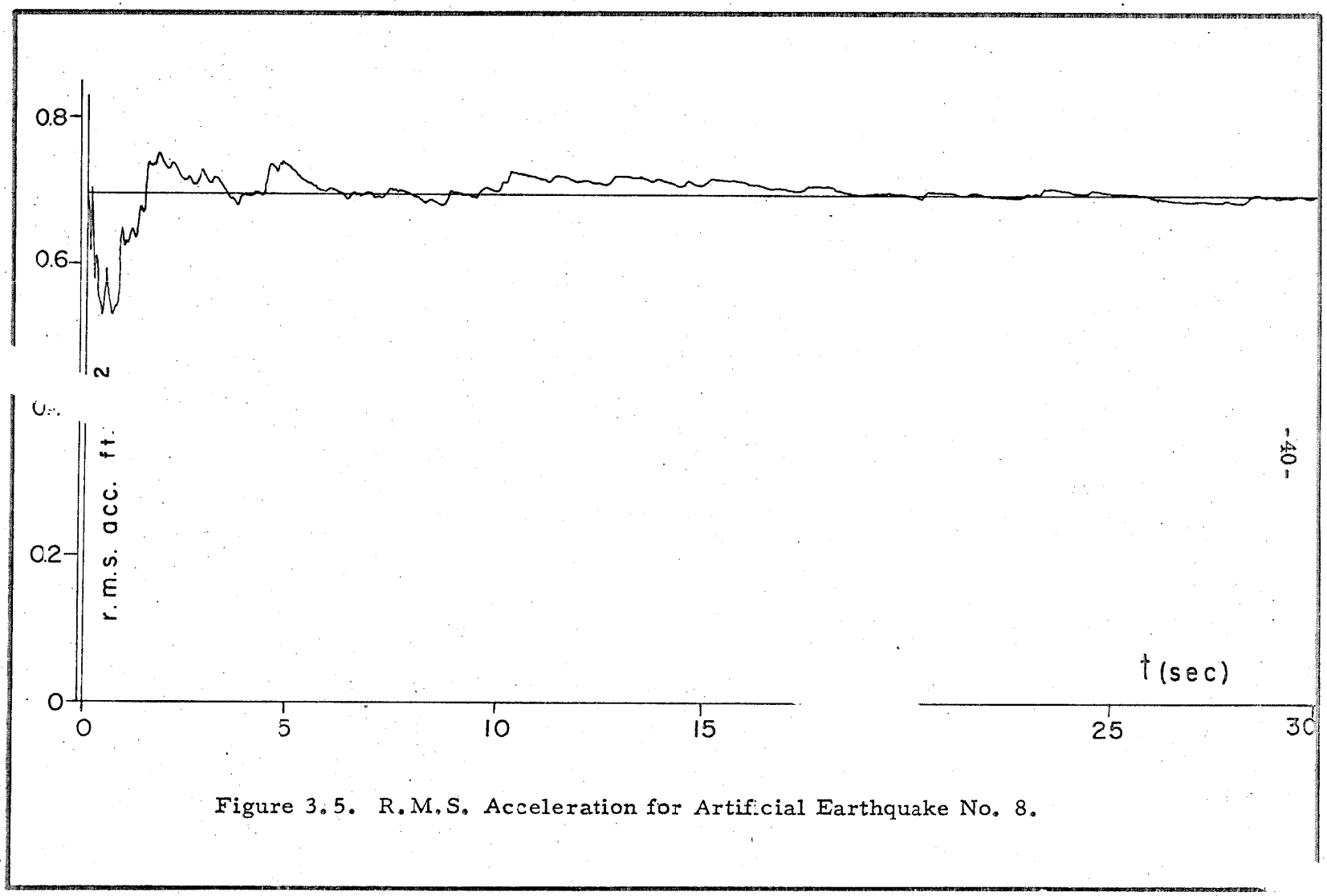


Figure 3.5. R.M.S. Acceleration for Artificial Earthquake No. 8.

TABLE IV

Artificial Earthquake Properties

| Item | Accelerogram Number | | | | | | | |
|---|---|---|---|---|---|---|---|---|
| | 1 | 2 | 3 | 4 | 5 | 6 | 7 | 8 |
| r.m.s. $= \left[\frac{1}{30}\int_0^{30} \ddot{y}^2(t)\,dt\right]^{\frac{1}{2}}$ | 0.665 | 0.684 | 0.698 | 0.734 | 0.689 | 0.709 | 0.700 | 0.694 |
| Average r.m.s. | | | 0.697 | | | | | |
| Percentage of average r.m.s. | 95.5 | 98.1 | 100.3 | 105.3 | 98.9 | 101.8 | 100.5 | 99.6 |
| Spectrum intensity $SI_o = \int_{0.1}^{2.5} S_v(0,\omega,30)\,d(\frac{2\pi}{\omega})$ | 3.02 | 3.49 | 2.99 | 3.22 | 3.23 | 2.89 | 3.18 | 3.38 |
| Average spectrum intensity | | | 3.18 | | | | | |
| Percentage of average intensity | 95.4 | 110.1 | 94.2 | 101.5 | 101.9 | 91.0 | 100.2 | 106.4 |
| Zero crossings accelerogram | 6.9 | 7.8 | 7.5 | 7.0 | 7.8 | 7.3 | 7.3 | 8.3 |
| Average zero crossings | | | 7.5 | | | | | |

acceleration of 0.697 ft/sec$^2$. This intensity was chosen to represent earthquakes whose average damped velocity spectra corresponds closely to the standard spectra computed by Housner[12]. A velocity spectra for one of the artificial earthquakes is shown in Figure 3.6.

One way to vary the severity of the excitation is to define a parameter E, a multiplicative constant used to produce a pseudo-earthquake of a desired intensity from any sample of the ensemble. As reported in reference 34, a value of E = 2.9 produces an ensemble whose strength is comparable to the El Centro 1940 earthquake, and an E = 2.1 corresponds to an ensemble whose strength is like that of the Taft 1952 accelerogram.

Period of Vibration

Four different values of the period for small amplitudes were selected which cover most of the range of interest in the earthquake problem. The values considered are T = 0.5, 1.0, 1.5 and 2.0 seconds ($\omega_o = 2\pi/T$). It is noted that the present study is not aimed at real one-story buildings. A range of T = 1/2 to T = 2 seconds was selected because it includes the periods of most multi-story buildings. This thesis represents a first step in the analysis of the effects of gravity; a prelude to the study of multi-story buildings. Although the analysis may apply to some special one-story structures, most modern one-story buildings are constructed in such a way that collapse is not a problem.

Figure 3.6

VELOCITY SPECTRA

OF PSEUDO-EARTHQUAKE NO.2

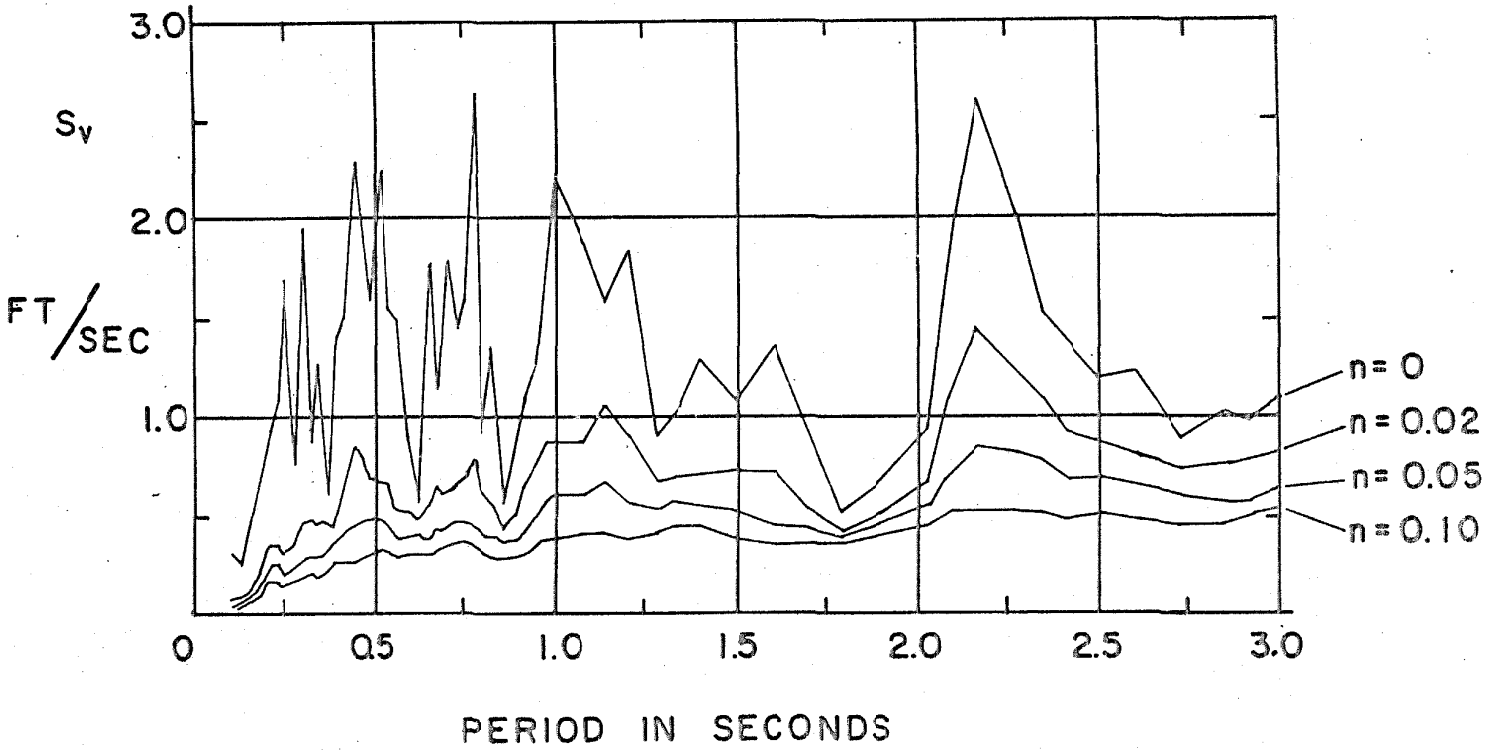

Damping

Because of time and computational limitations the amount of viscous damping was not varied in this study. The choice of the damping was the result of the following considerations: It is not advisable to consider undamped structures because 1) it is known that response statistics are very sensitive when no damping is assumed and 2) real structures always have some damping. On the other hand, a large amount of viscous damping is unrealistic and may mask the influence of other parameters on the collapse. Finally, based on the experimental results obtained by Nielsen[43] from vibrations of multi-story buildings, 2 per cent of critical viscous damping was selected as the value to be used throughout the present study.

Height of the Structures

When gravity is ignored, the response of a yielding structure does not depend on the length of the columns, $\ell$. However, if interest is focused on the collapse of the structure and gravity is included in the analysis, it is clear from the equation of motion 2.36 that the length of the column will have an important influence on the failure of the structure under consideration. Several values for $\ell$ were selected when analyzing its effects on the time necessary for a given yielding structure to collapse. The values of $\ell$ used in the calculations are $\ell$ = 5, 10, 15, 20, 25 and 30 ft. This range extends well below and above the heights of typical story heights in structures.

Yield Level

It proved convenient to use two parameters, $\phi_y$ and $a_y/g$, to describe the yield level of the structure. These two parameters are related by equation 2.33. $a_y/g$ represents the lateral yield level of the structure and for most of the work reported in this chapter two values of this parameter were selected: $a_y/g = 0.05$ and $a_y/g = 0.10$. A value of $a_y = 0.05g$ means that a horizontal force equal to 5 per cent of the weight of the structure will just produce yielding. In addition to these two values a few others were used for special calculations. As will be shown below, the use of another dimensionless parameter will permit the results obtained for $a_y/g = 0.05$ and $a_y/g = 0.10$ to be extrapolated to other cases of interest.

The yielding level for the springs, $\phi_y$, represents the angle at which the structure starts to yield. The values of $\phi_y$ selected for this study are obtained from 2.33 and the previously selected values of the lateral yield level.

Angle of Static Failure

Dynamic collapse of the yielding structure will be defined as the state in which the angle that the columns make with the vertical exceeds $\phi_s$, the angle of static failure, and does not again become less than that angle. The angle of static failure is defined by relations 2.38 and 2.39, and the values considered below are those which correspond to the previously selected values of $a_y/g$ and $\phi_y$.

Equation of Motion. Final Form

When E and a new parameter, $\theta = Eg/a_y$ are introduced, the equation of motion 2.36 may be written:

$$\frac{d^2\phi}{d\tau^2} + 2n\frac{d\phi}{d\tau} + F(\phi,\dot{\phi}) + \frac{g}{\ell\omega_o^2}\left\{F(\phi,\dot{\phi}) - \sin\phi\right\} + \frac{\theta}{g}\phi_y\sigma(\tau)\cos\phi = 0 \quad (3.1)$$

The significance of the parameter $\theta$ will be discussed later in the chapter.

B. Response and Failure of the Elasto-Plastic Structure

Equation 3.1 was used in the numerical integration of the response of the yielding structure to the artifical earthquakes. The computations were donc on an IBM 7094 digital computer, using both a $4^{th}$ order Runge-Kutta method[44] and also a third order Runge-Kutta method[44,45]. The Runge-Kutta method was used because of the self-starting feature and the long range stability. In no case was the integration step used longer than 1/20 of the natural period for small oscillations. Because further reduction of the integration step size did not modify the response of the structures, it was concluded that the step size was sufficiently small.

The influence of gravity in the response of elasto-plastic one degree of freedom structures near collapse can be made clear by an example. From the four 60 seconds-duration pseudo-earthquakes available, one was selected (3+4) and used to excite a structure with the following characteristics:

$$
\begin{aligned}
T &= 0.5 \text{ sec} \\
\ell &= 10 \text{ ft} \\
E &= 3.45 \\
\phi_y &= 0.00204 \text{ rad} \\
a_y &= 0.1g \\
\phi_s &= 0.10204 \text{ rad}
\end{aligned}
\qquad (3.2)
$$

From 3.2 it can be shown that the structure selected is of practical interest. Having $E = 3.45$, the r.m.s. acceleration of the pseudo-earthquake is 2.42 ft/sec$^2$, which represents an earthquake about 20 per cent stronger than the most severe recorded in the United States (see table V).

A value of $a_y = 0.1g$ is realistic and within the range of values considered in design. A period of half a second and a height of 10 ft represent a structure that is relatively flexible but not impossibly so.

The values of $\phi_y = 0.00204$ rad and $\phi_s = 0.10204$ rad imply that the 10 ft tall structure will begin yielding when the deflection at the top is 1/4 inch and will collapse statically when the deflection reaches 12.2 inches.

The results of four cases are presented in order that the significance of the results will be clear. For all cases the excitation was artificial earthquake (3+4).

In case a), the structure is linear, i.e., $\phi_y$ was selected very large, and gravity was neglected. In case b) the structure is still linear but gravity is considered. For case c), the structure is

elasto-plastic and defined by 3.2, but gravity is again neglected. Finally in case d), the structure is elasto-plastic as in case c) and the effect of gravity is included.

In Figures 3.7, 3.8, 3.9 and 3.10, the responses of the structure for these four cases are given as a function of time. The ordinate, in radians, is the angle that the columns make with the vertical.

From these figures it is seen that for the structure defined by Equation 3.2, the effect of gravity upon the response in the linear case is negligible. This was also the result found from similar calculations for other linear structures and other excitations. For the elasto-plastic structure with gravity neglected (case c) appreciable drift of the equilibrium position is obtained and at the end of the excitation a permanent set remains.

A different type of response was obtained in the case of the elasto-plastic structure with gravity. It is seen that the effect of gravity is to increase significantly the development of permanent set over that found when gravity is not considered, and in this case the displacement eventually exceeds $\phi_s$, the failure angle. Because the gravity effect increases as the deflection grows, the effects are accelerative and the permanent set increases rapidly as the failure angle is approached.

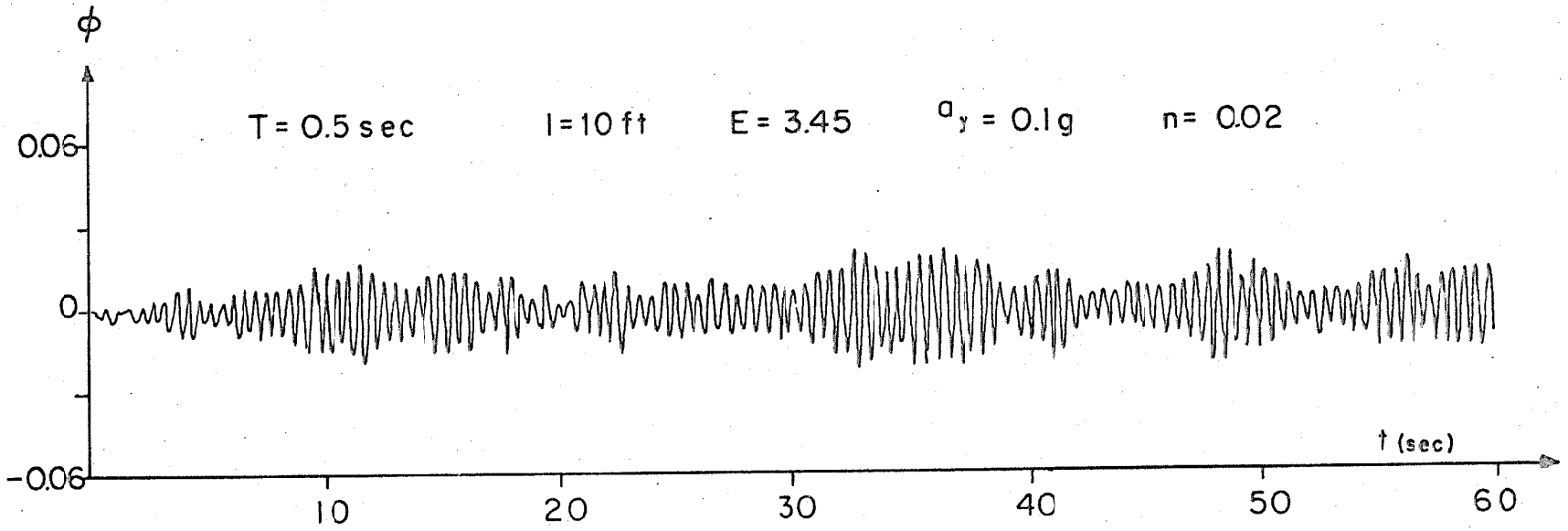


Figure 3.7. Response to Art. Earthq. (3+4). Linear structure, no gravity.

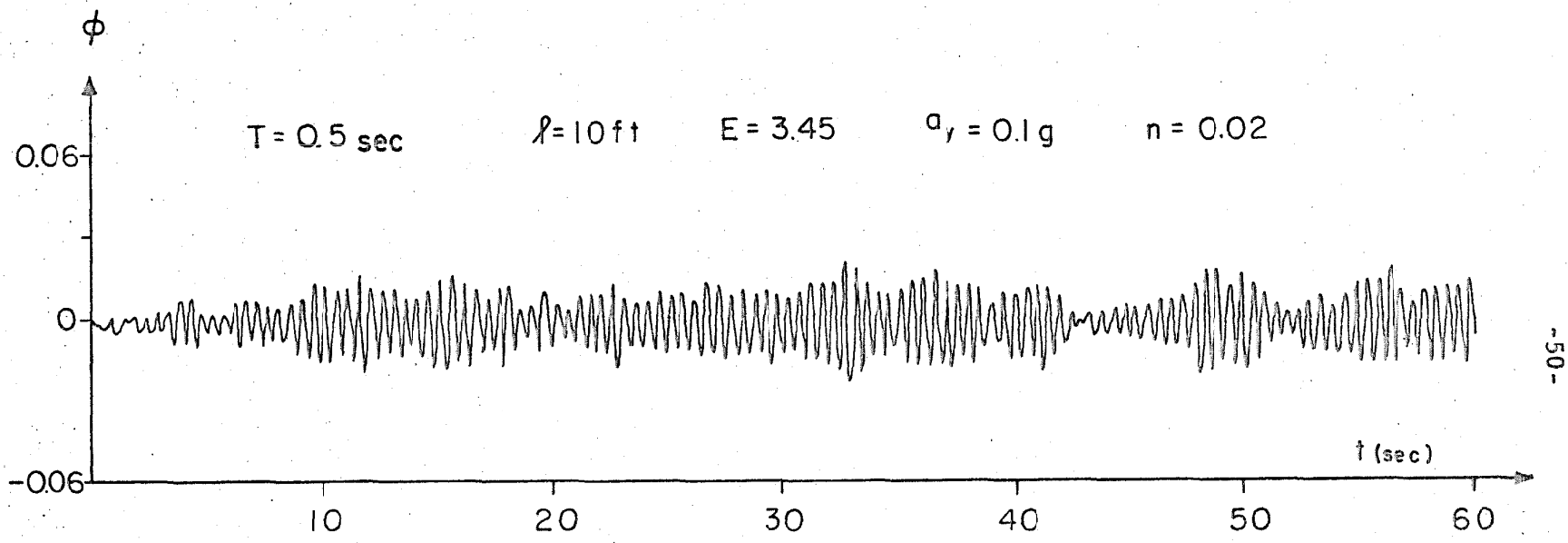


Figure 3.8. Response to Art. Earthq. (3+4). Linear structure, with gravity.

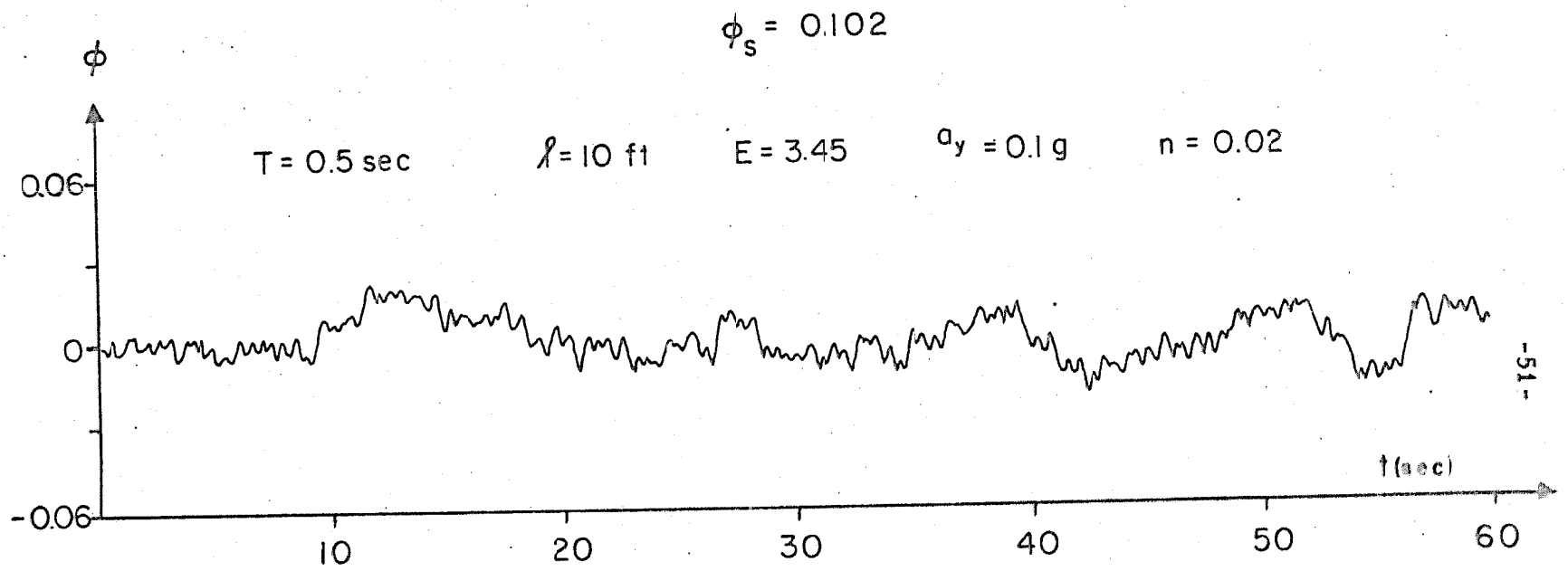


Figure 3.9. Response to Art. Earthq. (3+4). Elasto-plastic structure, no gravity.

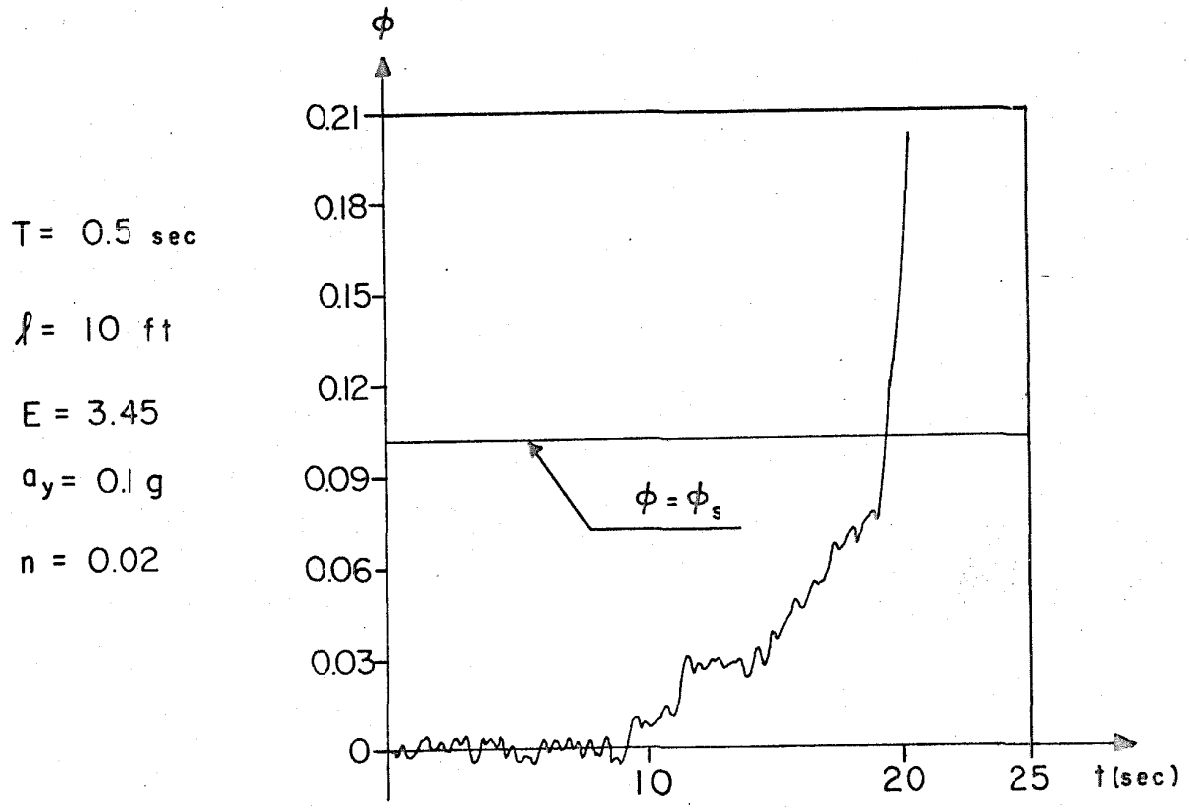


Figure 3.10. Response to Art. Earthq. (3+4). Elasto-plastic structure with gravity.

C. Analysis of Preliminary Results

It would appear that, when the response and collapse of structures are being studied, the intensity of the excitation should be discussed in relation to the strength of the structure under consideration. More precisely, it seems reasonable to expect that a structure with a high yield level subjected to strong earthquake excitation would collapse in about the same time as a structure with a lower yield level subjected to a proportionally weaker earthquake. That this is indeed the case for $\phi$ sufficiently small can be shown by writing equation 3.1 as:

$$\frac{d^2\phi}{d\tau^2} + 2n\frac{d\phi}{d\tau} + (1+\lambda)\phi_y f\left(\frac{\phi}{\phi_y}, \frac{\dot{\phi}}{\phi_y}\right) - \lambda \sin\phi = -\frac{E}{a_y/g}\phi_y \frac{\sigma(\tau)}{g}\cos\phi \qquad (3.3)$$

where

$$F(\phi, \dot{\phi}) = \phi_y f\left(\frac{\phi}{\phi_y}, \frac{\dot{\phi}}{\phi_y}\right)$$

writing $z = \phi/\phi_y$, and taking

$$\sin\phi \approx \phi, \quad \cos\phi \approx 1 \qquad (3.4)$$

equation 3.3 becomes

$$\frac{d^2z}{d\tau^2} + 2n\frac{dz}{d\tau} + (1+\lambda)f(z, \dot{z}) - \lambda z = -\frac{E}{a_y/g}\frac{\sigma(\tau)}{g} \qquad (3.5)$$

For a given structure, $\lambda$ is a constant depending only on the geometry; therefore with the conditions that $\sin\phi \approx \phi$, $\cos\phi \approx 1$, the response $z$ will not be affected by a simultaneous and equal magnification of the intensity of the earthquake (E) and of the yield

level $(a_y/g)$.

It can be seen from 2.33 and 3.4 that the effect of varyi T and $a_y/g$ proportionally is that the yield level $\phi_y$ and the respo. $\phi$ are modified proportionally. However, the response, z, is unchanged and, hence, the time of failure remains the same, provided that conditions 3.4 are satisfied. The range of this approximation was investigated by computing the exact responses of three structures having the following properties:

$$T = 1.0 \text{ sec}$$
$$\ell = 10 \text{ ft} \qquad (3.6)$$
$$\frac{E}{a_y/g} = 23$$

Using artificial earthquake (7+8) and Equation 3.1 the response was calculated for the following three pairs of values of E and $a_y/g$:

$$\text{a)} \begin{cases} E = 6.9 \\ a_y/g = 0.30 \end{cases}$$

$$\text{b)} \begin{cases} E = 2.3 \\ a_y/g = 0.10 \end{cases} \qquad (3.7)$$

$$\text{c)} \begin{cases} E = 1.15 \\ a_y/g = 0.05 \end{cases}$$

For all three the ratio $E/(a_y/g)$ is equal to 23.

The angle of yielding $\phi_y$ and the angle of failure $\phi_s$, are determined by 3.6, 3.7 and the definitions given in Chapter II:

$$
\begin{aligned}
&\text{a)} \quad \left\{ \begin{array}{l} \phi_y = 0.0246 \text{ rad} \\ \phi_s = 0.3246 \text{ rad} \end{array} \right. \\
&\text{b)} \quad \left\{ \begin{array}{l} \phi_y = 0.0082 \text{ rad} \\ \phi_s = 0.1082 \text{ rad} \end{array} \right. \\
&\text{c)} \quad \left\{ \begin{array}{l} \phi_y = 0.0041 \text{ rad} \\ \phi_s = 0.0541 \text{ rad} \end{array} \right.
\end{aligned} \tag{3.8}
$$

It should be noted that the ratio of the angle of static failure to the angle of yielding has the same value, $\phi_s/\phi_y = 13.2$, for the three cases.

The results of the computations can be summarized as follows: 1) The time for failure in all three cases was 35.5 sec within a tolerance of 0.2 per cent; and 2) The fact that the three times of failure were the same is a verification of the fact that $\phi$ was small enough so that the motion is described by 3.5. During the 35.5 seconds that preceeded the collapse, there were plastic deformations only for about 2.0 seconds, i.e., less than 6 per cent of the time. The largest values of $\phi$ were obtained in case a):

$$
\left| \frac{\phi_s}{\sin \phi_s} \right|_{max} \approx 1.02 \quad , \quad \cos \phi \approx 0.95
$$

It is concluded that for most cases of interest the time to collapse depends only on the ratio of the intensity of the earthquake to the lateral yield level and not upon their individual values. The parameter $\theta = E/(a_y/g)$, which is the ratio of the relative strength

of the earthquake motion to the strength of the structure, is thus of special significance in interpreting the responses.

The values of the parameter E are given in Table V for the earthquakes listed in Table I. The durations and r.m.s. accelerations were taken from reference (23).

Recalling that the yield levels of many real structures typically lie between 0.05g and 0.10g, it is possible to estimate the range of values of $\theta$ that are of interest for real earthquakes and real structures. On the basis of the data in Table V and the above values of lateral yield level, it is concluded that for most practical cases, $\theta$ will lie in the range between 20 and 60. The value of 20 was obtained for the 1934 El Centro earthquake when 0.10g was selected for the yield level and the value of 60 resulted when the 1940 El Centro earthquake was used with a yield level of 0.05g.

## D. Calculations of Response to Artificial Earthquakes

### 1. Introduction

Four sixty second pseudo-earthquakes were used for excitation in order to study the statistical fluctuations of the time of collapse when the remaining parameters were not varied. Values of the parameter E were varied between $E_{min} = 1.15$ and $E_{max} = 6.9$ to represent the range of interest of the earthquake intensity. The response and the time of collapse of simple elasto-plastic structures were determined numerically by integration of equation 3.1.

The ranges of the parameters selected for this study were

TABLE V

Strong-Motion Earthquake r.m.s. and E Values

| Location and Date | Strong-Motion Duration (seconds) | Component | Acceleration r.m.s. ft/sec$^2$ | Average r.m.s. | E From Average r.m.s. |
|---|---|---|---|---|---|
| El Centro, Calif. 18 May 1940 | 25 | N.S.<br>E.W. | 2.20<br>1.82 | 2.01 | 2.88 |
| El Centro, Calif. 30 Dec. 1934 | 17 | N.S.<br>E.W. | 1.43<br>1.27 | 1.35 | 1.93 |
| Olympia, Wash. 13 April 1949 | 21 | S80°W<br>S10°E | 1.95<br>1.57 | 1.76 | 2.51 |
| Taft, California 21 July 1952 | 14 | S69°E<br>N21°E | 1.45<br>1.42 | 1.44 | 2.06 |

based on the analysis presented in Chapter II. Particular values of the parameters were used and general trends were investigated. Appendix I gives a complete list of the elasto-plastic cases solved numerically, and includes angles of failure, $\phi_s$, time of collapse $t_o$, together with other characteristics of the structures. For the elasto-plastic oscillator, a total of 169 response calculations was made.

2. Effect of Different Inputs

At first, the length of the columns was kept fixed at $\ell = 10$ ft and the response and failure of different structures were obtained for four values of the period, $T = 0.5$, 1.0, 1.5 and 2.0 seconds and for four values of the parameter $\theta$, $\theta = 23.0$, $\theta = 34.5$, $\theta = 46.0$ and $\theta = 69.0$, for the four 60 second duration artificial earthquakes. Calling $t_o$ the time of failure for a given structure when subjected to an artificial earthquake and $\bar{t}_o$ the average of $t_o$ over the ensemble of earthquakes when the structural parameters are kept constant, it is of interest to learn if the times of failure for individual samples of the ensemble of earthquakes will show a dependence trend upon the period of vibration. In Figures 3.11, 3.12, 3.13 and 3.14 the results are shown plotting the ratio between the individual and average times of failure $\bar{t}_o$ as the ordinate. The abscissa is the value of the natural period of the structure for small oscillations. Each line plotted represents the results for a different artificial earthquake. In these figures no consistent trend is apparent in the responses to individual earthquakes, as the period varies from 1/2

$\theta = 23$ $\ell = 10$ft $n = 0.02$

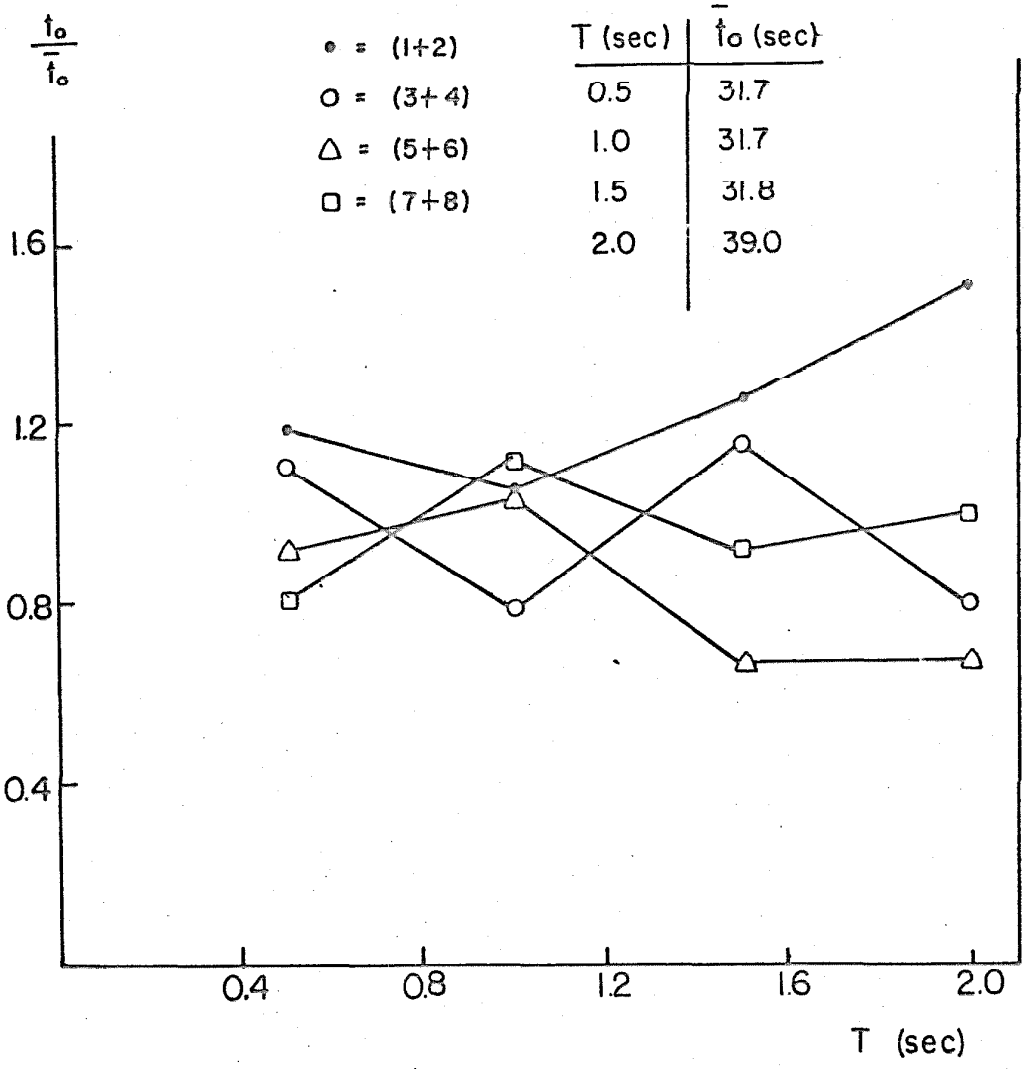


Figure 3.11. Normalized times of failure.

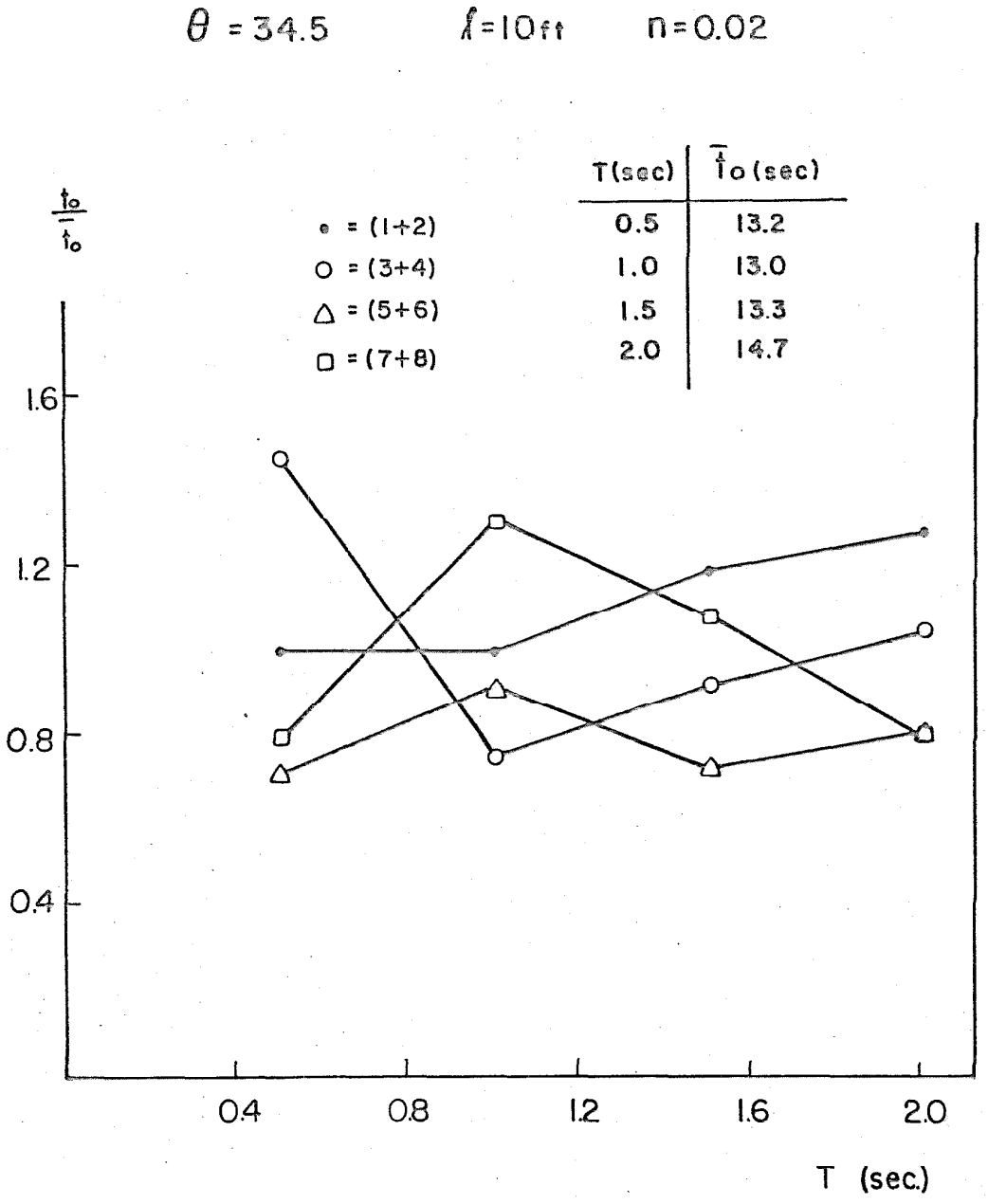


Figure 3.12. Normalized times of failure.

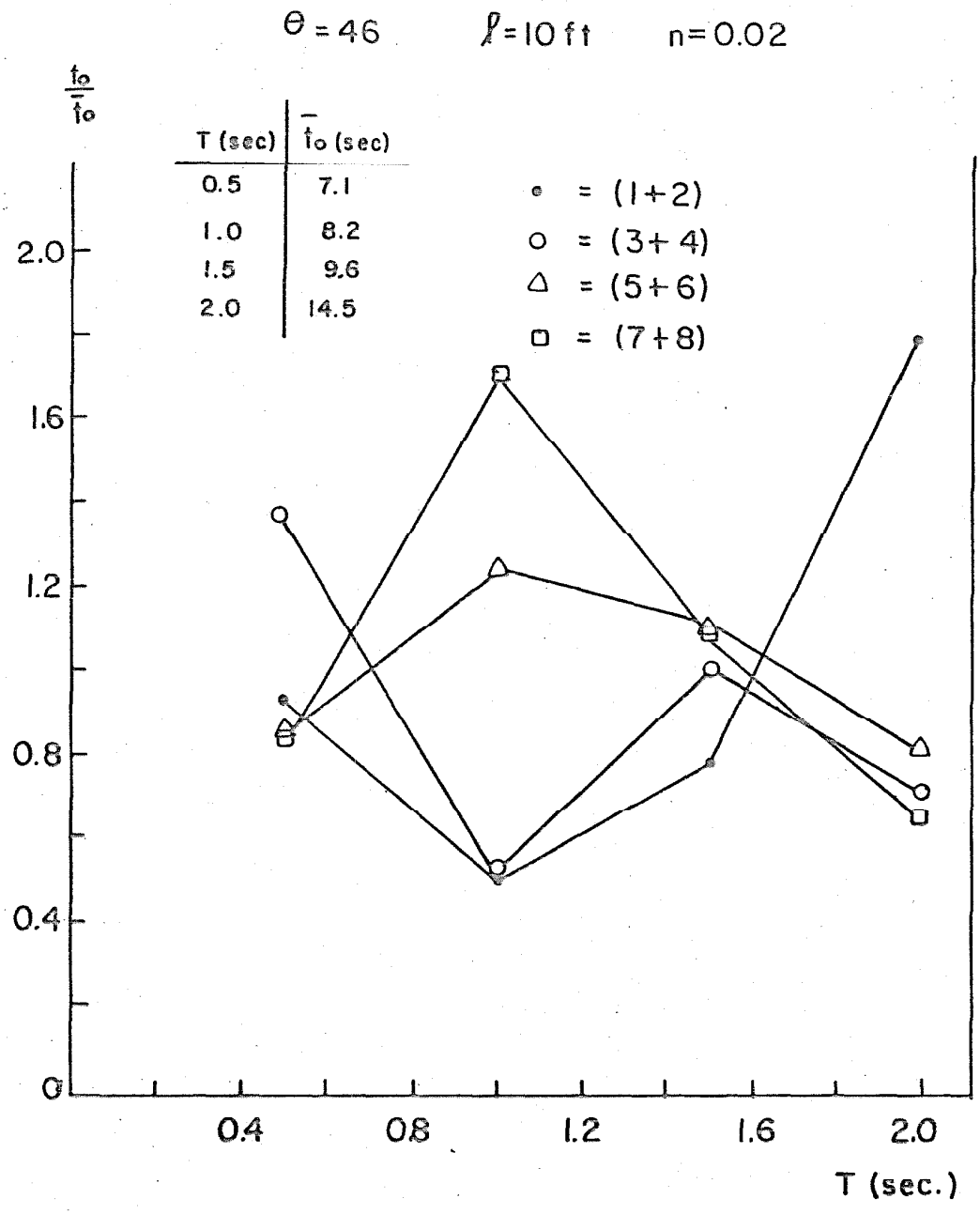


Figure 3.13. Normalized time of failure.

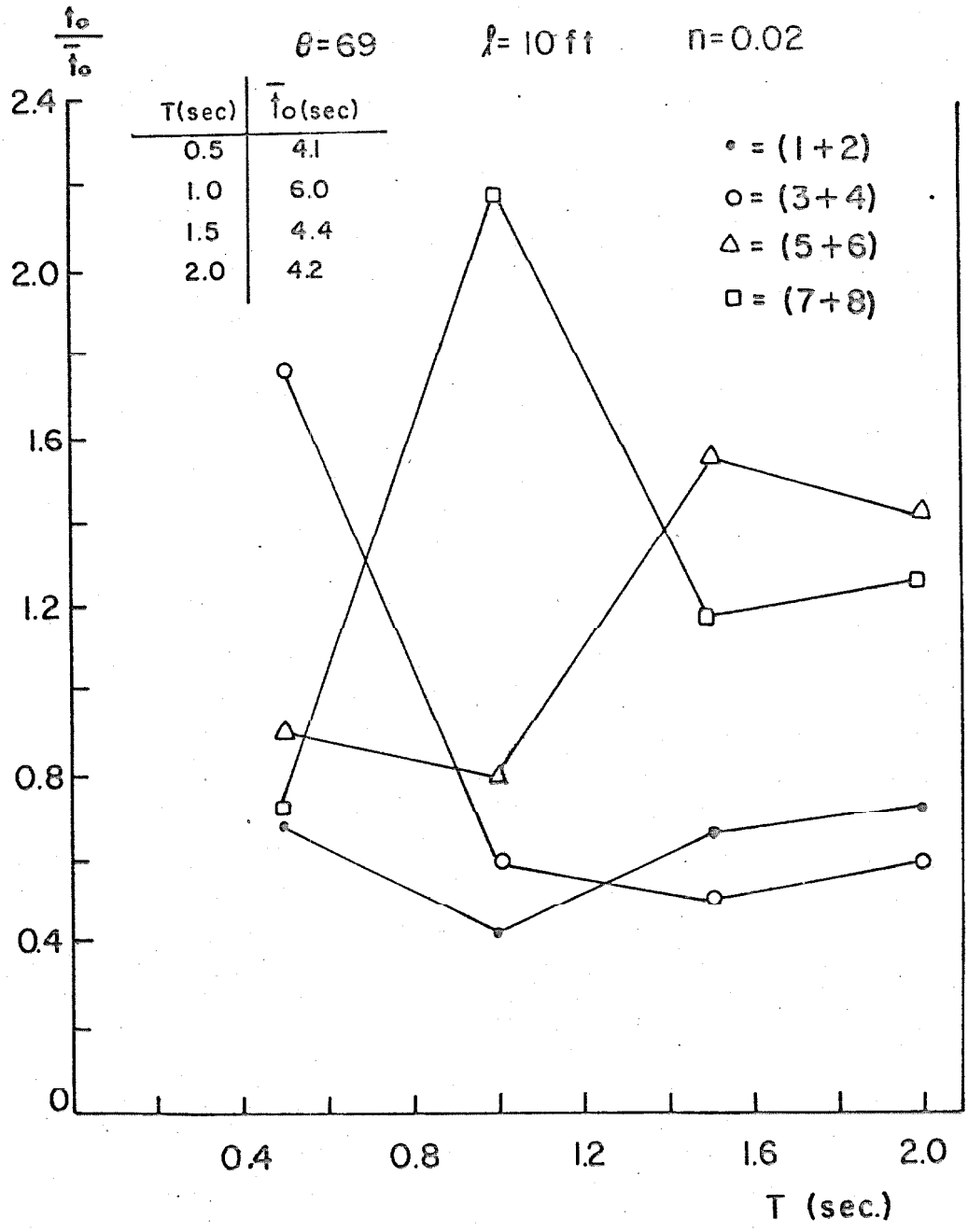


Figure 3.14. Normalized time of failure.

to 2 seconds.

It is clear from the results, however, that large dispersions can be obtained when different earthquakes of the same intensity are utilized. This indicates the necessity of obtaining statistical averages of the times of failure.

To obtain a better insight into the dispersion obtained with individual earthquakes the ratio $t_o/\bar{t}_o$ was plotted in Figure 3.15 as a function of $\theta$, where $t_o$ is the time of failure for the case considered, and $\bar{t}_o$ is the average time for failure for the corresponding natural period. It is seen in Figure 3.15 that there is no strong trend in the dispersion when the period changes from 0.5 to 2.0 seconds, four artificial earthquakes are considered, and $\theta$ is kept constant. When $\theta$ varies between 23 and 69 there appears to be a tendency for the dispersion of the results to increase somewhat. This indicates more variations in times of failure of rather weak structures subjected to strong earthquakes (large $\theta$) than for strong structures subjected to weak earthquakes (small $\theta$).

Rather small values for the time of collapse $t_o$ are obtained when large values of $\theta$ are considered. It is noted that for small values of $t_o$, the r.m.s. acceleration for different artificial earthquakes is not well represented by the parameter $E$ and this fact is thought to be responsible for the increase in the dispersion observed in Figure 3.15.

It can be said that Figures 3.11, 3.12, 3.13, 3.14 and 3.15 show no marked dependency of the time of failure upon the period of the yielding structure. Because of this, it seems permissible to

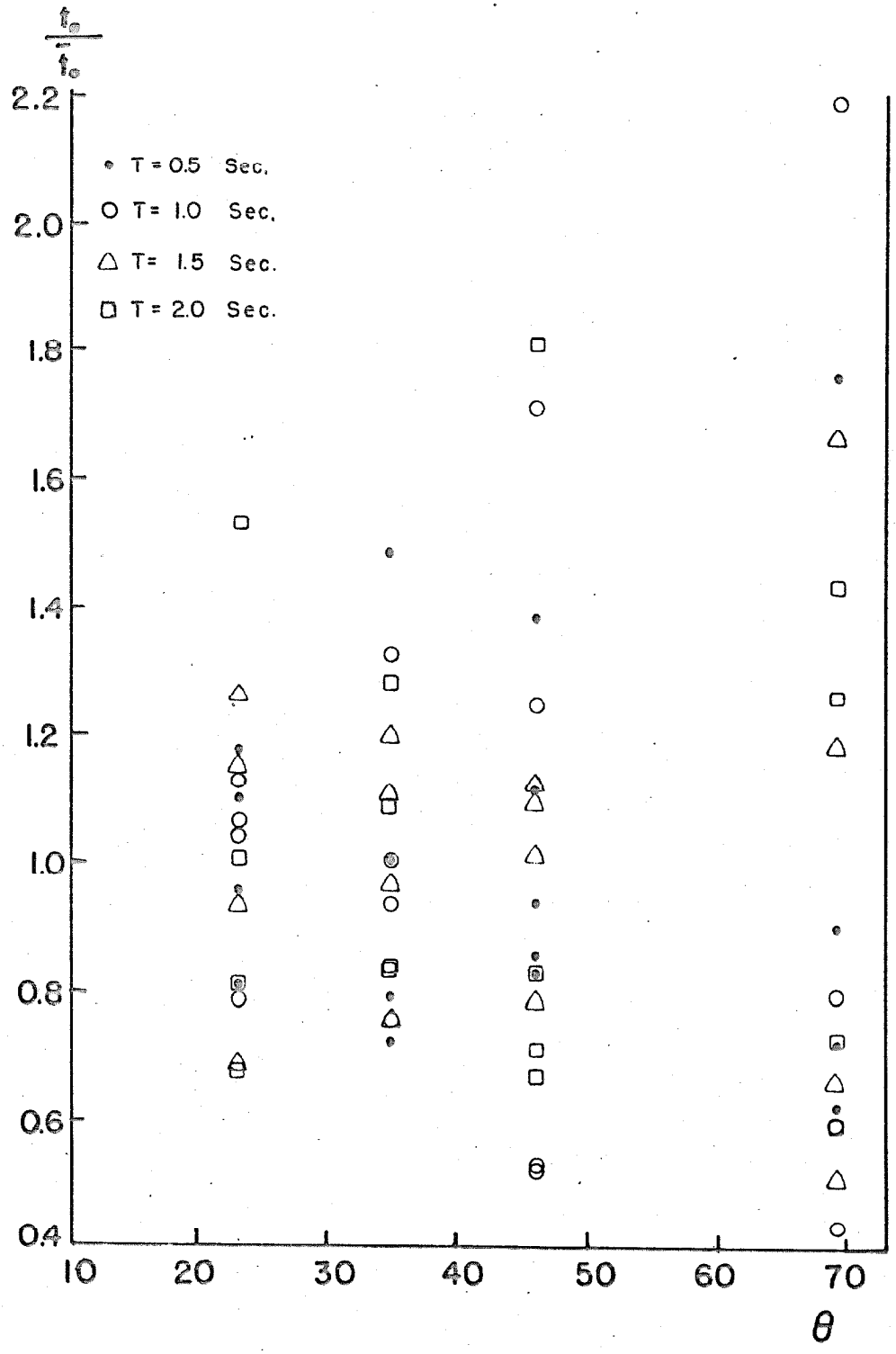


Figure 3.15. Normalized time of failure.

combine the data for different periods, but for singles values of $\theta$. Figures 3.16, 3.17, 3.18 and 3.19 are histograms for $\theta = 23$, $\theta = 34.5$, $\theta = 46$ and $\theta = 69$. The ratio $t_o/\bar{t}_o$ for all periods is plotted as the abscissa and the frequency of occurrence as the ordinate. Although the dispersion varies, no conclusive trends are observed in these four figures as $\theta$ varies between $\theta = 23$ and $\theta = 69$. In Figure 3.20, a histogram is presented constructed from the data contained in the four preceeding pictures. In this figure $\bar{t}_o$ is not the average from the previous four figures, but is the $\bar{t}_o$ appropriate to each different $\theta$.

From the above discussion it is concluded that $\bar{t}_o$ does not depend strongly on the period T and Figure 3.15 suggests that $t_o/\bar{t}_o$ is also independent of the period. However, $\bar{t}_o$ is strongly dependent upon $\theta$, decreasing as $\theta$ increases. Some dependence of $t_o/\bar{t}_o$ on $\theta$ is indicated from Figures 3.15 and 3.16 through 3.18, but it is thought that the relation is too weak to be determined from the statistics available.

### 3. Dependence of $\bar{t}_o$ on $\theta$

It was shown above that the time of collapse for a yielding structure is strongly dependent on $\theta$. Using the same data contained in Figure 3.15, but separating the results obtained for the four values of the natural period, it was possible to study the dependence of the average time for collapse $\bar{t}_o$ upon the parameter $\theta$ when the amount of viscous damping was constant, and the length of the columns was fixed at 10 ft.

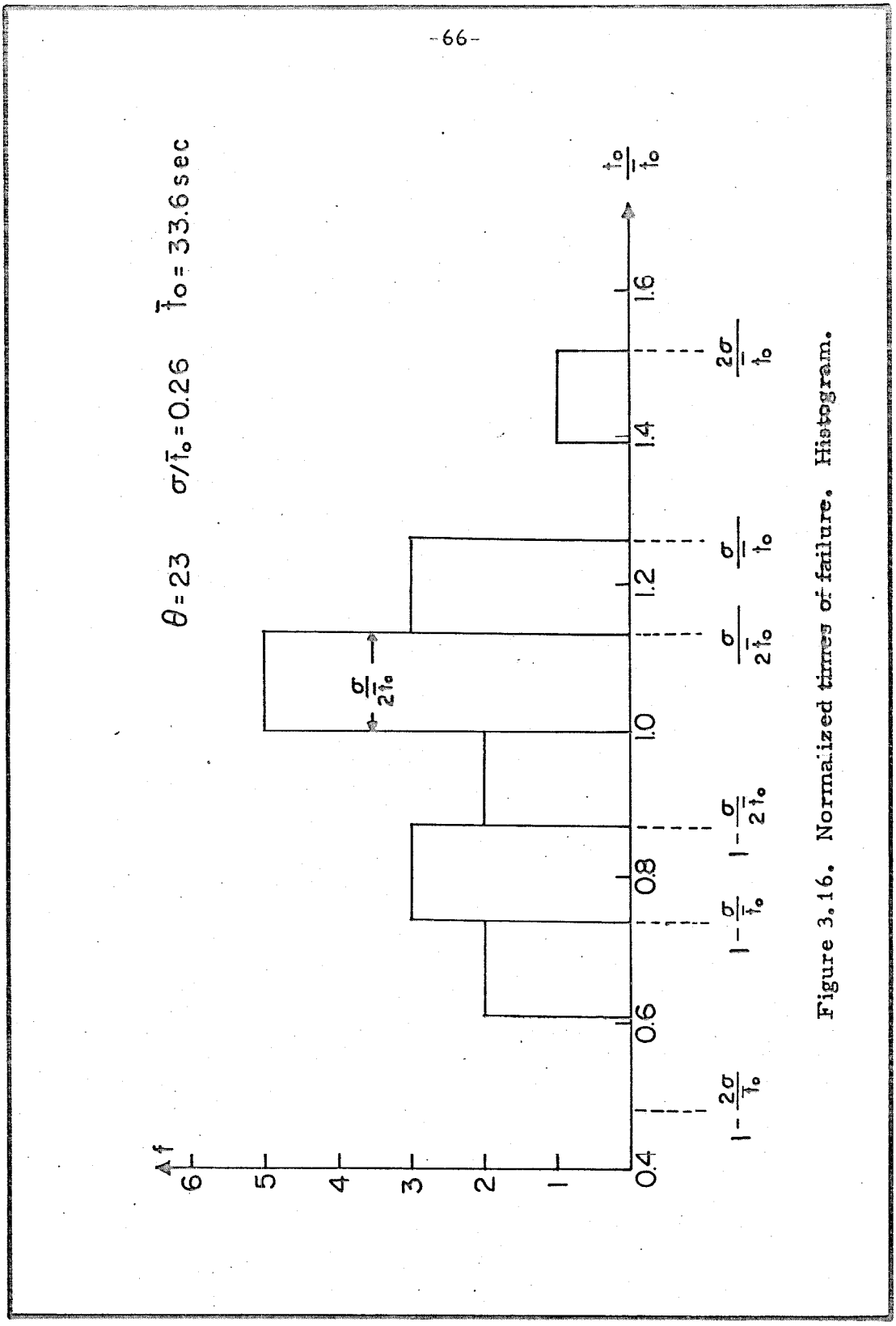


Figure 3.16. Normalized times of failure. Histogram.

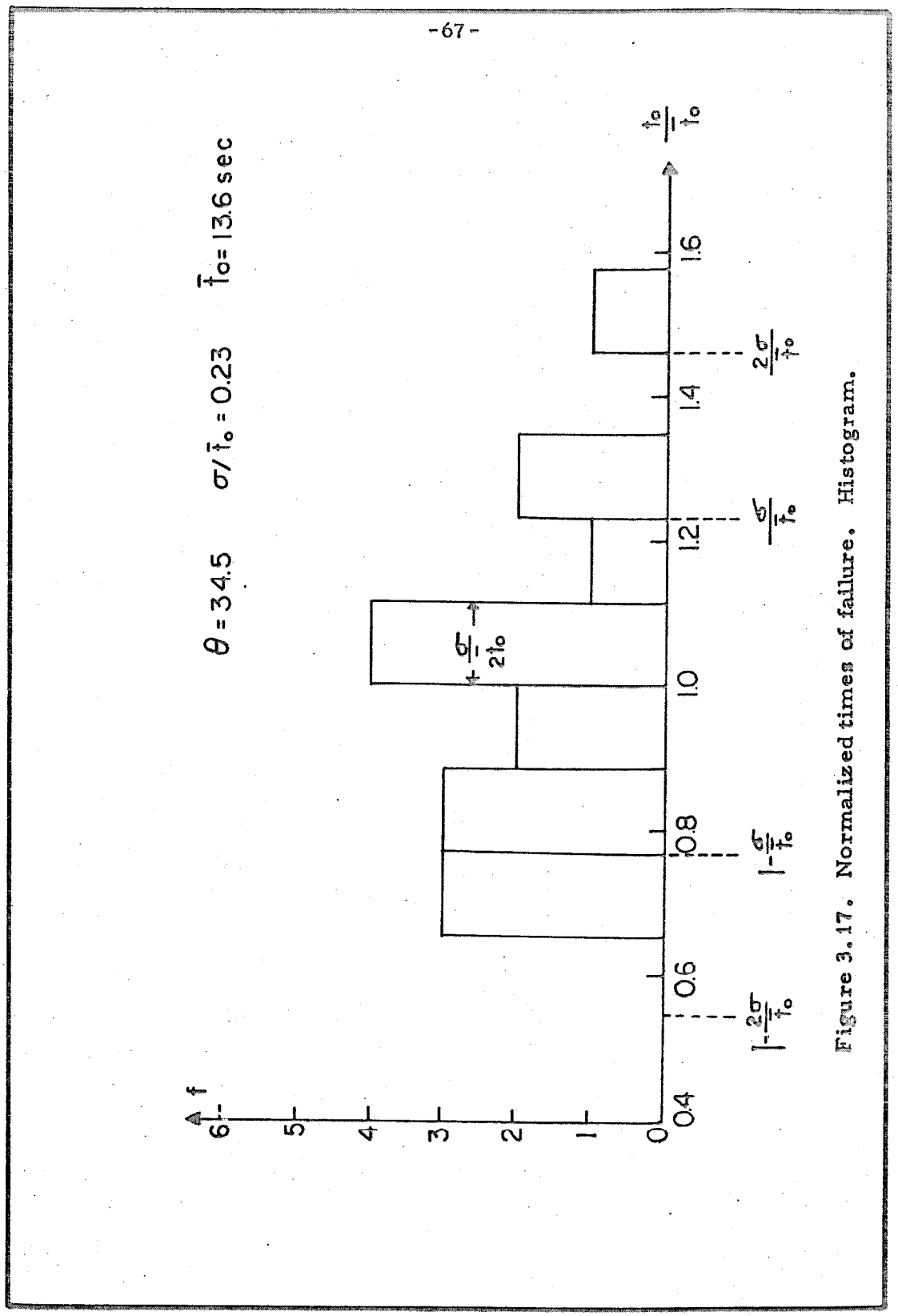


Figure 3.17. Normalized times of failure. Histogram.

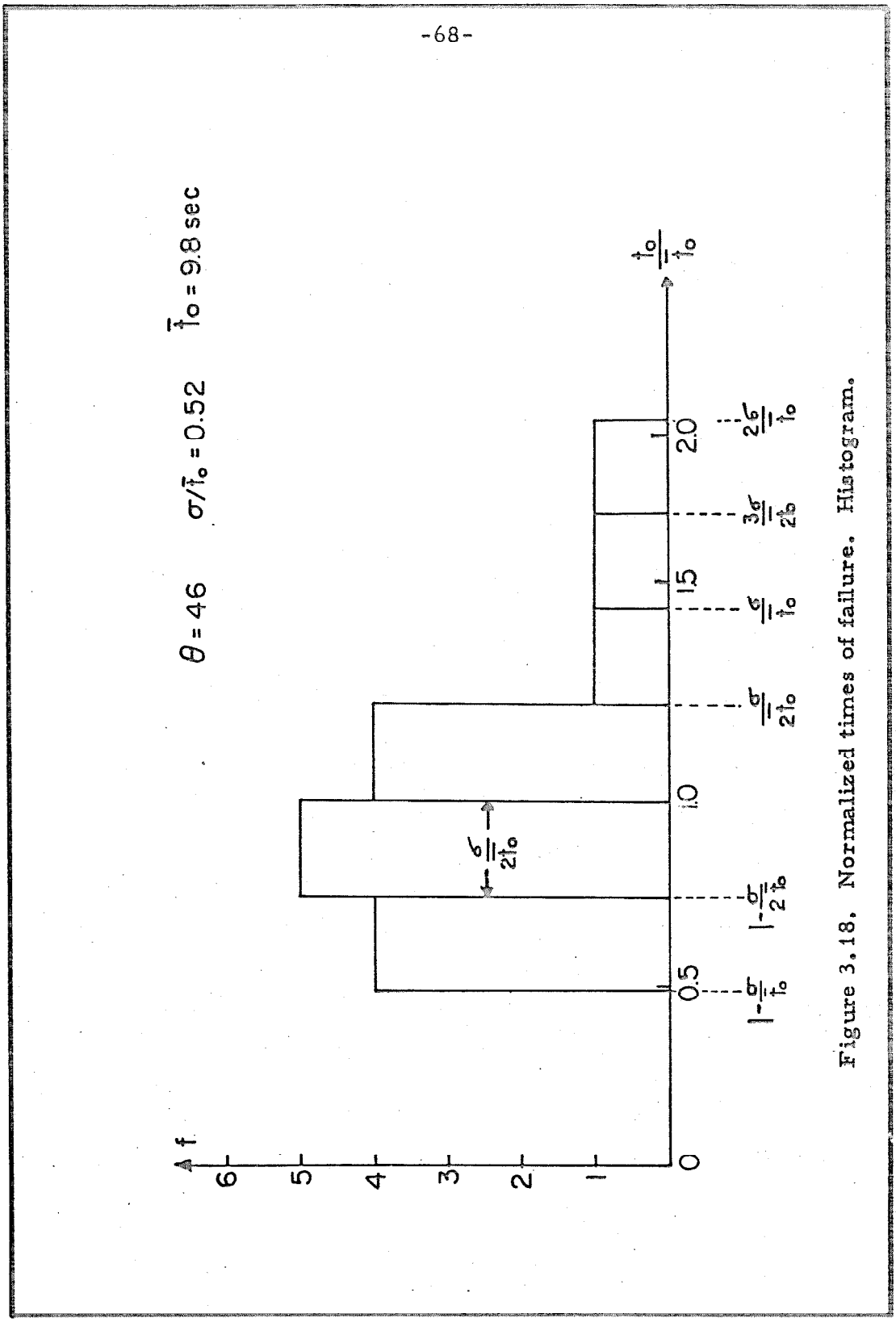


Figure 3.18. Normalized times of failure. Histogram.

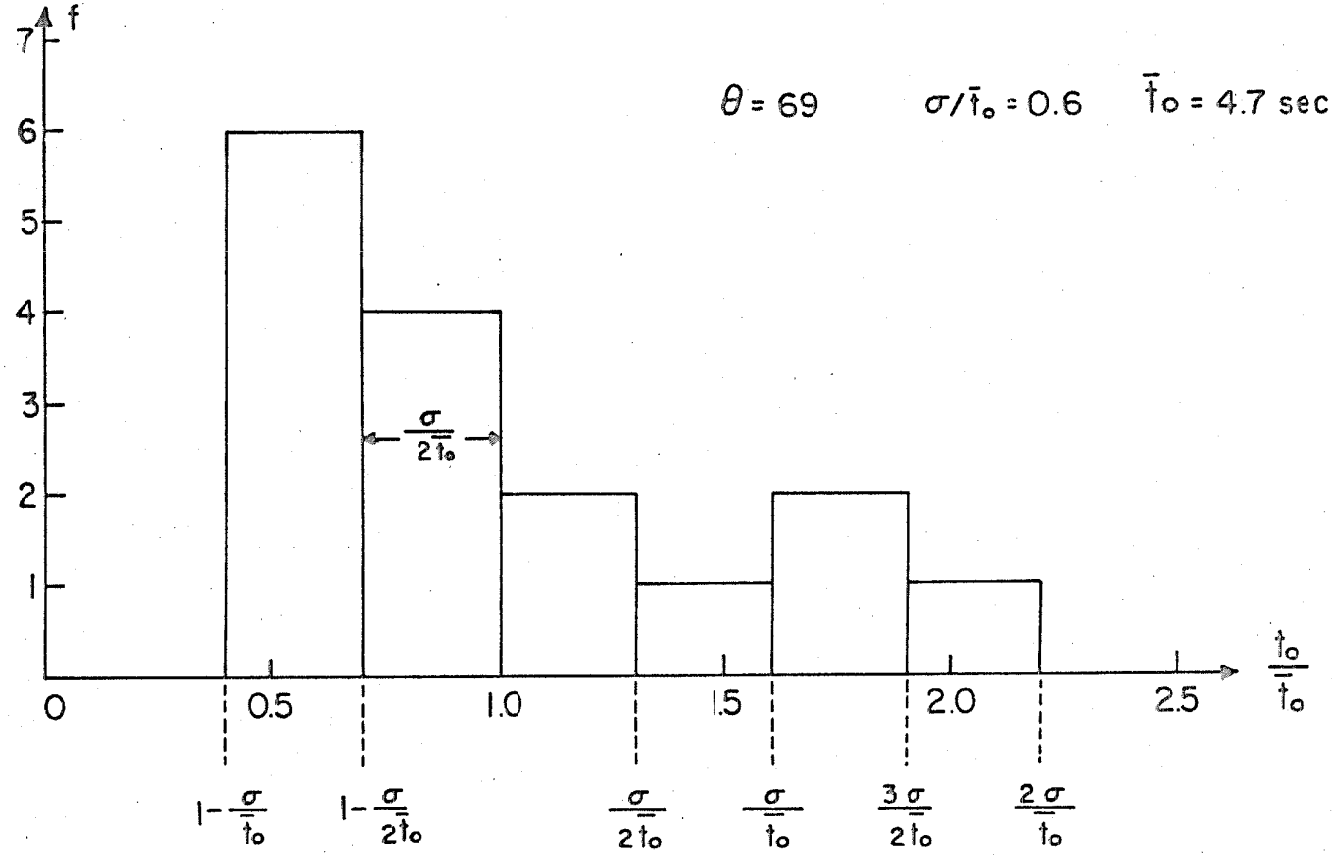


Figure 3.19. Normalized times of failure. Histogram.

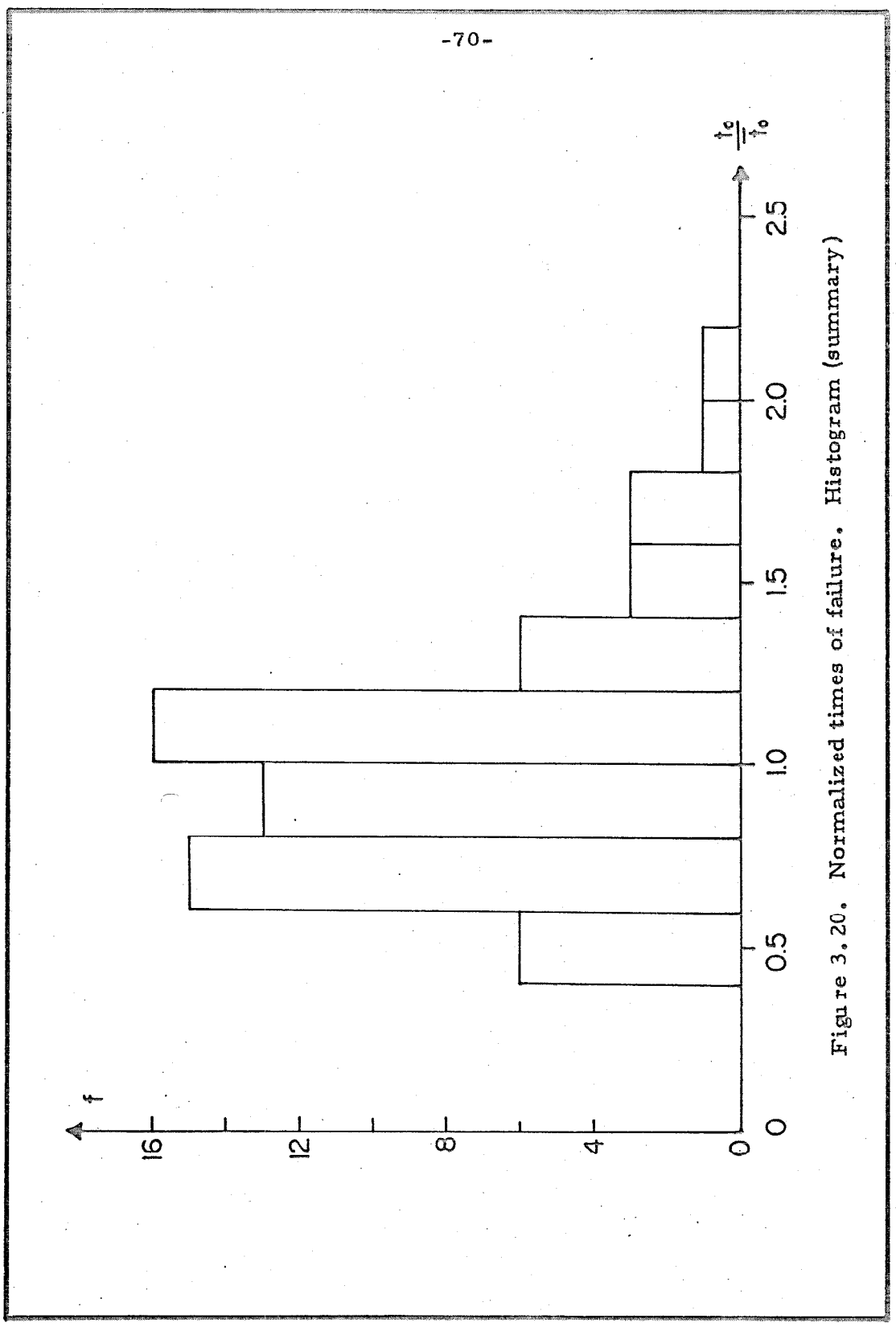


Figure 3.20. Normalized times of failure. Histogram (summary)

Using four artificial earthquakes, some extra calculations were done on the digital computer for one particular value of the period of the yielding structure, i.e., $T = 1.0$ sec. Those cases correspond to the values of $\theta = 90$ and $\theta = 17$ and the purpose of those computations was to define for a more extensive range the dependence of $\bar{t}_o$ on $\theta$ for fixed $\ell$, n and T.

From Figure 3.21 it is clear that the relation between $\bar{t}_o$ and $\theta$ is nearly hyperbolic. For each value of $\theta$, Figure 3.21 shows $\bar{t}_o$ and also the range of individual times of collapse.

In Figure 3.22 the dependence of $\bar{t}_o$ on $\theta$ is studied for the four values of T considered, and from the picture it seems that if $\bar{t}_o$ depends on the natural period of the structure then that influence is comparable to the statistical dispersion of the data. The empirical formula describing the data of Figure 3.22 will be discussed later in this chapter.

Assuming that the average time for collapse does not depend appreciably on the period of the structure, it is legitimate to consider all the data contained in Figure 3.22 as belonging to the same ensemble. New averages for the time of failure were computed across the ensemble of earthquakes for the several values of the natural period studied and the results are also plotted on Figure 3.22.

4) Effect of Story Height

The influence of the height, $\ell$, of the columns upon time to collapse was next studied. An investigation was made to see if changes in $\ell$ alone would produce significant variations in $\bar{t}_o$. The

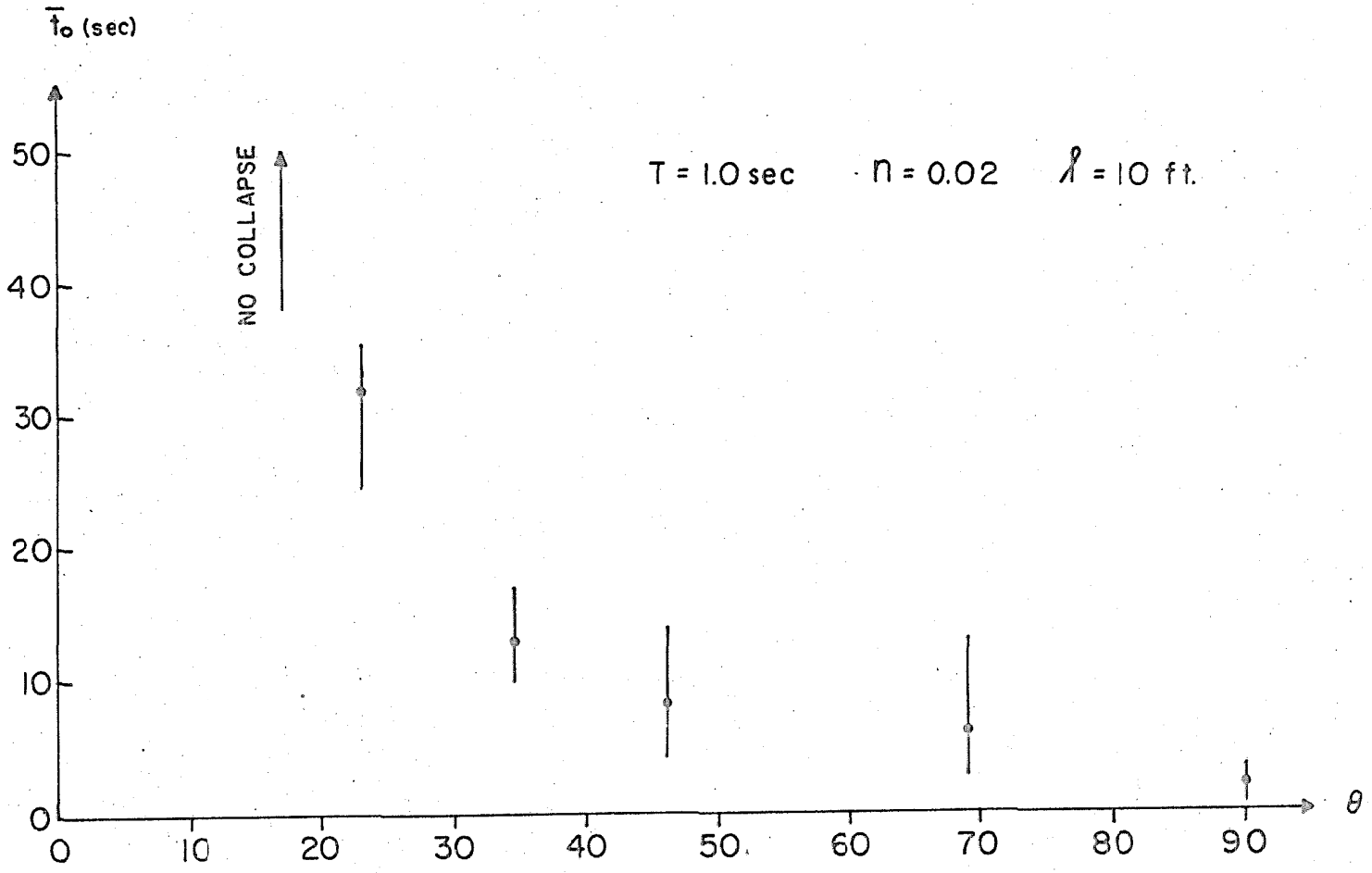


Figure 3.21. Times of failure for variable θ. Elasto-plastic structures.

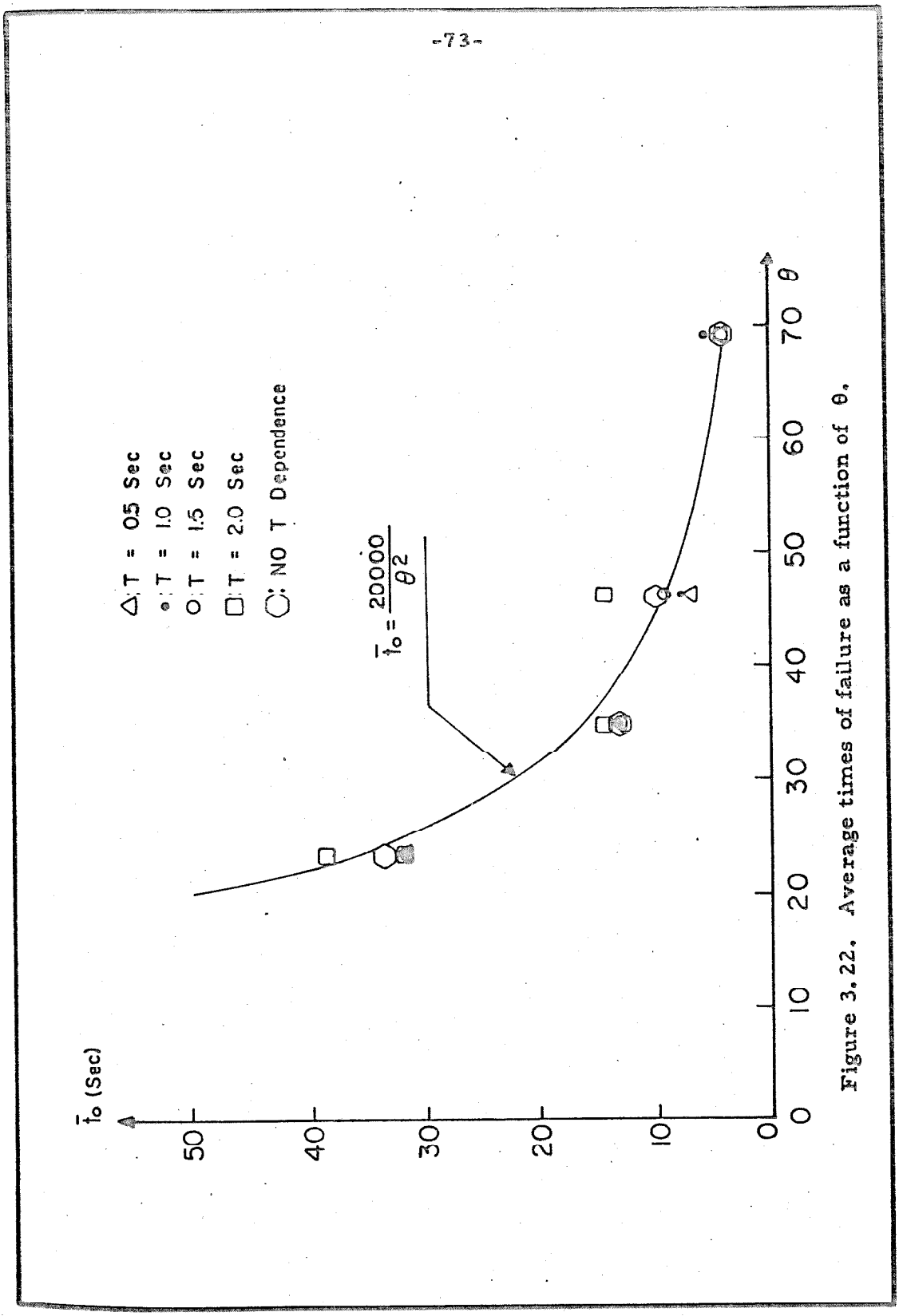


Figure 3.22. Average times of failure as a function of θ.

influence of $\ell$ was investigated for different natural periods of the structure.

For the purpose of this study values of 5, 10, 15, 20, 25 and 30 ft of the height of the columns $\ell$ were selected and a lateral yield level of $a_y/g = 0.05$ was used together with an intensity of the earthquakes given by $E = 2.3$. This gives a value of $\theta = 46$ for all cases considered in this particular analysis. Computations of the response to the ensemble of artificial earthquakes were done for six different values of $\ell$, and the average time of failure across the ensemble was determined for each of the cases. The results that were obtained show an almost perfect linear relationship between $\ell$ and the average time of failure $\bar{t}_o$. It should be noted that there was an appreciable dispersion of the values of $t_o$ for a particular artificial earthquake. The computations were done for structures whose periods of oscillation for small displacements were $T = 0.5$, 1.0, 1.5 and 2.0 seconds. The results, shown in Figure 3.23, indicate a linear relationship between average time of failure and the height of the columns when the rest of the parameters are not varied.

Since four values of $T$ were used for the selected range of $\ell$, it is possible to check if there is any significant dependence of $\bar{t}_o$ on $T$, when only $\ell$ is varied. All the data available for $\theta = 46$ were used to prepare Figure 3.23. From that figure it is concluded that if a clear influence upon the average time of failure could be assigned to the period of the structure, it is such that it is not more important than the fluctuations obtained with different

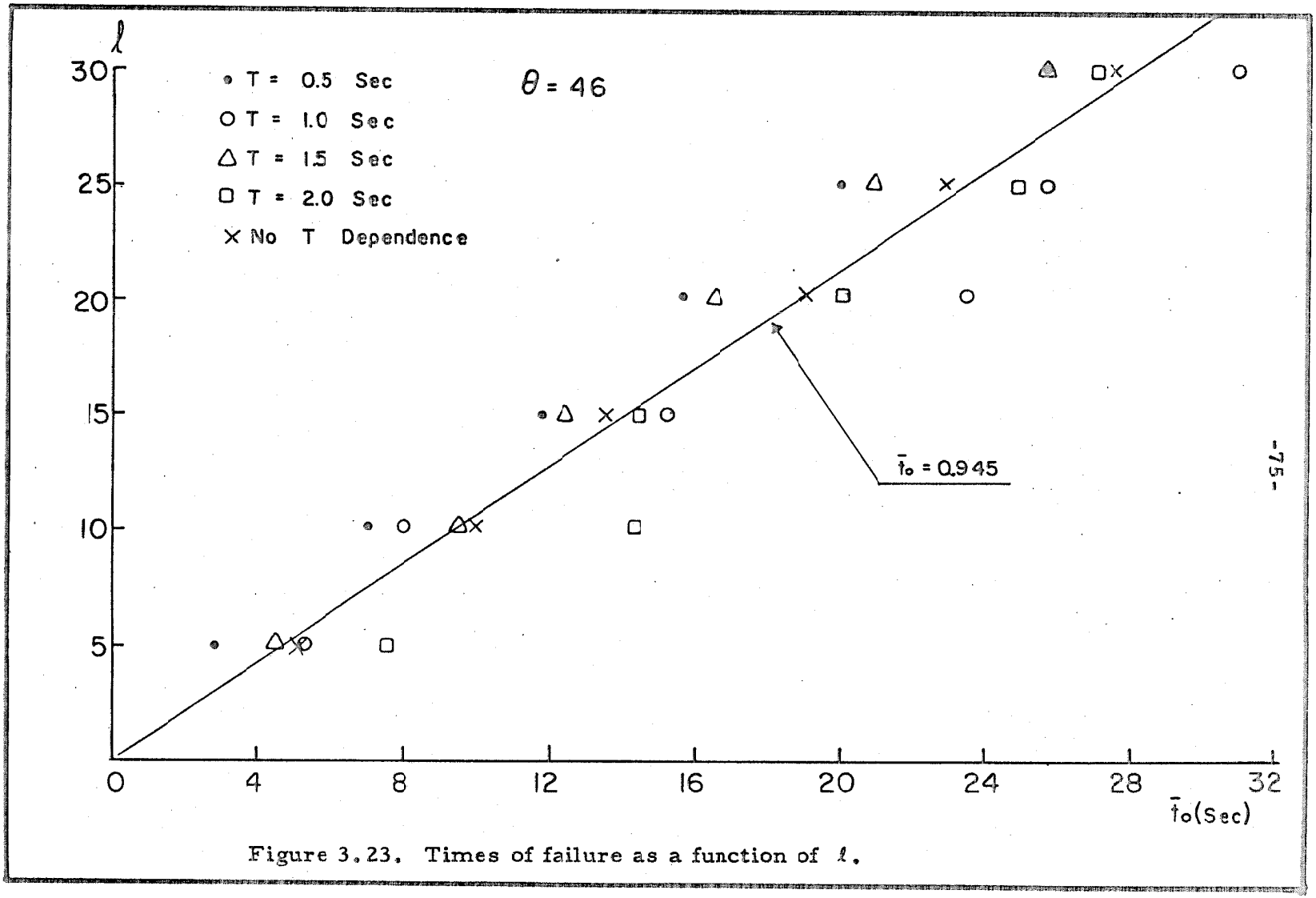


Figure 3.23. Times of failure as a function of $l$.

samples of the ensemble of artificial earthquakes, and it is thought that many more samples would have to be used before being able to determine the effects of T on the response statistics.

The trend of $\bar{t}_o$ toward zero as $\ell$ decreases, which is apparent in Figure 3.23 arises because the lateral displacement necessary to cause failure diminishes as $\ell$ decreases, and it takes a correspondingly smaller time for the displacement to reach this value.

5) Correlation Analysis

It is informative to do a study of correlations and regressions[46,47,48] in order to decide if the influence of T on the time of failure should be considered, or if it may be eliminated as being less important than the statistical dispersion of the data used for the analysis.

Based on the results obtained from the digital response, a statistical study was made with the objective of finding out if the variables $\ell$, T and $\theta$ are adequate to estimate the time of collapse for simple elasto-plastic structures. The relation that has been studied is of the form

$$\bar{t}_o = A\ell^{\alpha}\theta^{\beta}T^{\gamma} \qquad (3.9)$$

where A, $\alpha$, $\beta$, $\gamma$ are constants to be determined.

It is convenient to introduce the variables:

$X_1 = \log \bar{t}_o$ $\qquad$ $X_3 = \log \theta$

$X_2 = \log \ell$ $\qquad$ $X_4 = \log T$

that transform 3.9 into a linear relation.

First examined was the total correlation between $X_1$ and each one of the variables $X_2$, $X_3$ and $X_4$. The resulting correlation coefficients are:

$$\begin{aligned} r_{12} &= 0.656 \\ r_{13} &= -0.681 \\ r_{14} &= 0.118 \end{aligned} \qquad (3.10$$

From 3.10 it follows that $\ell$ and $\theta$ are suitable variables to estimate $\bar{t}_o$, and that the influence of $T(r_{14})$, is small.

It is informative to examine also the coefficients of partial correlation and of multiple correlation. They are given below and the formulas that define the three different types of correlation coefficients are presented in Appendix II.

$$\begin{aligned} r_{12.3} &= 0.964 & r_{12.4} &= -0.656 \\ r_{13.2} &= -0.966 & r_{13.4} &= -0.683 \\ r_{14.2} &= 0.121 & r_{14.3} &= 0.141 \\ r_{24.3} &= 0.042 & r_{34.2} &= -0.025 \\ r_{12.34} &= 0.968 & r_{13.24} &= -0.970 \\ r_{14.23} &= 0.375 & R_{1(23)} &= 0.981 \\ R_{1(24)} &= 0.662 & R_{1(34)} &= 0.688 \\ R_{1(234)} &= 0.983 \end{aligned} \qquad (3.11)$$

where $r_{ij.k}$ represents the degree of correlation between the two

variables x and y when the other variable z has an assigned value. In the same way $r_{xy.zv}$ is the correlation between x and y when the variables z and v are kept constant. $R_{x(yz)}$ denotes the coefficient of multiple correlation between x and the variables y and z and $R_{x(yzv)}$ represents the coefficient of multiple correlation between x and the variables y, z and v.

From 3.11 it is seen that the multiple correlation coefficients where the variables $X_2$ and $X_3$ appear simultaneously have a value that is practically unity, reinforcing the conclusion that $\ell$ and $\theta$ are suitable variables to estimate the average time for collapse of simple yielding structures.

A comparison of $r_{12.3}$ and $r_{12.34}$, $r_{13.2}$ and $r_{13.24}$, $r_{12.4}$ and $R_{1(24)}$ shows conclusively that the influence of T on the time of failure is (within the data obtained in the digitial response of elasto plastic structures) less important than the statistical dispersion of the data used for this work. Finally, a comparison of two multiple correlation coefficients $R_{1(23)}$ and $R_{1(234)}$, shows that nothing will be gained by trying to express the time of failure $\bar{t}_o$ as a function of $\ell$, $\theta$ and T; it suffices to use $\ell$ and $\theta$.

6) Regression Analysis

Considering the conclusions of the correlation study, it is of interest to find a regression of the type:

$$\bar{t}_o = B \ell^{\alpha_1} \theta^{\beta_1} \qquad (3.12)$$

Using all the information obtained from the digital response

calculations, presented in Appendix I, it is found that

$$\bar{t}_o = 1060 \frac{\ell^{0.98}}{\theta^{1.83}} \tag{3.13}$$

where $\ell$ is measured in ft, $\bar{t}_o$ in sec, and $\theta$ is dimensionless.

Observation of the regression presented above suggests a new relation that may be more suitable for the estimation of the time of collapse of simple elasto-plastic structures. The relation is:

$$\bar{t}_o = \frac{C\ell}{\theta^2} \tag{3.14}$$

The numerical determination of C gives:

$$\bar{t}_o = \frac{2000\ \ell}{\theta^2} \tag{3.15}$$

which is valid for values of $\ell$ in the range 5 to 30 ft and for $\theta$ ranging between 20 and 70. Figures 3.24 and 3.25 show the observed values of $\bar{t}_o$ on the abscissa and the computed values of $\bar{t}_o$ according to 3.13 and 3.15, respectively, on the ordinates. Observation of Figures 3.24 and 3.25 shows that relation 3.15 is adequate to estimate the average time of failure for the elasto-plastic structure.

Considering that the statistical study was made with only four different artificial earthquakes, and recalling that large dispersions were obtained when estimating average times of collapse, it seems of no advantage to use a relation more complicated than 3.15 to estimate $\bar{t}_o$.

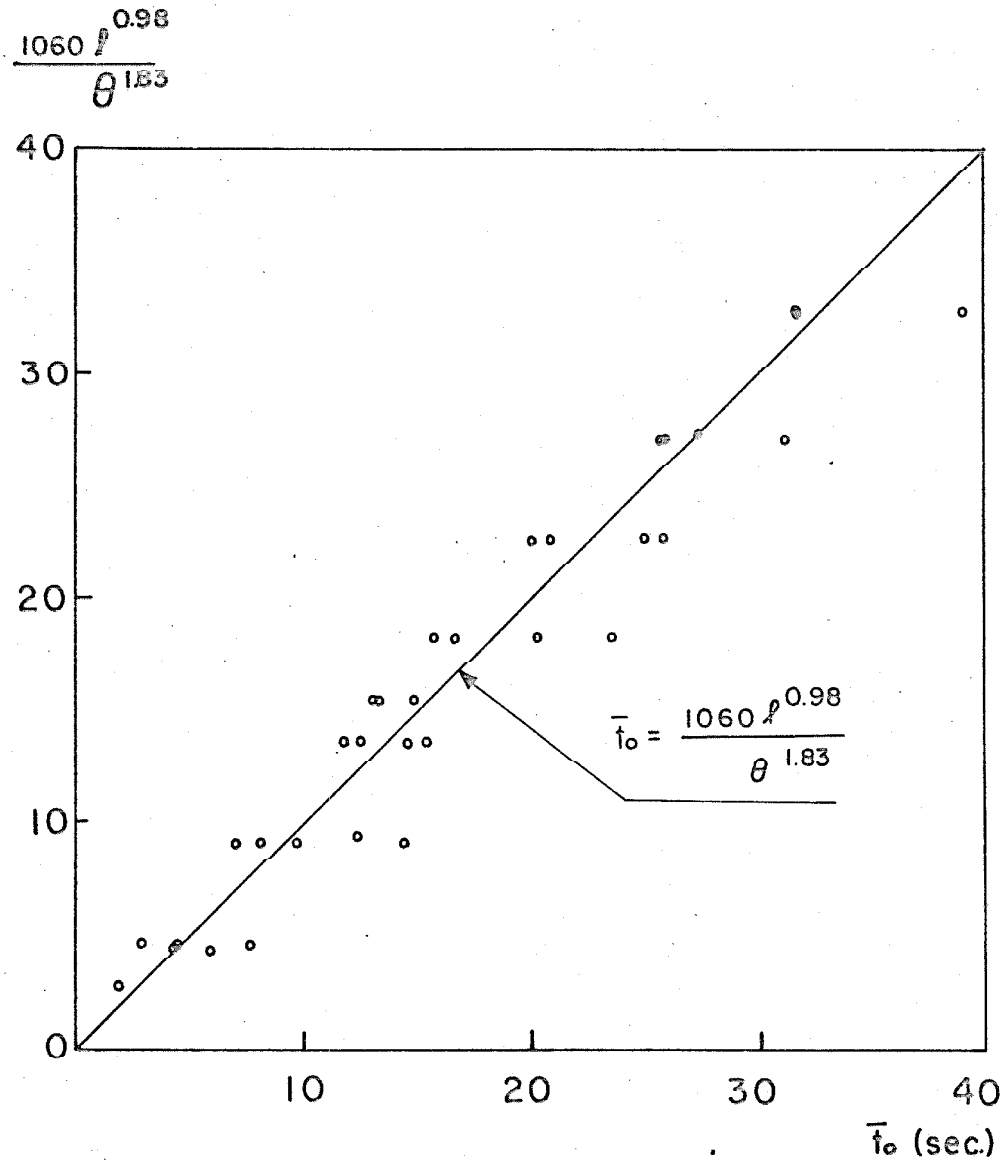


Figure 3.24. Times of failure for Elasto-plastic structures. Dispersion.

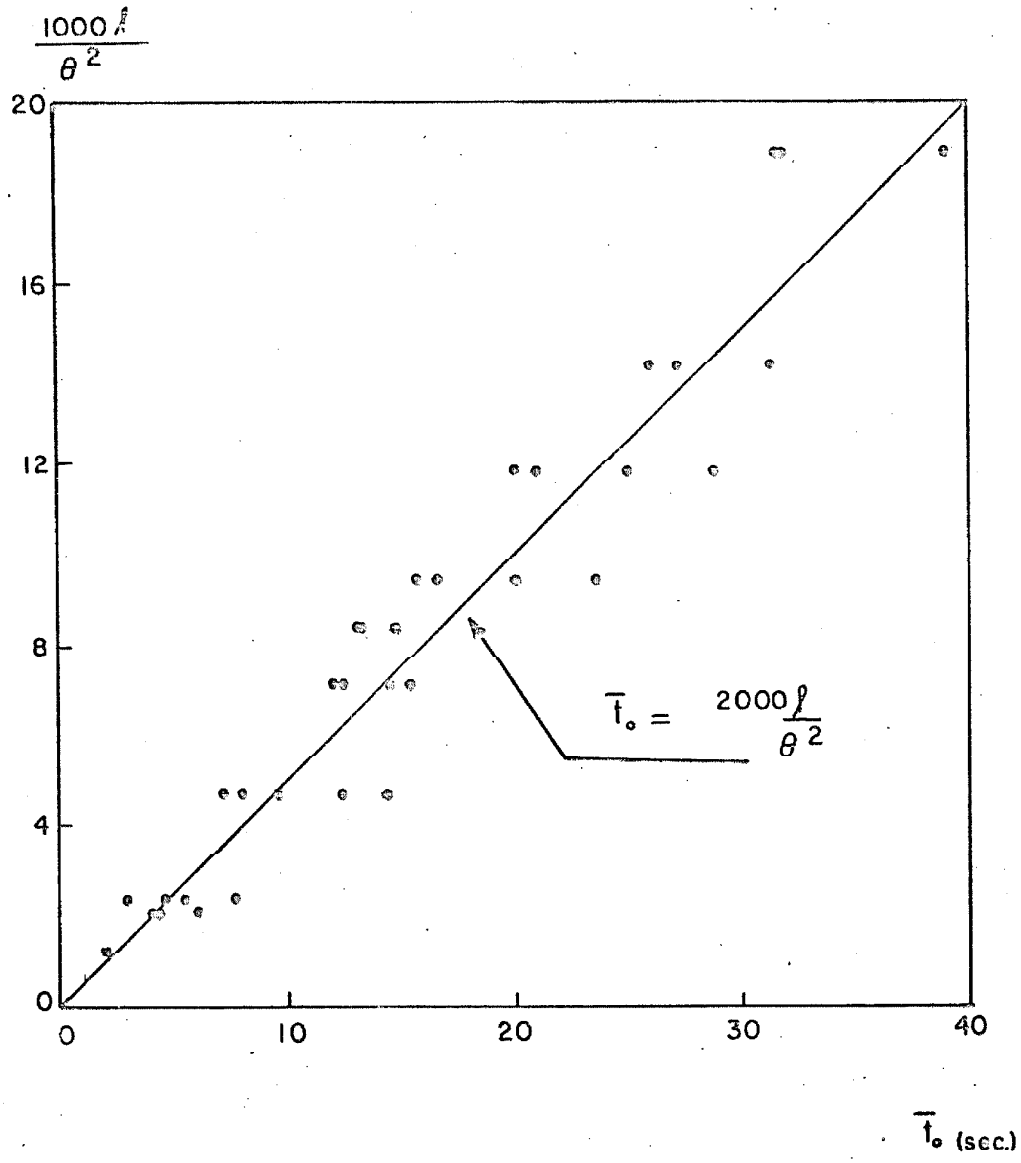


Figure 3.25. Times of failure for elasto-plastic structure. Dispersion.

For $\theta = 46$ relation 3.15 gives

$$\bar{t}_o = 0.945\, \ell \tag{3.16}$$

The straight line represented by 3.16 is plotted in Figure 3.23 and it is seen that 3.16 gives an adequate representation of the dependence of $\bar{t}_o$ on $\ell$ for this value of $\theta$.

Equation 3.15 is plotted also with the data for $\ell = 10$ ft shown in Figure 3.22. Again it is seen that Equation 3.15 adequately describes the results.

The results presented are pertinent to the response of simple elasto-plastic structures subjected to very short duration earthquakes. Examples of such earthquakes are the Port Hueneme earthquake of March 18, 1957[9] and the Parkfield earthquake of June 27, 1966, both of which have a very short strong part. The latter, for which an accelerogram is shown in Figure 3.26, did not produce major damage in spite of the large maximum acceleration.

To examine the effects of duration, consider a structure with a yield level $a_y/g$ and height $\ell$, and let $E_1$ be the intensity of the acceleration. Take first an earthquake 25 seconds long and assume that the structure collapses at the end of the earthquake. Using Equation 3.15, the minimum necessary intensity of the earthquake is

$$E_1 = \sqrt{80\ell\,(a_y/g)^2} \tag{3.17}$$

Consider next an earthquake like Parkfield with an intensity

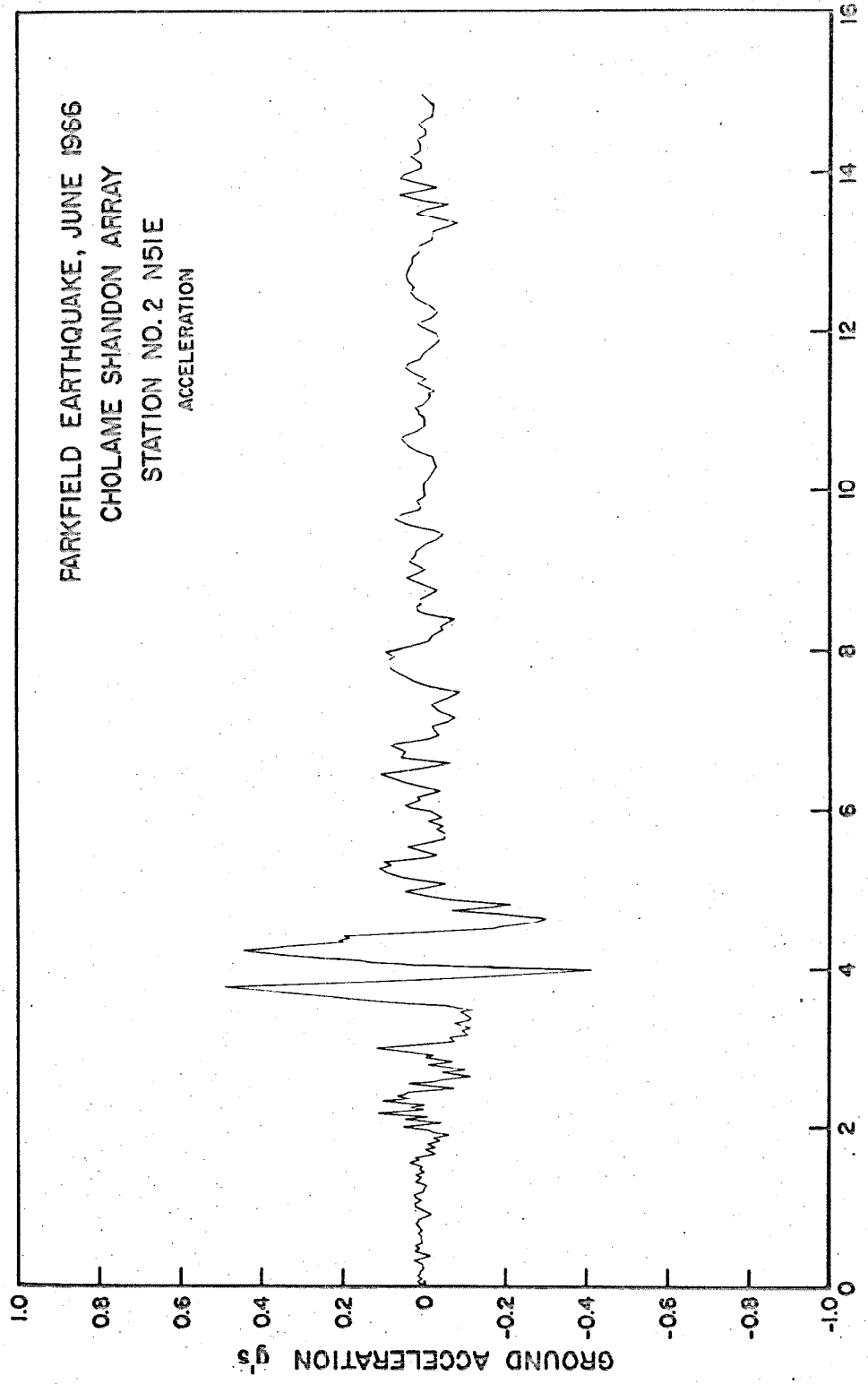
PARKFIELD EARTHQUAKE, JUNE 1966
CHOLAME SHANDON ARRAY
STATION NO. 2 N51E
ACCELERATION
GROUND ACCELERATION g's
1.0
0.8
0.6
0.4
0.2
0
-0.2
-0.4
-0.6
-0.8
-1.0
0
2
4
6
8
10
12
14
16
TIME, SECONDS

Figure 3.26

$E_2$ and assume that the structure collapses at the end of the strong part of the excitation, i.e., after one second. Applying Equation 3.15 again and comparing $E_2$ with $E_1$ shows that $E_2 = 5E_1$, indicating that it would take approximately 5 times the intensity of earthquake shaking to fail the elasto-plastic structure in one second, compared to the intensity causing failure in 25 sec.

Although real structures are usually not elasto-plastic, the above analysis does indicate that the intensity of shaking necessary for collapse is probably significantly larger for earthquakes of short duration.

# IV. SPECIAL EFFECTS IN YIELDING STRUCTURES

## A. Examination of Bilinear Hysteretic Structures. Analysis and Digital Response.

A bilinear hysteretic model often is a more realistic representation of real yielding structures than the elasto-plastic model and it is interesting to see how the results obtained for the elasto-plastic structure are modified when the yielding relation is changed to bilinear hysteretical. V. V. Bertero and G. J. Iragorry[49], J. P. Colaco[50], M. A. Sozen and N. N. Nielsen[51], M. Yamada and I. Nakaza[52] and E. P. Popov[53] have authored recent publications treating the bilinear properties.

Again, a complete analytical study of the transient response of hysteretic structures to earthquake-like excitation is not possible but numerical solutions of particular cases can be found and these provide means for understanding the response and its dependence on important parameters.

It is evident that for a given earthquake, the time of failure will increase when the slope of the second line in Figure 4.1 is increased, because then the restoring moment will be greater for the bilinear structure than for the elasto-plastic structure, and also the angle of static failure for the bilinear model will be greater. In this study calculations are made only for two specific structures so that the entire range of possible bilinear structures is not covered. It was decided to select the two structures having the following characteristics:

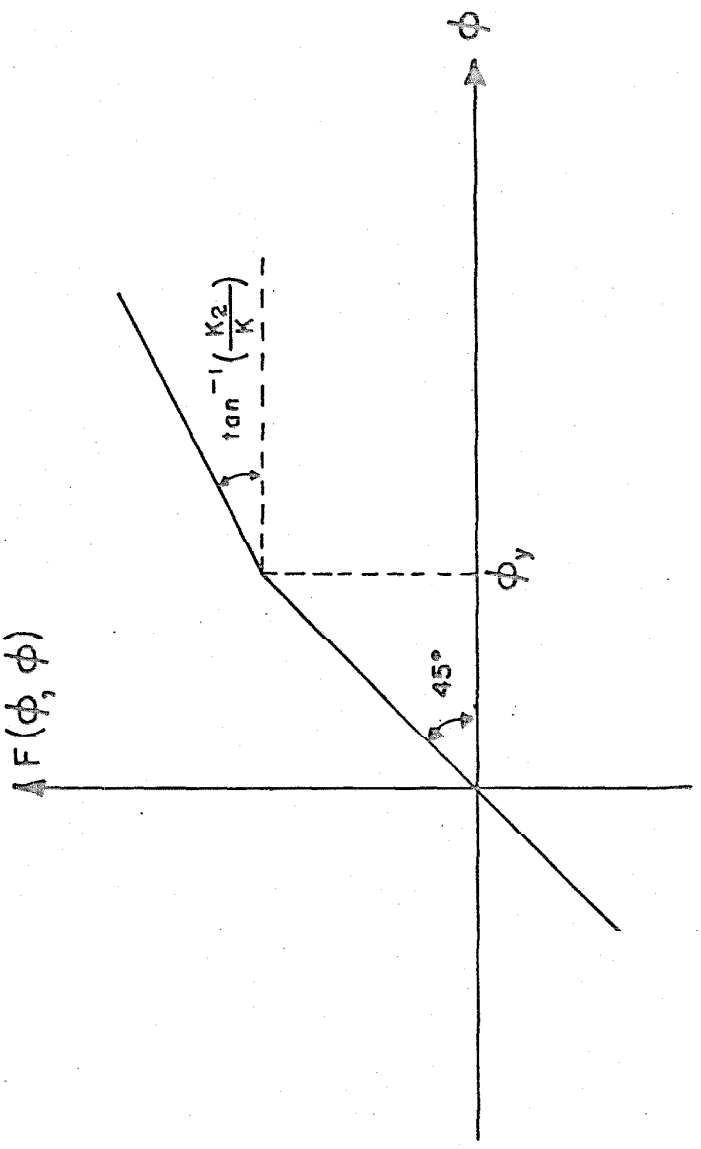


Figure 4.1. Bilinear hysteretic moment-angle relation.

Structure I

$$\begin{aligned} \ell &= 10 \text{ ft.} \\ n &= 0.02 \\ T &= 1.0 \text{ sec.} \\ a_y &= 0.05g \\ E &= 2.3 \\ \theta &= 46 \end{aligned} \tag{4.1}$$

Structure II

$$\begin{aligned} \ell &= 10 \text{ ft.} \\ n &= 0.02 \\ T &= 1.5 \text{ sec.} \\ a_y &= 0.1g \\ E &= 3.45 \\ \theta &= 34.5 \end{aligned} \tag{4.2}$$

These parameters are consistent with those considered in the previous chapter and are thought to lie in the range of realistic structures. The severity of the earthquakes selected (E) represent medium and strong earthquakes.

Computations of the response were made using equation 2.32 for the numerical integration, with $F(\phi,\dot{\phi})$ representing the bilinear hysteretic moment deflection relation. The method used (Runge-Kutta), and the size of the integration step were selected in the same way as in Chapter III. The equation that relates the yielding angle and the yield level for the bilinear model is the same as for the elasto-plastic one and is given by Equation 2.36. The angle of static failure, $\phi_s$, is derived from equilibrium considerations which give:

$$K\phi_y + K_2(\phi_s - \phi_y) = mg\ell \sin \phi_s \tag{4.3}$$

In this expression $\phi_y$ is the angle at which the stiffness changes

and K and $K_2$, the spring stiffnesses, are defined by equation 2.2 and Figure 4.1. Transformation of Equation 4.3 gives:

$$\frac{\phi_s}{\phi_y} = \frac{K_2 - K}{K_2 - mg\ell(\sin \phi_s/\phi_s)} \tag{4.4}$$

For $\sin \phi_s \approx \phi_s$, and defining $K_2/K = \alpha$, this equation can be written:

$$\frac{\phi_s}{\phi_y} = \frac{1 - \alpha}{\frac{mg\ell}{K} - \alpha} \tag{4.5}$$

When this equation is expressed in terms of the frequency parameter:

$$\omega_o^2 = \frac{K}{m\ell^2} - \frac{g}{\ell} \tag{4.6}$$

there is obtained:

$$\frac{\phi_s}{\phi_y} = \frac{(1 - \alpha)\left[1 + \frac{g}{\ell\omega_o^2}\right]}{\frac{g}{\ell\omega_o^2} - \alpha\left[1 + \frac{g}{\ell\omega_o^2}\right]} \tag{4.7}$$

It is of interest to note that for small displacements, $\sin \phi_s \approx \phi_s$, there is a singular case for which gravity does not tend to make $\phi$ increase beyond $\phi_s$. This is when the denominators in the foregoing equations are zero. In this case, the effect of the spring $K_2$ just balances the effect of gravity, that is:

$$K_{2c} = mg\ell \tag{4.8}$$

Calculated Responses

The responses of the two bilinear structures specified by Equations 4.1 and 4.2 were calculated for each of four artificial earthquakes. The cases that were computed are listed in Table VI. Figure 4.2 shows the average times to failure, $\bar{t}_o$. The abscissa is the ratio between the time of failure for the elasto-plastic structure and for the bilinear structure with the same lower slope. The ordinate is the ratio between $K_2$ and $K_{2c}$, i.e., $K_2/mg\ell$ and the curves representing different periods are expected to be bounded by the line $K_2/mg\ell = 1$. The most important feature of the results is the appreciable increase in the time of collapse when the second slope $K_2$ increases from zero towards $K_{2c}$.

With the limited computational data available it is not possible to determine the dependence, if any, of $\bar{t}_o/\bar{t}_{o_{el.pl.}}$ upon the period $T = 2\pi/\omega_o$. Since no such dependence was indicated for the elasto-plastic case it will also be assumed here that there is no such dependence in the data used to plot Figure 4.2. Under these assumptions, a least square fit of the data was performed and the following expression was obtained:

$$\frac{\bar{t}_o}{\bar{t}_{o_{\text{elast-plast}}}} = \frac{1}{1 - \left(\frac{K_2}{mg\ell}\right)^{0.8}} \tag{4.9}$$

It should be noted that large dispersion about the average time of failure were obtained for the bilinear model when the ensemble of artificial earthquakes were used. The size of the

TABLE VI-a. Summary of Bilinear Response Calculations for $T = 1.0$ sec; $\ell = 10$ ft; $a_y/g = 0.05$; $E = 2.3$; $\phi_y = 0.0041$ rad

| Case | Earthuuake | $\alpha = \frac{K_2}{K}$ | $\phi_s$ (rad) | $t_o$ (sec) | $\frac{K_2}{mg\ell}$ |
|---|---|---|---|---|---|
| 1 | (1+2) | 0.01 | 0.0615 | 5.65 | |
| 2 | (3+4) | 0.01 | 0.0615 | 5.92 | 0.132 |
| 3 | (5+6) | 0.01 | 0.0615 | 10.41 | |
| 4 | (7+8) | 0.01 | 0.0615 | 17.22 | |
| 5 | (1+2) | 0.02 | 0.0715 | 12.75 | |
| 6 | (3+4) | 0.02 | 0.0715 | 7.74 | 0.265 |
| 7 | (5+6) | 0.02 | 0.0715 | 12.15 | |
| 8 | (7+8) | 0.02 | 0.0715 | 20.05 | |
| 9 | (1+2) | 0.025 | 0.0774 | 15.72 | |
| 10 | (3+4) | 0.025 | 0.0774 | 9.64 | 0.331 |
| 11 | (5+6) | 0.025 | 0.0774 | 12.50 | |
| 12 | (7+8) | 0.025 | 0.0774 | 21.84 | |
| 13 | (1+2) | 0.03 | 0.0860 | 21.62 | |
| 14 | (3+4) | 0.03 | 0.0860 | 9.95 | 0.397 |
| 15 | (5+6) | 0.03 | 0.0860 | 12.92 | |
| 16 | (7+8) | 0.03 | 0.0860 | 24.27 | |
| 17 | (1+2) | 0.04 | 0.1090 | 32.88 | |
| 18 | (3+4) | 0.04 | 0.1090 | 11.82 | 0.530 |
| 19 | (5+6) | 0.04 | 0.1090 | 16.00 | |
| 20 | (7+8) | 0.04 | 0.1090 | 31.17 | |
| 21 | (1+2) | 0.05 | 0.1500 | 37.80 | |
| 22 | (3+4) | 0.05 | 0.1500 | 19.00 | 0.662 |
| 23 | (5+6) | 0.05 | 0.1500 | 26.50 | |
| 24 | (7+8) | 0.05 | 0.1500 | 41.00 | |

TABLE VI-b. Summary of Bilinear Response Calculations for $T = 1.5$ sec; $\ell = 10$ ft; $a_y/g = 0.10$; $E = 3.45$; $\phi_y = 0.0184$ rad

| Case | Earthquake | $\alpha = \frac{K_2}{K}$ | $\phi_s$ (rad) | $t_o$ (sec) | $\frac{K_2}{mg\ell}$ |
|---|---|---|---|---|---|
| 25 | (1+2) | 0.01 | 0.1256 | 19.97 | |
| 26 | (3+4) | 0.01 | 0.1256 | 13.03 | 0.065 |
| 27 | (5+6) | 0.01 | 0.1256 | 10.47 | |
| 28 | (7+8) | 0.01 | 0.1256 | 14.65 | |
| 29 | (1+2) | 0.02 | 0.1330 | 24.02 | |
| 30 | (3+4) | 0.02 | 0.1330 | 13.16 | 0.129 |
| 31 | (5+6) | 0.02 | 0.1330 | 10.67 | |
| 32 | (7+8) | 0.02 | 0.1330 | 14.80 | |
| 33 | (1+2) | 0.05 | 0.1660 | 35.95 | |
| 34 | (3+4) | 0.05 | 0.1660 | 15.85 | 0.323 |
| 35 | (5+6) | 0.05 | 0.1660 | 12.50 | |
| 36 | (7+8) | 0.05 | 0.1660 | 20.50 | |
| 37 | (1+2) | 0.075 | 0.2130 | 40.22 | |
| 38 | (3+4) | 0.075 | 0.2130 | 23.17 | 0.484 |
| 39 | (5+6) | 0.075 | 0.2130 | 15.90 | |
| 40 | (7+8) | 0.075 | 0.2130 | 23.43 | |
| 41 | (1+2) | 0.10 | 0.3020 | 56.37 | |
| 42 | (3+4) | 0.10 | 0.3020 | 30.95 | 0.645 |
| 43 | (5+6) | 0.10 | 0.3020 | 39.80 | |
| 44 | (7+8) | 0.10 | 0.3020 | 41.32 | |

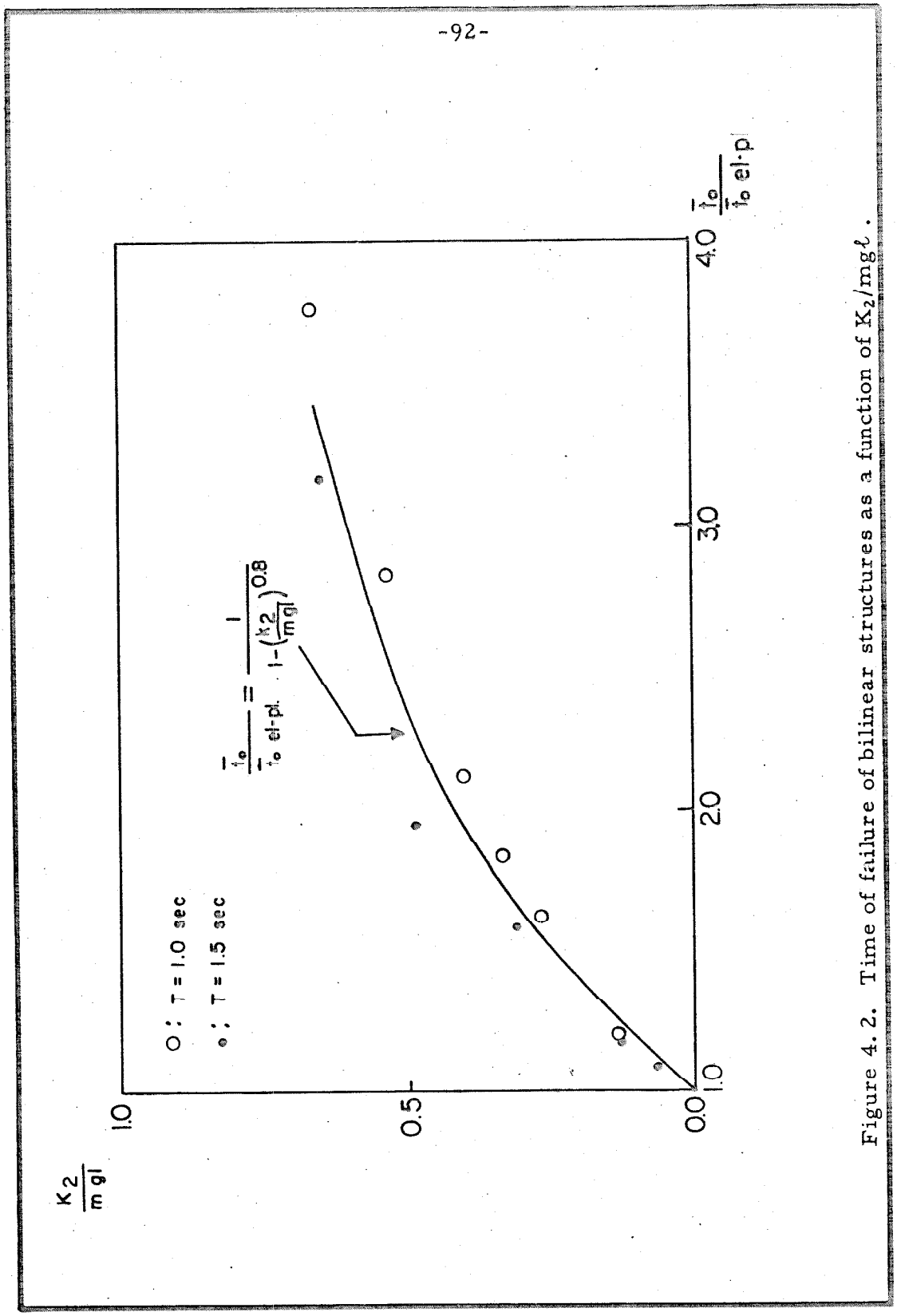


Figure 4.2. Time of failure of bilinear structures as a function of $K_2/mg\ell$.

dispersion appears to be approximately the same as for the elasto-plastic model.

Figures 4.3, 4.4, 4.5 and 4.6 show the time history of the response of structure I, defined by Equation 4.2 for the elasto-plastic case, and for $K_2/K = 0.02$, 0.05 and 0.075 respectively, when earthquake (3 + 4) was used. For this structure $K_{2c} = 0.075\,K$. It is seen that for the case when $K_2 = K_{2c}$ the structure does not collapse and the response shows two predominant periods that can be associated with the first and second slopes in the moment-angle relation under consideration.

On the basis of Figure 4.2 and relation 4.9 it can be concluded that the time of failure of a bilinear hysteretic structure can be strongly influenced by the second slope, $K_2$, of the moment-angle relation. This agrees with experimental results for stationary random response of bilinear hysteretic systems. In such systems, Lutes[54] found that the low-frequency power spectral density of the response was governed by the smaller of the two slopes of the restoring moment curve.

When Equation 4.9 is combined with Equation 3.15, there is obtained, for $K_2 < mg\ell$:

$$\bar{t}_o = \frac{2000\,\ell}{\left(\frac{E}{a_y/g}\right)^2 \left\{1 - \left(\frac{K_2}{mg\ell}\right)^{0.8}\right\}} \qquad (4.10)$$

This equation gives the mean time to failure of a bilinear system subjected to earthquake shaking of intensity E. The yield

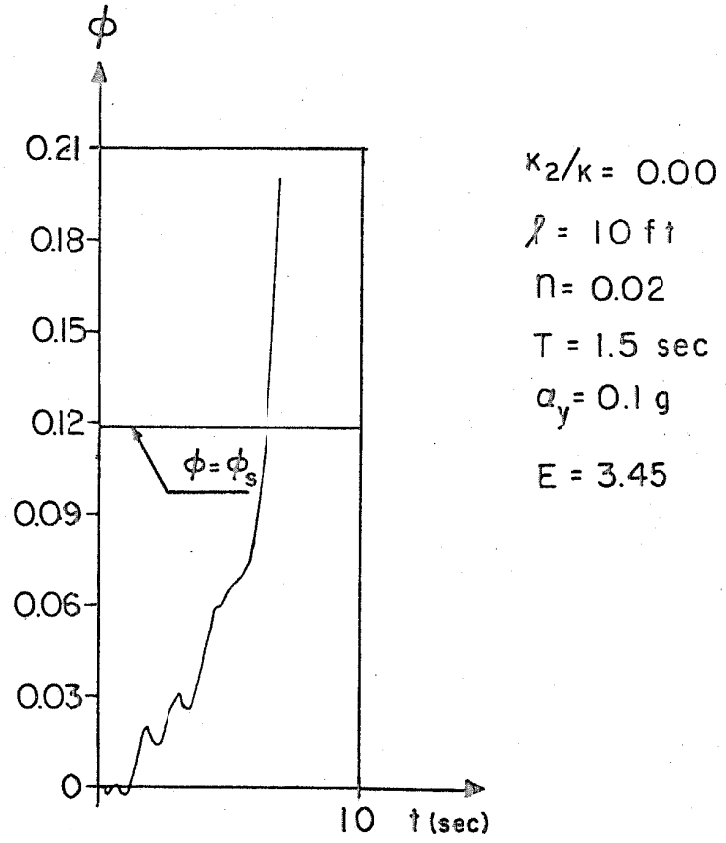


Figure 4.3. Response of structure I to earthquake (3+4).

$\kappa_2/\kappa = 0.02$

$\ell = 10$ ft

$n = 0.02$

$T = 1.5$ sec

$a_y = 0.1\,g$

$E = 3.45$

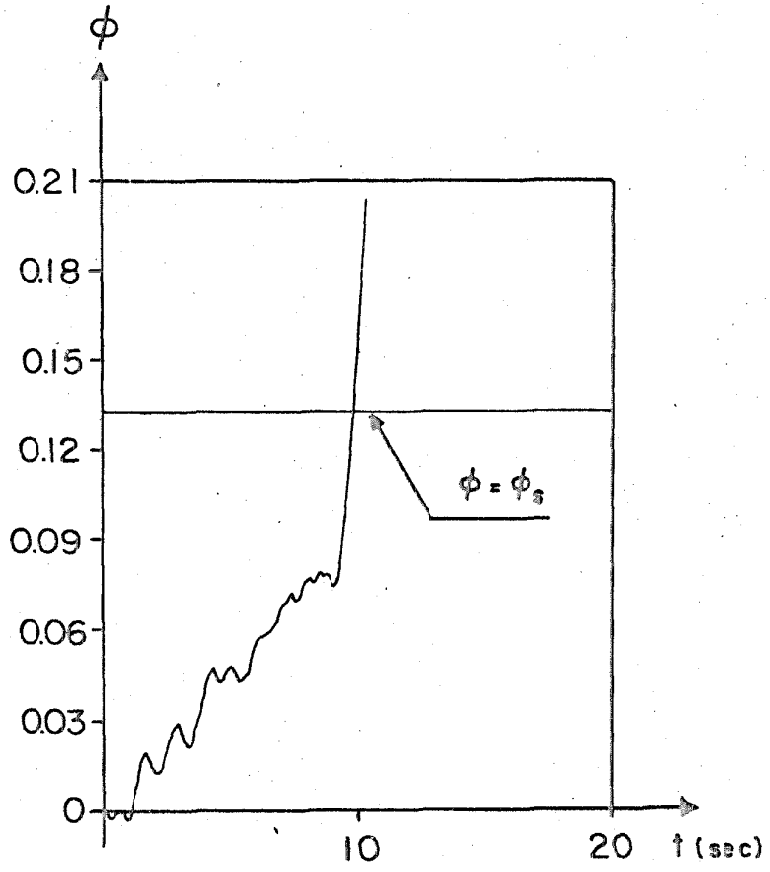


Figure 4.4. Response of structure I to earthquake (3+4).

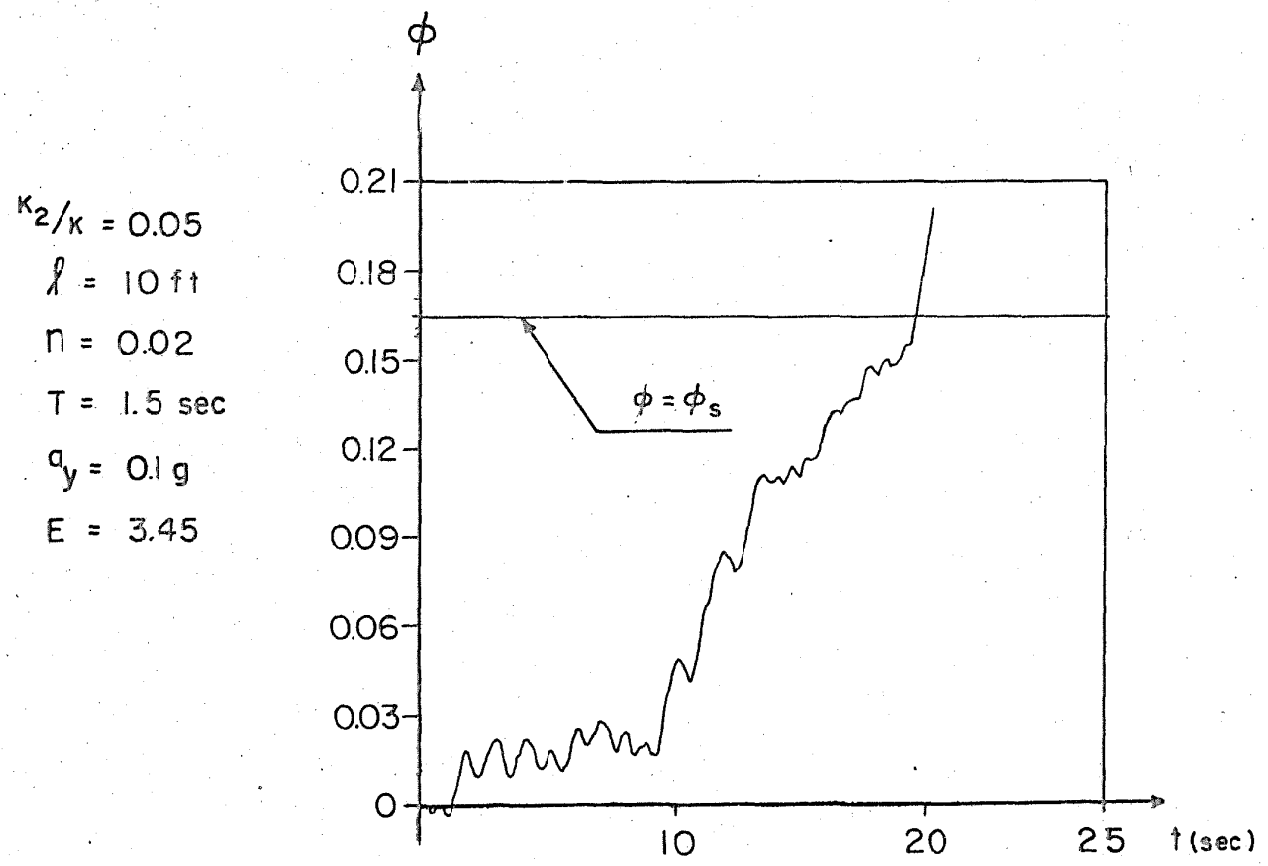


Figure 4.5. Response of structure I to earthquake (3+4).

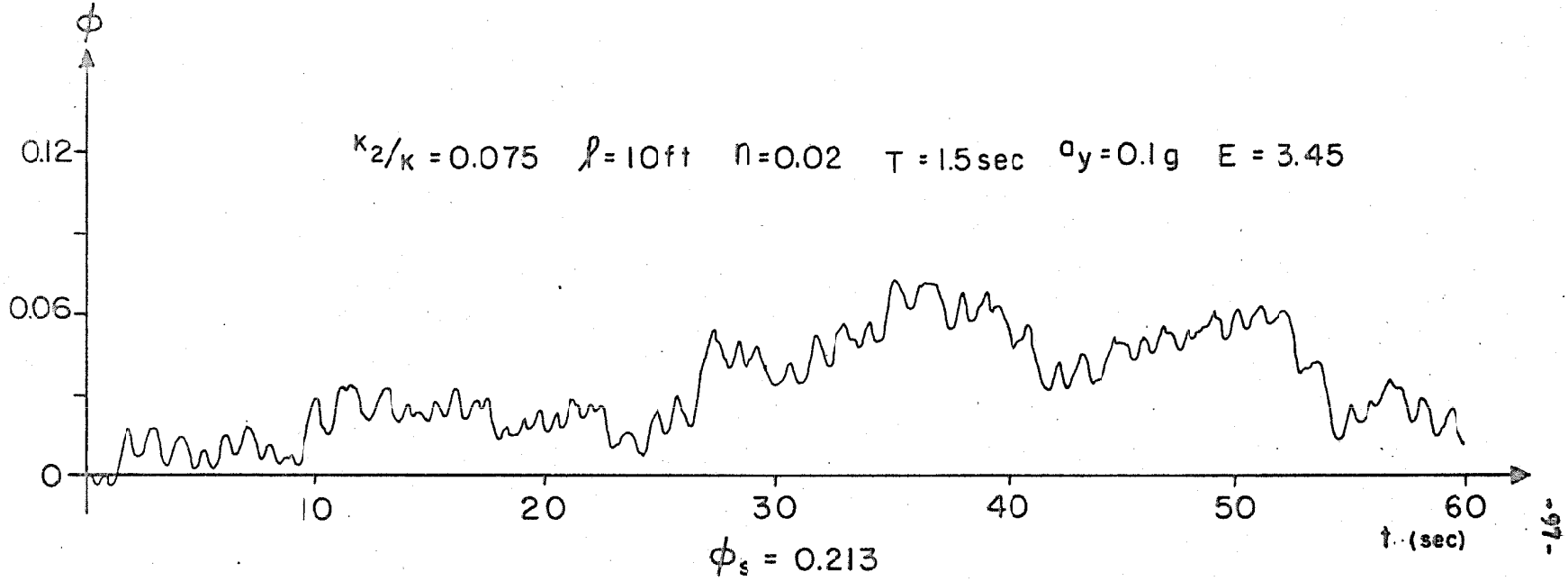


Figure 4.6. Response of structure I to earthquake (3+4).

level, as specified by $a_y/g$, corresponds to the knee of the bilinear curve. It should be noted that this equation gives the mean time to failure and that it does not predict the actual failure time. Because of the statistical fluctuations in the calculated $t_o$ for different artificial earthquakes, Equation 4.10 is informative as to the influence of the properties of the structure and the strength of the earthquake, but gives only an approximate idea of the actual failure time.

B. Response and Failure of Elasto-plastic Structures Subjected to Real Earthquakes

It has been shown[23,24] that when the effect of gravity is ignored, collapse of the structure not being the subject of consideration, the ensemble of artificial earthquakes used in this study is suitable for earthquake engineering research. Having now the results for artificial earthquake excitation with the effect of gravity included, it is of interest to examine similar calculations when real earthquakes are used, to see if the results are consistent with those obtained using the artificial earthquakes. Three recorded earthquake ground accelerations were used for this purpose:

(1) The N.S. horizontal component of the 1940 El Centro earthquake, which will be called the El Centro earthquake.

(2) The S.10E. horizontal component of the 1949 Olympia earthquake (Olympia earthquake).

(3) The N.21E. horizontal component of the 1952 Taft earthquake (Taft earthquake).

Some of the principal characteristics of these earthquakes are given in Table V in Chapter III. In Figures 4.7, 4.8 and 4.9 the accelerograms for the three real earthquakes are presented in order to provide a visual comparison with similar graphs of artificial earthquakes.

What makes the problem under investigation more difficult is the fact that when the time of failure is studied, the relative position and duration of the strong part of the earthquake become of primary importance, in contrast to the problem of linear response in which the maximum response, i.e., the spectrum value, is more directly dependent on just the intensity of the shaking.

Recorded earthquake ground motions can be classified into three types:

(a) The initial portion of the record is of relatively short duration and is very strong, and the following portion decays quite rapidly. Examples of such earthquakes are those recorded at Vernon, March 10, 1933, and October 2, 1933, Helena, Montana, October 31, 1935, Ferndale, September 11, 1938, and Santa Barbara, June 30, 1941.

(b) The initial portion of the accelerogram has large amplitudes and is of relatively long duration, the following portion being of small amplitude. Examples of such earthquakes are: the one at Los Angeles Subway Terminal, March 10, 1933, El Centro, December 30, 1934, and May 18, 1940, Olympia, April 13, 1949, Seattle, April 13, 1949, and Taft, July 12, 1952.

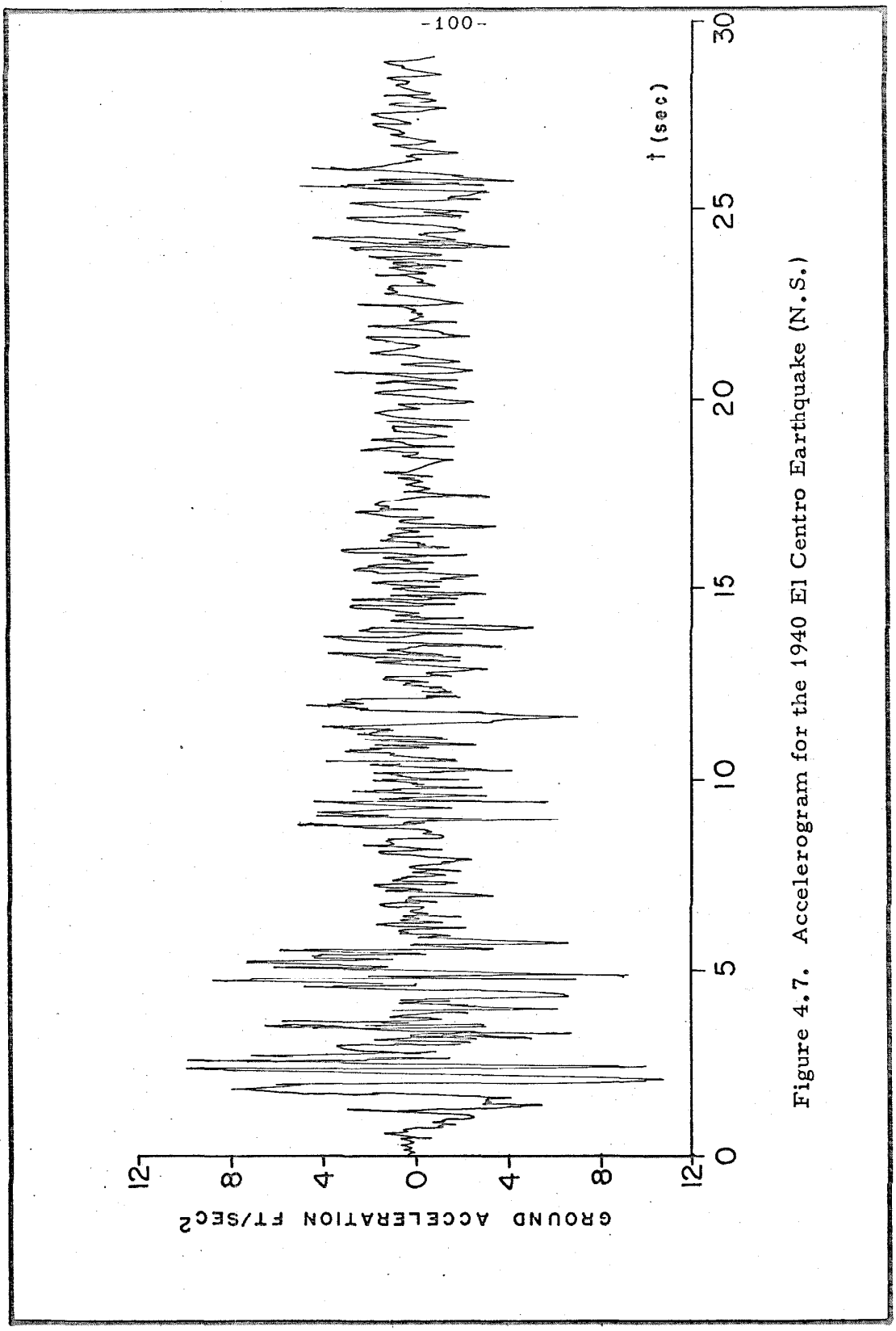


Figure 4.7. Accelerogram for the 1940 El Centro Earthquake (N.S.)

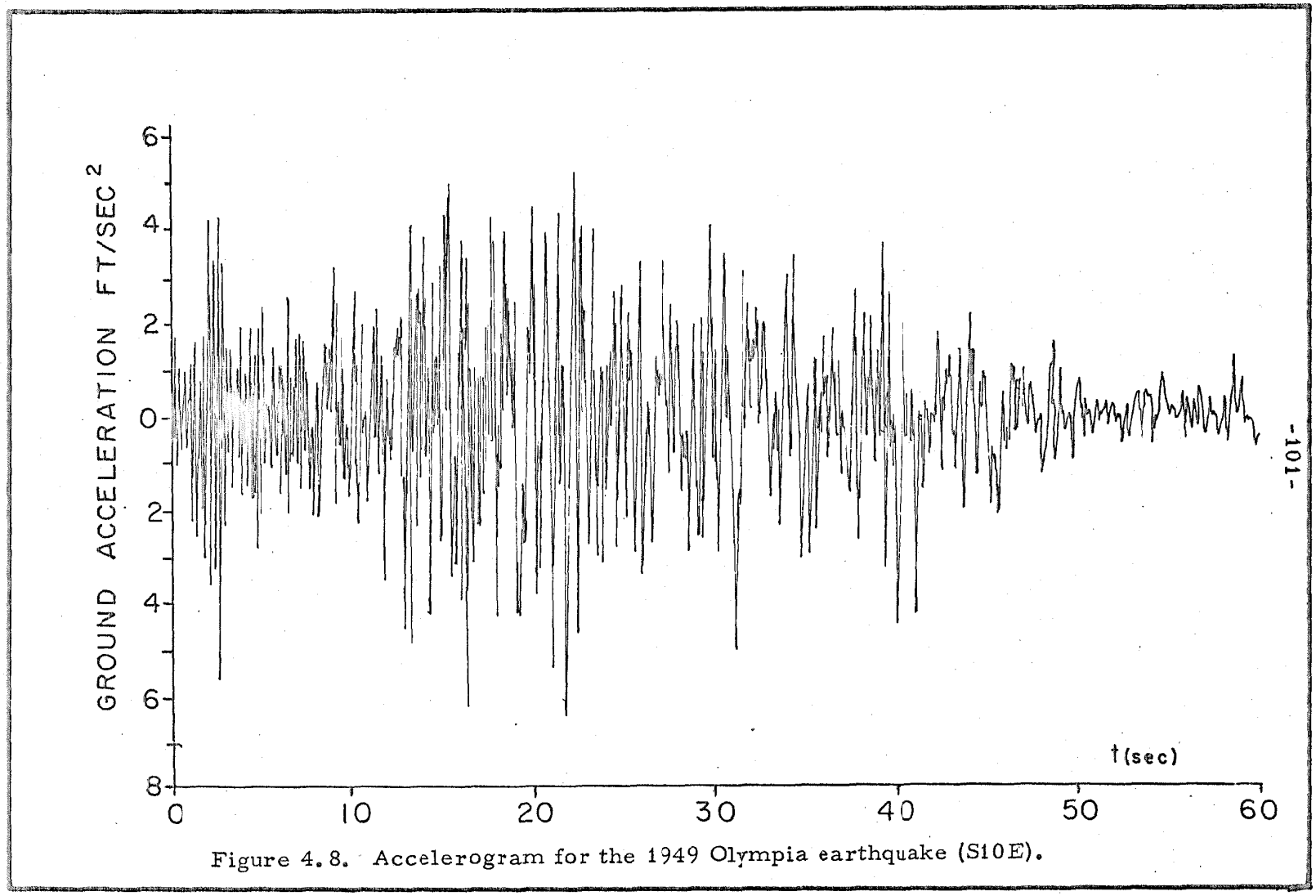


Figure 4.8. Accelerogram for the 1949 Olympia earthquake (S10E).

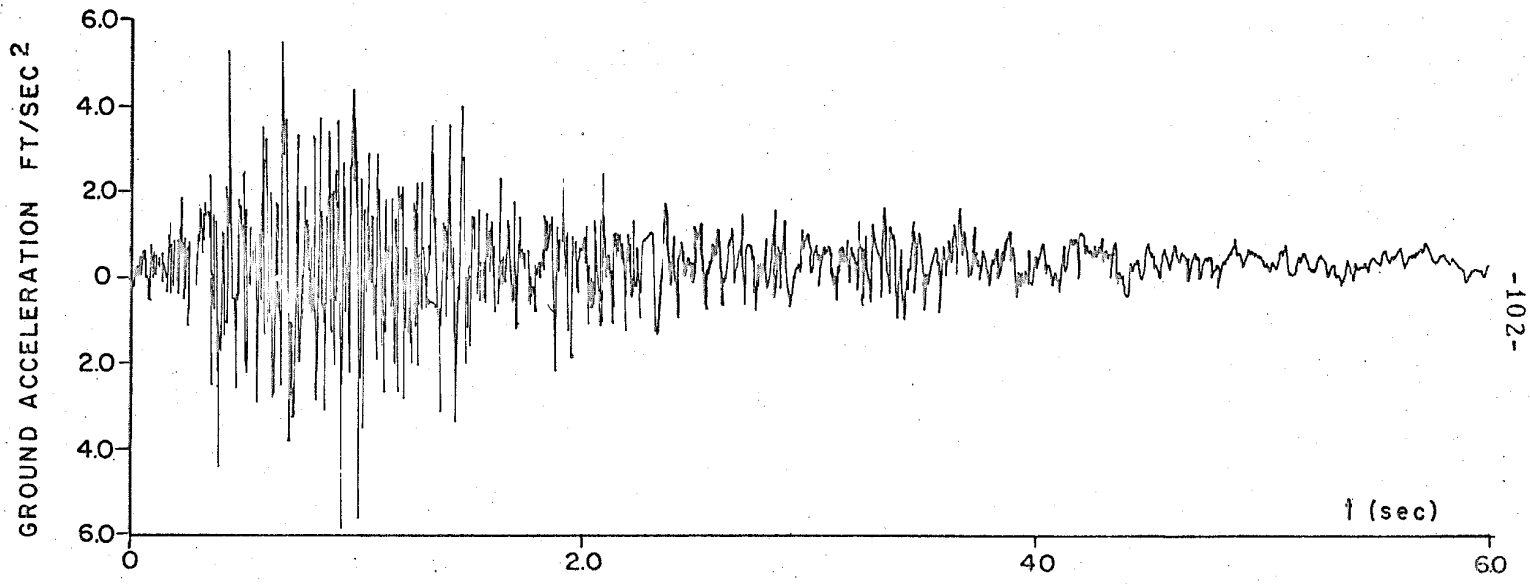


Figure 4.9. Accelerogram for the 1952 Taft earthquake (N 21 E).

(c) A considerable part of the record at the beginning has small amplitudes compared with the middle part, which has large amplitudes. The middle part is short, decreasing to the final part, which has small amplitudes. Examples of such earthquakes are: the one for Ferndale, October 3, 1941, and the one for Hollister, March 9, 1949.

All of the earthquakes just mentioned are presented with their respective spectra in reference 9. For the purposes of this study three earthquakes of group (b) were selected because they were the strongest recorded in the U.S.A. and probably typify excitations likely to produce collapse of real structures. They are also nearest to representing a stationary process and, hence, should compare better with artificial earthquakes than will types (a) and (c).

A typical one degree of freedom elasto-plastic structure was selected for the purpose of comparing the results of Chapter III with those obtained when real earthquakes are used. The structure is defined by the following constants:

$$a_y = 0.05g$$
$$n = 0.02 \qquad (4.11)$$
$$\ell = 10 \text{ ft}$$

Two different values for the period of the structure were considered, T = 0.5 and 1.0 seconds. The structure was subjected to the ensemble of four 60 sec. artificial earthquakes with a value E = 3.16

(r.m.s. = 2.2 ft/sec$^2$; $\theta$ = 63.2).

In Table VII the results are given for the three real earthquakes and Table VIII shows the corresponding results for the ensemble of artificial earthquakes.

TABLE VII. Results for Real Earthquakes

| | r.m.s. at failure | | r.m.s. | $t_o$ (sec) | | |
|---|---|---|---|---|---|---|
| Earthquake | T = 0.5 | T = 1.0 | ref. 23 | T = 0.5 | T = 1.0 | Average |
| El Centro | 3.65 | 3.80 | 2.20 | 3.26 | 4.44 | 3.8 |
| Taft | 1.05 | 1.40 | 1.42 | 32.8 | 13.8 | 23.3 |
| Olympia | 1.67 | 1.57 | 1.57 | 11.8 | 11.9 | 11.8 |

TABLE VIII. Results for Artificial Earthquakes (r.m.s. = 2.2 ft/sec$^2$)

| Artificial | $t_o$ (sec) | |
|---|---|---|
| Earthquake | T = 0.5 sec | T = 1.0 sec |
| (1+2) | 2.90 | 2.67 |
| (3+4) | 7.85 | 3.69 |
| (5+6) | 4.67 | 6.02 |
| (7+8) | 3.32 | 24.80 |

Average of 8 cases, $\bar{t}_o$ = 7.0 sec.

Assuming that an extrapolation is permissible, and recalling that the mean time of failure was found to be inversely

proportional to the square of the severity of the earthquake, as shown in Equation 3.15, it is possible to estimate the time of failure for the structure defined in 4.11 for the three real earthquakes considered. The results are shown in Table IX together with the observed times of collapse. The r.m.s. used to calculate $\theta$ is taken from column 3 of Table VII.

TABLE IX. Computed and Predicted Times of Failure

| Earthquake | $t_o$ (sec) | $\bar{t}_o$ (Equation 3.15) |
|---|---|---|
| El Centro | 3.8 | 5.0 |
| Taft | 23.3 | 12.0 |
| Olympia | 11.8 | 9.8 |

The discrepancies between observed and predicted values in Table IX, though large, are not inconsistent with the spread in values in Table VIII. The predicted value of $\bar{t}_o$ for artificial earthquakes with an r.m.s. of 2.20 is 5.0 sec, from Equation 3.15, which is to be compared with the calculated average of 7.0, and the individual values in Table VIII.

Considering the data in these three tables, it appears that the statistics are roughly comparable for the artificial and real earthquake excitation; no significant differences were found. There is some reason to suppose that the predicted $\bar{t}_o$ might be larger than the calculated value from earthquake excitation if enough cases were done to define the statistics accurately. This is what would be

expected if the real earthquakes are not stationary processes, as then some portions would have greater intensities than indicated by the r.m.s. values. Since $\bar{t}_o$ varies inversely as $E^2$, a smaller $\bar{t}_o$ would be expected for a nonstationary process having the same r.m.s.

It is informative also to see how the time-history response of a real earthquake compares with those of artificial earthquakes. Figure 4.10 shows the response of the structure defined by Equation 4.11 with T = 1.0 sec. to the El Centro earthquake and Figure 4.11 shows the response of the same structure to artificial earthquake (5+6) with the same r.m.s.

It is concluded that real earthquakes, to the degree that they are approximately segments of a stationary process, produce responses similar to the artificial earthquakes. For real earthquakes that are not segments of a stationary process, for example, strong motion followed by weaker motion, it may be possible to model them by a sequence of artificial earthquakes of different intensities. Further research on this problem is desirable.

## C. Influence of Vertical Ground Motion on the Collapse of Simple Yielding Structures

The preceeding analyses were made for one component of horizontal earthquake motion only, the vertical ground motion being neglected. In this Chapter several of the structures that were investigated in Chapter III are re-examined when vertical and horizontal motions are acting simultaneously to check whether the

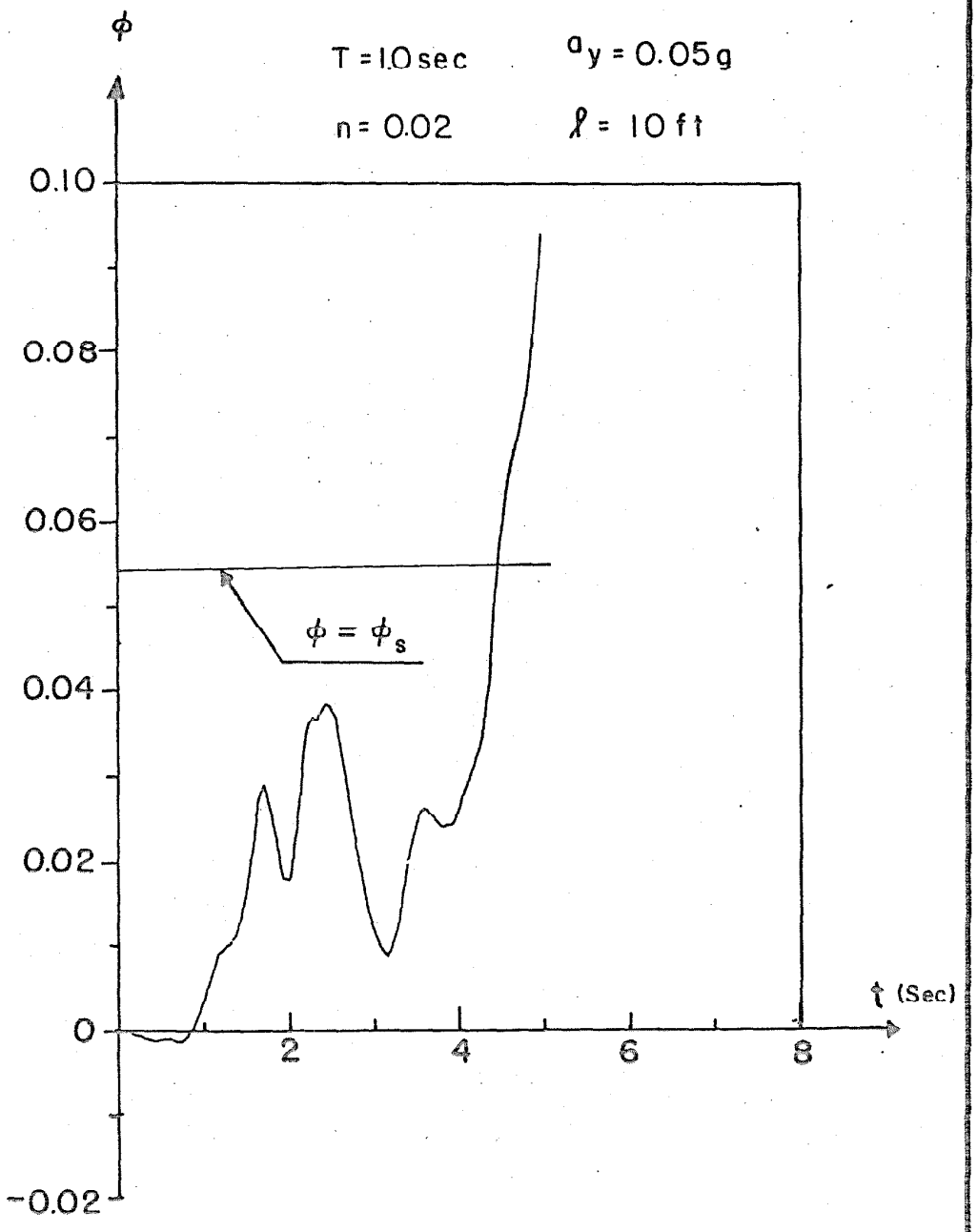


Figure 4.10. Response to El Centro earthquake.

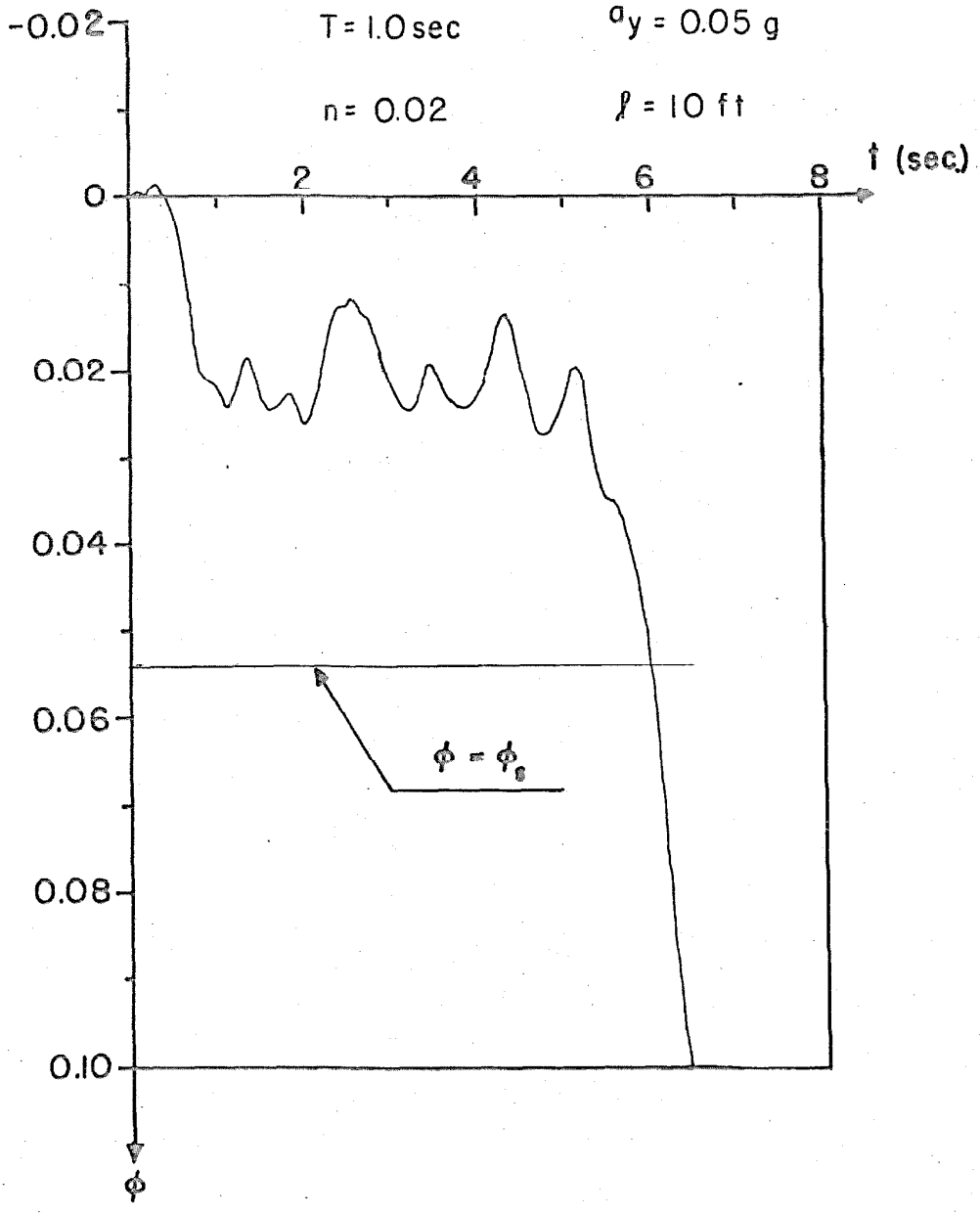


Figure 4.11. Response to art. earthquake (5+6).

vertical motion will appreciably shorten the time to failure.

The differential equation of motion for the structure when a horizontal component $u(t)$ and a vertical component $Z(t)$ of an earthquake are acting, is:

$$\ddot{\phi} + 2n\omega_o\dot{\phi} + \frac{K}{m\ell^2}F(\phi,\dot{\phi}) - \frac{g}{\ell}\sin\phi + \frac{\ddot{u}(t)}{\ell}\cos\phi - \frac{\ddot{Z}(t)}{\ell}\sin\phi = 0 \tag{4.12}$$

Equation 4.12 differs from Equation 2.31 only by the addition of the term $\ddot{Z}(t)\sin\phi/\ell$. Recalling that for the range of values of interest in this study $|\sin\phi_s| \leq \frac{1}{10}|\cos\phi_s|$ and so, the vertical motion term, even if $\ddot{Z}(t)$ is as intense as $\ddot{u}(t)$, will be smaller than one tenth of the $\ddot{u}$ term. This will be the case only near $\phi = \phi_s$, for during the first part of the response the $\ddot{Z}$ term will be less than one per cent of the $\ddot{u}$ term. Even though the differential equation is nonlinear it can be anticipated that the influence of the vertical motion will be small.

The recorded earthquakes in the U.S.A. have vertical components that are smaller than the horizontal components, the r.m.s. values being approximately 1/2 as great. This is further reason to expect that the time of collapse of a given structure will not be affected appreciably by the vertical excitation.

The following structure, which was analyzed in Chapter III, was reanalyzed with simultaneous vertical motion:

$$
\begin{aligned}
&T - 1.5 \text{ sec.} \\
&a_y = 0.1g \\
&E_h = E_v = 3.45 \\
&\ell = 10 \text{ ft.} \\
&n = 0.02
\end{aligned}
\tag{4.13}
$$

This structure is the same as structure II defined by relation 4.2. In the computations both components of ground motion were the same, that is, the same artificial earthquake was used for both components. The results of the computations are shown in Table X.

TABLE X. Horizontal and Vertical Excitation Results for Typical Structure

| Earthquake | $t_o$ horiz. comp. only | $t_o$ with both comp. |
|---|---|---|
| (1+2) | 15.85 | 17.50 |
| (3+4) | 12.78 | 13.05 |
| (5+6) | 10.19 | 10.37 |
| (7+8) | 14.50 | 14.37 |
| | $\bar{t}_o$ = 13.33 sec | $\bar{t}_o$ = 13.82 sec. |

In these calculations the two components are perfectly correlated so that the resultant ground motion was on a $45^o$ line. It is seen that the effect on the average time of failure is to increase it less than 4%. In three cases $t_o$ was increased so that the vertical component had a slightly stabilizing effect on the structure. It is

not evident why this should be so, and it is thought that it is not significant.

In addition, the structure defined below was used to determine the time of collapse when artificial earthquake (1+2) was used for horizontal excitation and (5+6) for vertical excitation, in which case the two components are practically uncorrelated.

$$\begin{aligned} T &= 0.5 \text{ sec.} \\ a_y &= 0.1g \\ E_h &= E_v = 3.45 \\ \ell &= 10 \text{ ft.} \\ n &= 0.02 \end{aligned} \qquad (4.14)$$

This structure collapsed in 13.36 seconds under the action of earthquake (1+2) when vertical motion was not included. When the vertical component was included the time of collapse was computed to be 13.33 seconds. This shows a negligible effect for the particular structure and earthquakes considered, in agreement with the analysis made at the beginning of this section.

It is concluded that the vertical component of earthquake motion does not appreciably affect the lateral vibrations and collapse of structures of the type considered in this thesis.

# V. RANDOM WALK AND UPPER BOUND ANALYSES.

## A. Random Walk with Bias

In contrast to linear response, an elasto-plastic one degree of freedom structure will yield when the deflection in the structure reaches a certain level. From the observation of the results obtained in the digital response study, it is clear that the total displacement of a yielding structure subjected to earthquake-like excitation is a combination of oscillations around the equilibrium position of the structure and drifts of its position. In order to be able to learn if appreciable deformations and permanent set develop in a yielding structure, it is important to observe the instantaneous location of its equilibrium position. This anticipates that the drift represents a very important factor when studying collapse of simple yielding structures. For the system without gravity, the inelastic drift is a sequence of steps, some positive and some negative, with no bias in either direction. However, when the effect of gravity is taken into account, it can be seen that after yielding once, there is an increase in the probability of yielding in the same direction.

Since no exact solution for the above problem has been found, one method of attack is to seek a simpler problem that will have the same general characteristics, namely, a system where successive equal increments of plastic deformation are positive or negative, but with a definite bias in the direction of the accumulative drift. A solvable problem which exhibits these characteristics is a biased one-dimensional random walk. It should be noted that the solution

obtained for the random walk problem is an ensemble average solution, so that to compare this solution with digital computations of the response of structures would require finding averages for many cases.

Consider a one dimensional random walk with bias[58]. A particle is at the origin at $t = 0$ and can move either $\Delta$ to the right or $\Delta$ to the left, and the duration of each step is $\tau$. Bias is introduced into the problem by allowing the probability of moving in either direction to depend on the position of the particle. M. C. Wang and G. E. Uhlenbeck[59] analyzed the random walk problem with an attractive center of force and were able to find average values. The probability distribution for this problem was found by M. Kac[59]. The same problem was also discussed by E. Schrödinger and F. Kohlraush[60].

A repulsive center of force at the origin of the random walk problem corresponds to the destabilizing effect of gravity in the vibration problem. At any one step, the probabilities for making a step $\Delta$ in the positive or negative directions are no longer equal but depend on the position of the particle. If the particle is at $K\Delta$, the probabilities of moving in the positive and negative directions are specified to be $\frac{1}{2}(1 + \frac{K}{R})$ and $\frac{1}{2}(1 - \frac{K}{R})$ respectively, where $R$ is an integer and the positions of the particle are restricted by the condition $-R \leq K \leq R$. According to this model, when the particle is at a location $K\Delta$, where $K > 0$, it will more likely move on its next step to $(K+1)\Delta$; only when $K = 0$ will it have the same probability of moving in either direction. When the particle reaches $\pm R\Delta$

there is zero probability of reversing its motion. This corresponds to failure.

$P(m\Delta, s\tau)$ is defined as the probability that the particle starting at the origin at $t = 0$, will be at the position $m\Delta$ after a time $s\tau$, where $\Delta$ is the length of each step, $\tau$ is the time elapsed between steps, and $m$ and $s$ are positive integers. Let $Q(K,m)$ be the probability that if at time $\alpha\tau$ the particle is at $K\Delta$, then at time $(\alpha+1)\tau$ it will be at $m\Delta$, or, in other words, the probability of going from $K\Delta$ to $m\Delta$ in the interval of time $\tau$.

$$Q(K,m) = \frac{1}{2}\left(1 - \frac{K}{R}\right)\delta(m,K-1) + \frac{1}{2}\left(1 + \frac{K}{R}\right)\delta(m,K+1) \qquad (5.1)$$

where $\delta$ is the Kronecker delta. Thus $Q(K,m) = 0$ except when $m = K - 1$ or $m = K + 1$.

Using Smoluchowski's equation, given in reference 59, one obtains the following difference equation satisfied by $P(m\Delta, s\tau)$:

$$P(m\Delta, s\tau) = \frac{1}{2}\left(1 - \frac{m+1}{R}\right)P\left((m+1)\Delta, (s-1)\tau\right)$$

$$+ \frac{1}{2}\left(1 + \frac{m-1}{R}\right)P\left((m-1)\Delta, (s-1)\tau\right) \qquad (5.2)$$

which is to be solved with the following initial condition:

$$P(m\Delta, 0) = \delta(m,0) \qquad (5.3)$$

The mean position, $\langle m(s)\rangle$, is given by

$$\langle m(s)\rangle = \sum_{n} nP(n\Delta, s\tau) \qquad (5.4)$$

Using Equation 5.2, it is found, as expected, after some algebra that

$$\langle m(s)\rangle = 0 \tag{5.5}$$

The variance of the location $m(s)$ is of special importance since its square root will give information about the location of the particle as a function of the elapsed time.

$$\langle m^2(s)\rangle = \sum_n n^2 P(n\Delta, s\tau) \tag{5.6}$$

From equations 5.2 and 5.6 it is found that

$$\langle m^2(s)\rangle = 1 + \left(1 + \frac{2}{R}\right)\langle m^2(s-1)\rangle \tag{5.7}$$

By repeated use of 5.7, the variance is determined to be

$$\langle m^2(s)\rangle = \frac{R}{2}\left\{\left(1 + \frac{2}{R}\right)^2 - 1\right\} \tag{5.8}$$

Equation 5.8 can be transformed to obtain the corresponding relation for the continuous problem. Assume that $\Delta$ and $\tau$ approach zero in such a way that when $R$ approaches infinity the relations written below are satisfied:

$$\begin{aligned} \frac{\Delta^2}{2\tau} &= D \quad ; \quad R\tau = \frac{1}{\gamma} \\ s\tau &= t \quad ; \quad m\Delta = x \end{aligned} \tag{5.9}$$

From equations 5.8 and 5.9 it follows that

$$\langle x^2\rangle = \frac{R\Delta^2}{2}\left[\left(1 + \frac{2}{R}\right)^s - 1\right] \tag{5.10}$$

Applying conditions 5.9

$$\langle x^2 \rangle = \frac{D}{\gamma}\left(e^{2\gamma t} - 1\right) \tag{5.11}$$

Figure 5.1 shows the r.m.s. value of $x$ as a function of time for several values of $D$ and $\gamma$ and it is seen that there is a resemblance between these figures, which are ensemble averages, and the calculated drift of elasto-plastic structures subjected to earthquake excitation when gravity effects are considered. Figures 5.2 and 5.3 give the response of particular elasto-plastic structures to artificial earthquake (7+8).

Relation 5.2 can be easily transformed and the limiting equation obtained when $\Delta$ and $\tau$ approach zero and $R$ tends to infinity, according to 5.9:

$$\frac{\partial P(x,t)}{\partial t} = -\gamma \frac{\partial}{\partial x}\left[xP(x,t)\right] + D\frac{\partial^2 P(x,t)}{\partial x^2} \tag{5.12}$$

with initial condition:

$$P(x,0) = \delta(x) \tag{5.13}$$

where $\delta$ is the Dirac delta function.

Using Fourier Transform techniques, equations 5.12 and 5.13, it is found that

$$P(x,t) = \sqrt{\frac{\gamma}{2\pi D(e^{2\gamma t} - 1)}}\ \exp\left\{\frac{-\gamma x^2}{2D(e^{2\gamma t} - 1)}\right\} \tag{5.14}$$

Equation 5.14 shows that $P(x,t)$ is a Gaussian distribution in

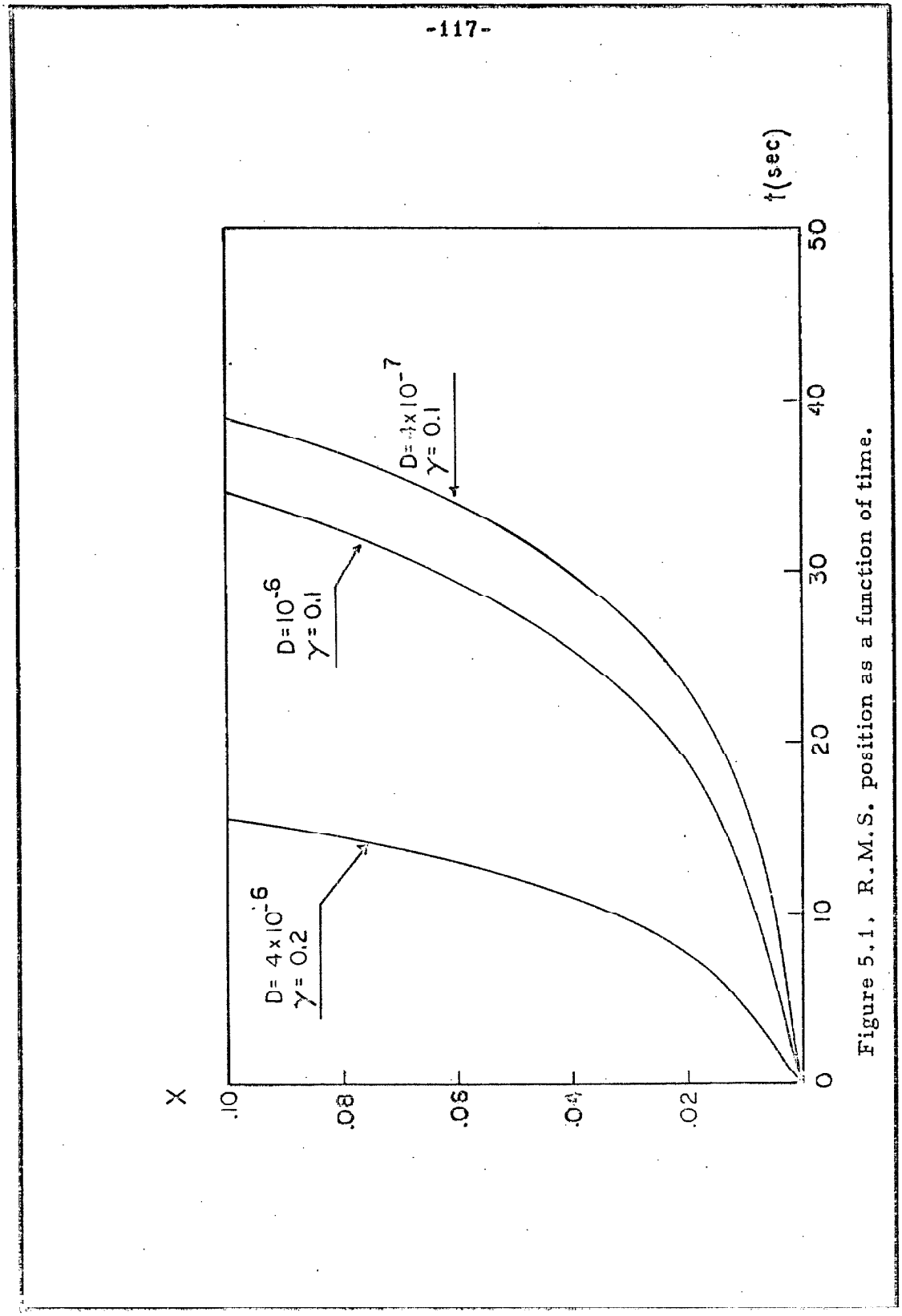


Figure 5.1, R.M.S. position as a function of time.

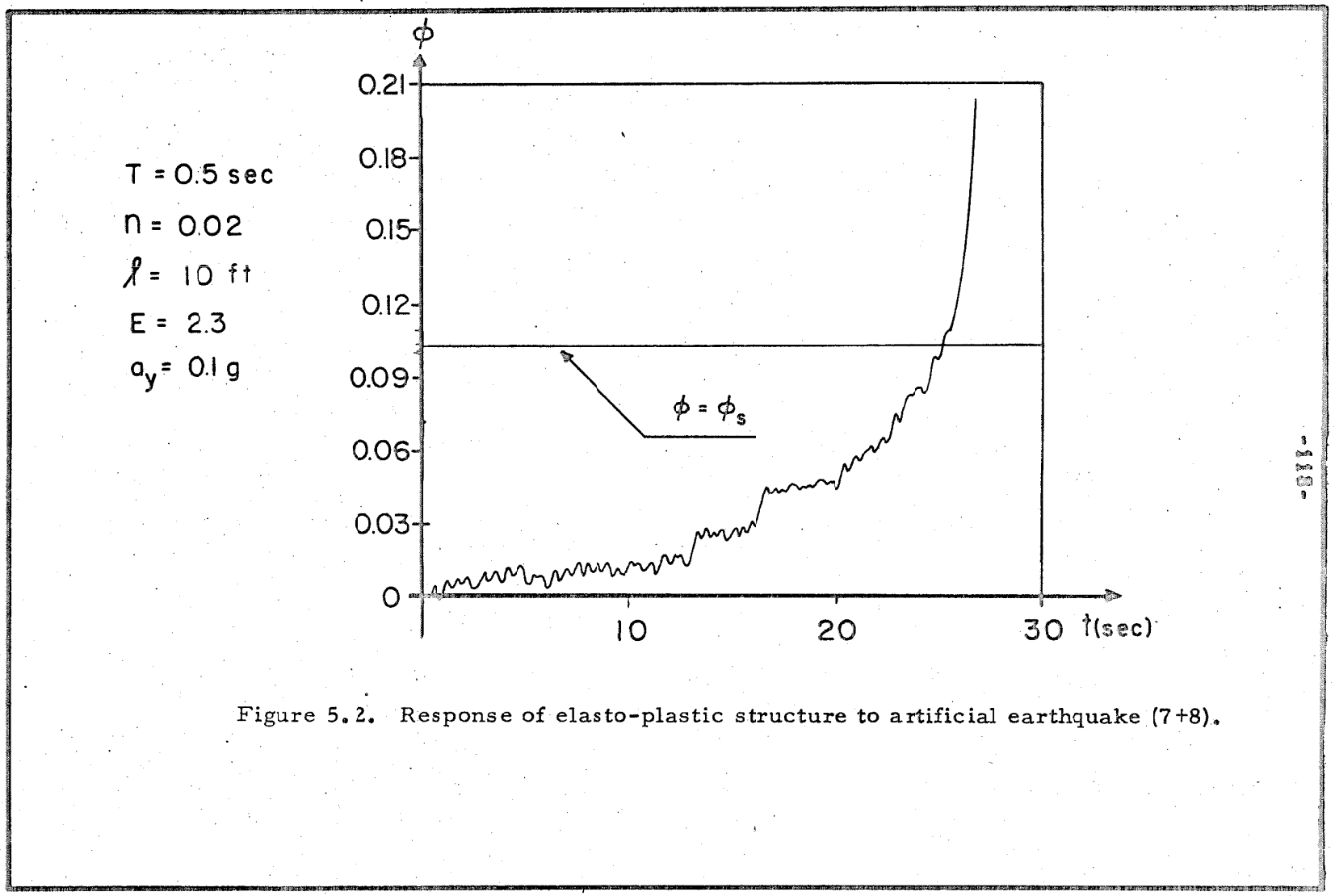


Figure 5.2. Response of elasto-plastic structure to artificial earthquake (7+8).

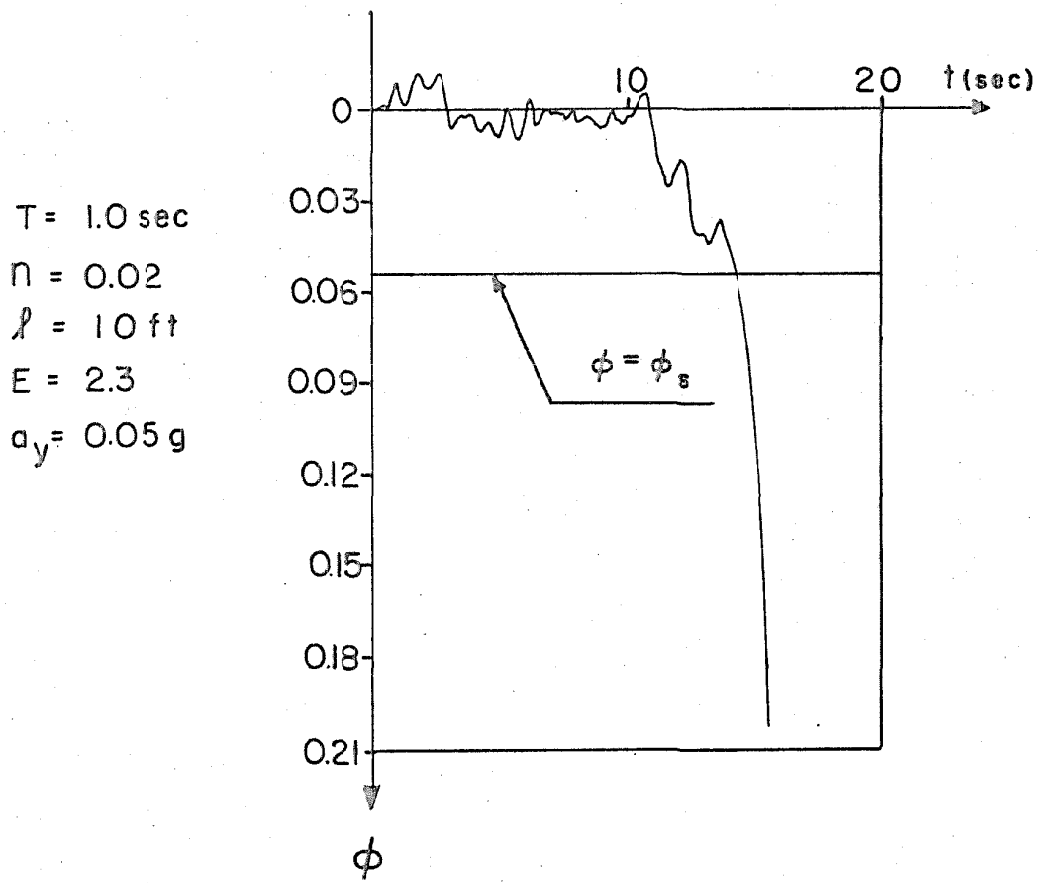


Figure 5.3. Response of elasto-plastic structure to artificial earthquake (7+8).

x with a variance that is a function of time. The peak of the distribution is infinite at $t = 0$ in accordance with Equation 5.13, and for large values of t the peak value of the distribution decreases exponentially with $\gamma t$. Thus the particle can be expected to wander far from the origin as time increases.

From the examination of relation 5.14 it follows that:

$$\bar{x} = 0 \tag{5.15}$$

where $\bar{x}$ denotes the average value for the location of the particle after a time t.

Knowing the probability density function and using Equation 5.15, the r.m.s. value for the displacement x can be obtained as follows:

$$\sigma_x = \text{r.m.s. } x = \sqrt{\int_{-\infty}^{\infty} x^2 P(x,t)\, dx} \tag{5.16}$$

Performing the integration in Equation 5.16 gives:

$$\sigma_x = \text{r.m.s. } x = \sqrt{\frac{D}{\gamma}} (e^{2\gamma t} - 1)^{\frac{1}{2}} \tag{5.17}$$

which is identical with that obtained directly from the discrete model. Hence, the biased random walk variance is given by

$$\sigma_x^2 = \frac{D}{\gamma}(e^{2\gamma t} - 1) = \frac{R\Delta^2}{2}(e^{\frac{2t}{R\tau}} - 1) \tag{5.18}$$

Since $x_s = R\Delta$ = the failure point, relation 5.18 can be written as

$$\frac{2\sigma_x^2}{\Delta x_s} = e^{\frac{2t}{R\tau}} - 1 \tag{5.19}$$

this equation then can be inverted to give:

$$t = \frac{R\tau}{2} \log \left\{ 1 + \frac{2\sigma_x^2}{\Delta x_s} \right\} \tag{5.20}$$

Let $\sigma_x$ be $\beta x_s$ $(\beta < 1)$ and obtain

$$t \approx \bar{t}_o = \frac{R\tau}{2} \log \left( 1 + \frac{2x_s \beta^2}{\Delta} \right) \tag{5.21}$$

Now let $x_s = \ell\phi_s$, $\Delta$ = the size of plastic increment, and note that $\Delta = C_1\theta^2$ for a given yield level $a_y$ since both $\Delta$ and $\theta^2$ are proportional to the average rate of energy input into the vibrating system. With these substitutions, relation 5.21 becomes for $\beta^2 C\ell\phi_s/\theta^2 << 1$,

$$\bar{t}_o \approx \frac{R\tau}{2} \left( \beta^2 C\ell\phi_s/\theta^2 \right) \tag{5.22}$$

This may be written

$$\bar{t}_o = \frac{C_o \ell}{\theta^2} \tag{5.23}$$

It is seen that this has the same form as the curve fitted to the calculated results in Chapter III and, hence, the biased random walk is analogous to the problem of earthquake collapse under gravity.

Equation 5.23 can also be written as follows:

$$\bar{t}_o = C_2 \frac{M_y}{E_o} \tag{5.24}$$

where: $C_2$ is a constant; $M_y$ is the static moment required to produce yielding; and $E_o$ is the average rate of energy input from white

noise acceleration. This might be an informative way of looking at the problem of collapse of simple yielding structures. For a given structure it follows from equation 5.24 that:

$$E_o \bar{t}_o = \text{constant} \tag{5.25}$$

which indicates that on the average, a yielding structure will collapse when a certain amount of energy has been fed into it.

B. Upper Bounds For the Displacement

An analysis of Equation 2.12 indicates that with the methods now available, there is very little hope for finding an analytical solution for the amplitude of displacement as a function of time. The equation is nonlinear and the input will be in general an earthquake or at best a white noise. Under those conditions, it was thought to be of some interest to look at estimations of upper bounds for the displacement, for systems with linear and with elasto-plastic restoring forces, even though it was not expected to obtain very good bounds. The procedure to be followed utilizes the fundamental solutions for the homogeneous linearized problem and certain bounds assumed to be known for the excitation.

Consider the following linearized equation:

$$\ddot{\phi} + 2A\dot{\phi} + B\phi + G(t) = 0 \tag{5.26}$$

with initial conditions given by

$$\phi(t_o) = \dot{\phi}(t_o) = 0 \tag{5.27}$$

where it is known only that the input $G(t)$ is bounded, i.e.,

$$|G(t)| \leq G_1 \tag{5.28}$$

From Equations 5.26 and 5.27 the solution can be written as

$$\phi(t) = -\int_{t_o}^{t} h(t-\tau)G(\tau)\, d\tau \tag{5.29}$$

in which $h(t)$ satisfies $\ddot{\phi} + 2A\dot{\phi} + B\phi = 0$ with initial conditions $\phi(0) = 0$ and $\dot{\phi}(0) = 1$. For Equation 5.26, $h(t)$ is given by

$$h(t) = \frac{e^{\alpha t} - e^{\mu t}}{\alpha - \mu} \tag{5.30}$$

where

$$\alpha, \mu = -A \pm \sqrt{A^2 - B} \tag{5.31}$$

Using $\xi = t - \tau$, 5.29 becomes:

$$\phi(t) = -\int_{o}^{t-t_o} h(\xi)G(t-\xi)\, d\xi \tag{5.32}$$

Letting $t_o$ approach $-\infty$, there is obtained

$$\phi(t) = -\int_{o}^{\infty} h(\xi)G(t-\xi)\, d\xi \tag{5.33}$$

Taking norms of both members of 5.33 gives:

$$|\phi(t)| \leq G_1 \int_{o}^{\infty} |h(\xi)|\, d\xi \tag{5.34}$$

Relation 5.34 will allow an estimation to be made of an upper bound for $\phi(t)$. There are three possible cases depending on whether

$A \lessgtr \sqrt{B}$. Only the Case $A < \sqrt{B}$ is discussed here. For $A < \sqrt{B}$ Equation 5.30 becomes

$$h(t) = \frac{e^{-At} \sin \sqrt{B-A^2}\, t}{\sqrt{B-A^2}} \tag{5.35}$$

Making use of 5.34 and 5.35 gives:

$$|\phi(t) \leq \frac{G_1}{\sqrt{B-A^2}} \int_o^\infty |e^{-At} \sin \sqrt{B-A^2}\, t|\, dt \tag{5.36}$$

Replacing the trigonometric function by unity in the last relation, a first estimation for an upper bound is obtained,

$$|\phi(t)| \leq \frac{G_1}{A\sqrt{B-A^2}} \tag{5.37}$$

A more accurate evaluation of Equation 5.36 can be made by replacing the integral by a series of integrals, as follows:

$$|\phi(t)| \leq \frac{G_1}{\sqrt{B-A^2}} \left\{ \int_o^{\pi/\sqrt{B-A^2}} e^{-A\xi} |\sin \sqrt{B-A^2}\, \xi|\, d\xi + \int_{\pi/\sqrt{B-A^2}}^{2\pi/\sqrt{B-A^2}} \% \; d\xi + \ldots \right\} \tag{5.38}$$

Making the substitution $\xi = \eta + (\pi/\sqrt{B-A^2})$ in the second integral, and $\xi = \gamma + (2\pi/\sqrt{B-A^2})$ in the third, etc., and using the identity:

$$\sin (\pi + \eta\sqrt{B-A^2}) = - \sin \eta\sqrt{B-A^2} \tag{5.39}$$

it is found that equation 5.38 gives:

$$|\phi(t)| \leq \frac{G_1 J}{\sqrt{B-A^2}} \left\{ 1 + e^{-A\pi/\sqrt{B-A^2}} + e^{-2A\pi\sqrt{B-A^2}} + \ldots \right\} \quad (5.40)$$

where

$$J = \int_0^{\pi/\sqrt{B-A^2}} e^{-A\xi} \sin\sqrt{B-A^2}\,\xi \; d\xi = \frac{\sqrt{B-A^2}}{B}\left(1 + e^{-A\pi/\sqrt{B-A^2}}\right) \quad (5.41)$$

The series in Equation 5.40 can be summed with the help of the identity

$$\sum_{j=0}^{\infty} e^{-jA\pi/\sqrt{B-A^2}} = \frac{1}{1 - e^{-A\pi/\sqrt{B-A^2}}} \quad (5.42)$$

So from 5.40, 5.41 and 5.42, it follows that

$$|\phi(t)| \leq \frac{G_1}{B} \coth\left(\frac{A\pi}{2\sqrt{B-A^2}}\right) \quad (5.43)$$

Since for small $\mu$, $\coth \mu \approx 1/\mu$, Equation 5.43 gives for the case when $A\pi/2\sqrt{B-A^2}$ is small,

$$|\phi(t)| \leq \frac{2G_1}{B} \frac{\sqrt{B-A^2}}{A\pi} \quad (5.44)$$

Equations 5.26 and 5.44 state that for usual structures (small damping, i.e. $B >> A^2$) the bound appears to be proportional to the maximum of the excitation, inversely proportional to the square root of the stiffness and also to the damping. The fact that the bound presented in 5.44 increases with $G_1$ and also increases with $1/A$ indicates that only weak bounds will be obtained if 5.44 is used to

estimate the response of lightly damped structures to strong ground motions.

Consider a second problem in which the system is governed by equations 5.26 and 5.27, and instead of 5.28 the following conditions are imposed:

$$|G(t)| \leq G_1$$
$$\left|\frac{d}{dt}\left(G(t)\right)\right| \leq G_2 \tag{5.45}$$

As before, it is possible to write,

$$\phi(t) = -\int_0^\infty h(\xi)G(t-\xi)\, d\xi \tag{5.46}$$

Integration by parts in 5.46 gives:

$$-\phi(t) = h^{-1}(\xi)G(t-\xi)\Big|_0^\infty + \int_0^\infty h^{-1}(\xi)G'(t-\xi)\, d\xi \tag{5.47}$$

where $h^{-1}(\xi)$ is defined as:

$$\frac{d}{dt}\left[h^{-1}(t)\right] = h(t) \tag{5.48}$$

The upper bound for the displacement is presented below for the case $A < \sqrt{B}$ and the other two cases are omitted. As in the problem solved before, $h(t)$ is given by 5.35 when $A < \sqrt{B}$ and therefore:

$$h^{-1}(t) = \frac{-e^{-At}}{\sqrt{B-A^2}}\left\{A \sin\sqrt{B-A^2}\,t + \sqrt{B-A^2}\cos\sqrt{B-A^2}\,t\right\} \tag{5.49}$$

From 5.47 and 5.49 it follows:

$$\phi(t) = -G(t) + \int_0^{\infty} G'(t-\xi) \frac{e^{-A\xi}}{\sqrt{B-A^2}} \left\{ A \sin \sqrt{B-A^2}\,\xi + \sqrt{B-A^2} \cos \sqrt{B-A^2}\,\xi \right\} d\xi \tag{5.50}$$

From 5.50 and 5.45, using an approximation similar to the one that replaced 5.36 by 5.37, it follows that

$$|\phi(t)| \leq G_1 + \frac{G_2}{A} \left\{ 1 + \frac{A}{\sqrt{B-A^2}} \right\} \tag{5.51}$$

Inspecting 5.51, it can be seen that for usual structures i.e., $A \ll \sqrt{B}$, the bound is inversely proportional to the value of $A$ and this again indicates that weak results are expected when 5.51 is used to describe the earthquake response of lightly damped structures.

In what follows, another upper bound for the displacement will be estimated for the structure represented by Equations 2.12 and 2.13. The following notation will be used in order to utilize some results already obtained:

$$\ddot{\phi} + 2A\dot{\phi} + B_2\phi + R(\phi,\dot{\phi}) - \frac{g}{\ell} \sin\phi = G(t) \cos\phi \tag{5.52}$$

where

$$\begin{aligned} g &= \frac{C_1}{m\ell^2} \\ B_2 &= \frac{K_2}{m\ell^2} \\ R(\phi,\dot{\phi}) &= \frac{K}{m\ell^2} \left\{ F(\phi,\dot{\phi}) - \frac{K_2}{K}\phi \right\} \\ G(t) &= \frac{-\ddot{u}(t)}{\ell} \end{aligned} \tag{5.53}$$

and where $K_2$ is defined through Figure 5.4 by the relation $\alpha = K_2/K$, and $K$ has the same meaning as in relation 2.2. Equation 5.52 can be transformed as follows:

$$\ddot{\phi} + 2A\dot{\phi} + B_2\phi = G(t) \cos \phi + \frac{g}{\ell} \sin \phi - R(\phi,\dot{\phi}) \tag{5.54}$$

From 5.54 and 2.13 it follows that

$$\phi(t) = \int_0^\infty h(\xi) \left\{ G(t-\xi) \cos \phi + \frac{g}{\ell} \sin \phi - R(\phi,\dot{\phi}) \right\} d\xi \tag{5.55}$$

The most interesting case is when $A < \sqrt{B_2}$ and then $h(t)$ is obtained from 5.35. The use of the techniques presented in the previous examples will provide an upper bound for $\phi$. It is easily verified that:

$$|\phi(t)| \leq \int_0^\infty (G_1 + \frac{g}{\ell} + R_1) |h(\xi)| \, d\xi \tag{5.56}$$

in which

$$G_1 = |G(t)|_{max}$$

$$R_1 = |R(\phi,\dot{\phi})|_{max}$$

therefore

$$|\phi(t)| \leq (G_1 + \frac{g}{\ell} + R_1) \int_0^\infty |h(\xi)| \, d\xi \tag{5.57}$$

Using 5.34, 5.43 and 5.57 produces

$$|\phi(t)| \leq \left( \frac{R_1 + \frac{g}{\ell} + G_1}{B_2} \right) \coth \left\{ \frac{A\pi}{2\sqrt{B_2 - A^2}} \right\} \tag{5.58}$$

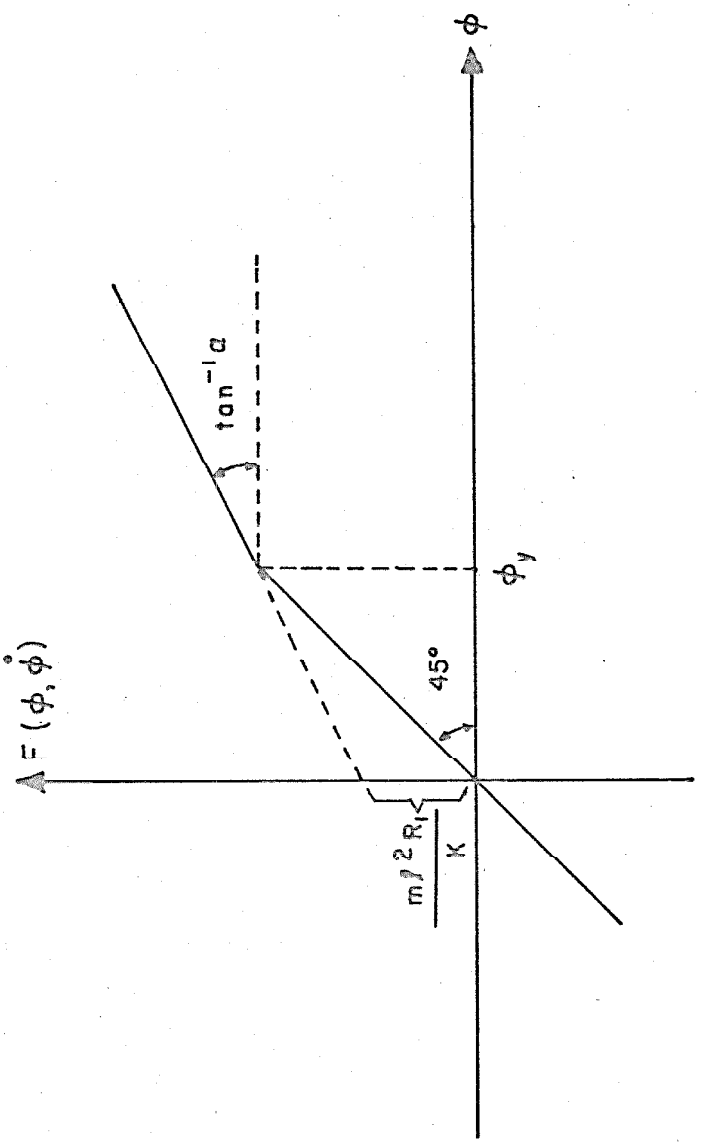


Figure 5.4. Bilinear hysteretic moment angle relation.

For an elasto-plastic structure, $B_2$ has a value of zero, since $B_2 = K_2/m\ell^2$, and $\alpha = K_2/K \equiv 0$. Therefore the amplitude of this system could reach infinite values. For a bilinear structure, depending on the value of $\alpha = K_2/K$, the upper bound will be finite but it is important to note that for small values of $\alpha$, amplitudes similar to the elasto-plastic response can be expected.

An example is now given to illustrate the practical suitability of the bounds just obtained. Consider the system described by Equation 5.52. Typical values for the parameters defining the structure were selected, i.e.,

$$\begin{aligned} \ell &= 10 \text{ ft} \\ \alpha &= 0.05 \\ n &= 0.02 \\ T &= 1.0 \text{ sec} \quad (\omega_o = 2\pi) \end{aligned} \tag{5.59}$$

An earthquake having the intensity of the El Centro earthquake (1940, N.S.) was used as input, i.e.,

$$|\ddot{u}(t)|_{max} = 9.6 \text{ ft/sec}^2$$

For these values of the parameters, it is possible to use the approximation that

$$\coth \frac{A\pi}{2\sqrt{B_2 - A^2}} \approx \frac{2\sqrt{B_2 - A^2}}{A\pi}$$

to get

$$|\phi(t)| \leq \frac{2(G_1 + \frac{g}{\ell} + R_1)}{\pi A B_2} \sqrt{B_2 - A^2} \qquad (5.60)$$

which is valid for $A < \sqrt{B_2}$. Recalling that

$$A = n\omega_o \quad ; \quad g = 32.2 \text{ ft sec}^2$$
$$B_2 = \frac{K_2}{m\ell^2} = \frac{K\alpha}{m\ell^2} \quad ; \quad \omega_o = \sqrt{\frac{K}{m\ell^2} - \frac{g}{\ell}}$$

it follows from 5.59 that $A = 0.126$ and $B_2 = 2.135$, therefore $A < \sqrt{B_2}$ and 5.60 is applicable, giving

$$|\phi(t)| \leq 14.42 + 3.45 R_1 \qquad (5.61)$$

where $|\phi(t)|$ is measured in radians.

Considering that real structures will collapse for values of $\phi(t)$ of the order of 0.1 radians, it is clear that the bounds just computed are much too weak to use in estimating the possibilities of the collapse of simple yielding structures.

It is known, of course, that for a linear 2% damped structure with a sinusoidal input, at resonance there is 25 times amplification of static displacement[61]. With earthquake excitation the amplification is found to be approximately 1.0, hence, assuming the same ratio applies for the present case, the upper bound for earthquake excitation should be approximately 1/25 of the bound 5.61, that is,

$$|\phi(t)| < 0.577 + 0.138 R_1$$

C. Time Dependent Bound for White Noise Excitation.

When a yielding structure subjected to white noise excitation is used, it is possible to find an upper bound for the displacement that gives a fairly good description of the drift observed in the previous chapters.

From Equation 2.12, with $C_1 = 0$, $\sin\phi \approx \phi$ and $\cos\phi \approx 1$ it follows that

$$\ddot{\phi} - g/\ell\,\phi + \frac{k}{m\ell^2} F(\phi, \dot{\phi}) = -\frac{\ddot{u}(t)}{\ell} \tag{5.62}$$

introducing the notation

$$\frac{k}{m\ell^2} F(\phi, \dot{\phi}) = G(\phi, \dot{\phi})$$

$$-\frac{\ddot{u}(t)}{\ell} = N(t) \tag{5.63}$$

$$g/\ell = \beta^2$$

produces

$$\ddot{\phi} - \beta^2 \phi + G(\phi, \dot{\phi}) = N(t) \tag{5.64}$$

The solution of Equation 5.64 with zero initial conditions is given by

$$\phi = \int_0^t \frac{\sinh \beta(t-\tau)}{\beta} \left\{N(\tau) - G(\phi, \dot{\phi})\right\} d\tau \tag{5.65}$$

The expected value of $\phi^2$, $E[\phi^2]$, can be calculated from Equation 5.65 as follows:

From Equation 5.65, $\phi^2$ can be written as

$$\phi^2 = \int_0^t \int_0^t \sinh \beta(t-\tau_1) \sinh \beta(t-\tau_2) \left\{N(\tau_2)-G\right\}\left\{N(\tau_1)-G\right\} d\tau_1, d\tau_2 \tag{5.66}$$

Taking expected values of both members in Equation 5.66 and recalling that for a white noise

$$\begin{aligned} E[N(\tau_1)N(\tau_2)] &= 2D\delta(\tau_1-\tau_2) \\ E[N(t)] &= 0 \end{aligned} \tag{5.67}$$

and calling

$$y = |G(\phi, \dot{\phi})|_{max} \tag{5.68}$$

it follows from Equations 5.66, 5.67 and 5.68 that

$$E[\phi^2] \leq \frac{2D}{\beta^3}\left\{\frac{\sinh 2\beta t - 2\beta t}{4}\right\} + \frac{y^2}{\beta^4}(\cosh \beta t - 1)^2 \tag{5.69}$$

For small values of time Equation 5.69 gives

$$E[\phi^2] \sim t^3 \tag{5.70}$$

Equation 5.70 agrees with many of the results given in Chapters III and IV, where rather small deformations were observed for small t.

For large values of time, from Equation 5.69 it is easily shown that

$$E[\phi^2] \sim e^{2\beta t} \tag{5.71}$$

and this result is also in agreement with the numerical computations of response done in Chapter III and IV.

It is noted that Equation 5.71 coincides for all practical purposes with the corresponding result obtained for the random walk problem. For small values of time, it is thought that Equation 5.69 gives a better representation of the phenomenon than the one provided by the random walk studied above.

# VI. SUMMARY AND CONCLUSIONS

## A. Summary

The effects of gravity on the earthquake response of one degree of freedom yielding structures were studied by subjecting elasto-plastic and bilinear hysteretic oscillators to earthquake-like excitation. The structures considered were one story frames with rigid girders and massless columns. The yielding characteristics were simplified by considering yielding in the columns to be a function of the bending deformation only. Interest was centered on the development of permanent set and on the parameters that influence the time required for yielding to progress to the point of collapse. It was the intent of this study that it provide a first step in the study of the effects of gravity on the yielding response of multistory buildings.

Four 60 sec long artificial earthquakes served as excitation for most of the cases studied. They were scaled to have intensities varying between weak motion and shaking 140 per cent stronger than the N.S. component of the 1940 El Centro earthquake. Four values of the period of the structure, in the range 0.5 to 2.0 sec were selected, because this range includes most multistory structures. The amount of viscous damping was 2% in all cases.

Six values of the height of the columns of the frame (see Figure 2.3) were used, ranging from 5 to 30 ft, which extends well below and above the heights of typical stories in structures. Two values of the lateral yield level of the structure, 0.05g and 0.10g

were selected for most of the work reported in this thesis. Two yielding mechanisms were used to model the nonlinear behavior of the structure: the elasto-plastic and the bilinear hysteretic.

For most cases of interest, the deflection at which yielding begins is small with respect to the column height, and under this condition it was found that the relative strength of the excitation is determined by the ratio of the earthquake strength to the lateral strength of the structure. Thus, the excitation could be characterized by a parameter $\theta$, defined as the ratio between the intensity of the earthquake acceleration (E) and the lateral yield level $(a_y/g)$.

For a total of 221 structures the response to earthquake-like excitation was computed and the time of collapse obtained. A statistical study of this data was then done to decide what parameters were suitable for estimating the time of failure for elasto-plastic structures. The following relation was found from a regression analysis.

$$\bar{t}_o = \frac{2000\,\ell}{\theta^2} \qquad (3.15)$$

This equation gives the average time of collapse of simple elasto-plastic structures, subjected to earthquakes of a given strength. In this expression $\ell$ is measured in ft, $\theta$ was defined above and $\bar{t}_o$ is the average time for collapse. It is significant that the average time to failure is independent of the period of the structure.

Three of the strongest earthquakes recorded in the U.S.A. were used to show that similar results are found under real earth-

quake excitation. Also, two simultaneous components of earthquake motions were used, one vertical and one horizontal (perfectly correlated and uncorrelated) and it was found that the effect of vertical motion on the time of failure was negligible.

Calculations were made of the response of two bilinear hysteretic structures to each of the four artificial earthquakes available. Using the results presented in Chapter III and IV it was found that the average time of collapse, $\bar{t}_o$, of bilinear hysteretic structures is described by

$$\bar{t}_o = \frac{2000\,\ell}{\theta^2\left\{1 - \left(\frac{K_2}{mg\ell}\right)^{0.8}\right\}} \tag{4.10}$$

This result shows a large increase in the time of failure when the second slope increases from zero (elasto-plastic) towards $K_{2c} = mg\ell$, the slope for which static failure is not possible.

Some of the features of the failure of simple yielding structures under earthquake excitation are comparable to those of a biased one-dimensional random walk. An analysis of this problem was done and the continuous probability distribution was obtained. The mean and variance of the position as functions of time were presented and it was shown that there is a resemblance between the results of the biased random walk problem and the thesis problem; for small values of time, the variance of the position as a function of time is given by the same type of relation as Equation 3.15 above.

Upper bounds for the displacement during earthquake response were found for systems with linear and elasto-plastic restoring

force relations.

Although the results showed the general stabilizing effects of viscous damping and finite upper slope on the bilinear yielding relation, it was not possible to obtain practically significant bounds with the techniques used.

B. Conclusions

The results demonstrate that for simple yielding structures, the effect of gravity is to increase significantly the amount of permanent set over that found when gravity is not considered. Large values of permanent set, of course, will lead to collapse of the structure.

The time of collapse does not appear to depend on the period of the structure for the range 0.5 to 2.0 sec considered. It is concluded that if $\bar{t}_o$ depends on the natural period of the structure, then that influence is masked by the statistical dispersion of the data. It is thought that many more samples would have to be used before being able to determine the effects of period on the response statistics.

Relations 3.15 or 4.10 have significant inplication on the collapse of simple yielding structures subjected to very short duration earthquakes like the Parkfield earthquake of June 27, 1966, that had a very short strong phase. The earthquake did not produce major damage in spite of the large accelerations recorded. It is concluded from this study that the intensity of shaking necessary for collapse is significantly larger for earthquakes of short duration,

and conversely that a lower excitation may cause failure if the duration is longer.

It appears that the statistics for the artificial and real earthquake excitations are comparable. No significant differences were found when studying the collapse of simple yielding structures. It is concluded that real earthquakes to the degree that they are approximately segments of a stationary process, produce responses similar to the artificial earthquakes.

It was concluded that the vertical component of the earthquake motion does not appreciably affect the lateral vibrations of structures of the type considered in this thesis.

It is concluded that the time of failure of a bilinear hysteretic structure of this type is strongly influenced by the second slope of the moment angle relation. In Figure 4.2 it is clearly seen that an appreciable increase in the time of collapse occurs when the second slope $K_2$ increases from zero towards $K_{2c} = mg\ell$.

Using the solution obtained for the biased one-dimensional random walk, it was shown that an analogy may be established between the random walk problem and the thesis problem. An interpretation of the results obtained permits the tentative conclusion that on the average, a yielding structure will collapse when a certain amount of energy is fed in. The random walk analogy appears as promising for further research on the collapse of simple yielding structures.

## REFERENCES


1. Jacobsen, L. S., "Steady Forced Vibration as Influenced by Damping," Transactions ASME, 1930, Paper APM-54-15.

2. Hudson, D. E., "Equivalent Viscous Friction for Hysteretic Systems with Earthquake-like Excitations," Proceedings, Third World Conference on Earthquake Engineering, New Zealand, 1965.

3. Caughey, T. K., "Sinusoidal Excitation of a System with Bilinear Hysteresis," Journal of Applied Mechanics, Vol. 27, No. 4, December, 1960.

4. Caughey, T. K., "Random Excitation of a System with Bilinear Hysteresis," Journal of Applied Mechanics, Vol. 27, No. 4, December, 1960.

5. Struble, R. A., Nonlinear Differential Equations. McGraw-Hill Book Company, 1962.

6. Heinbockel, J. H. and Struble, R. A., "Periodic Solutions for Differential Systems with Symmetries," J. Soc. Indust. Appl. Math., Vol. 13, No. 2, June, 1965.

7. Biot, M. A., "A Mechanical Analyzer for the Prediction of Earthquake Stresses," Bulletin of the Seismological Society of America, Vol. 31, April, 1941, No. 2.

8. Biot, M. A., "Analytical and Experimental Methods in Engineering Seismology," Transactions ASCE, Vol. 108, Paper No. 2183, 1943.

9. Alford, J. L., Housner, G. W. and Martel, R. R., Spectrum Analysis of Strong-motion Earthquakes. Pasadena: California Institute of Technology, Earthquake Research Laboratory, 1951.

10. Hudson, D. E., "Response Spectrum Techniques in Engineering Seismology," 1st World Conference on Earthquake Engineering, Berkeley, California, 1956.

11. Hudson, D. E., "Some Problems in the Application of Spectrum Techniques to Strong-motion Earthquake Analysis," Bulletin of the Seismological Society of America, Vol. 52, No. 2, April, 1962.

12. Housner, G. W., "Behavior of Structures During Earthquakes," Proceedings of the American Society of Civil Engineers, Vol. 85, No. EM4, October, 1959.

13. Caughey, T. K., "Classical Normal Modes in Damped Linear Dynamic Systems," Journal of Applied Mechanics, Paper No. 59-A-62.

14. Foss, K. A., "Coordinates Which Uncouple the Equations of Motion of Damped Linear Systems," Journal of Applied Mechanics, Paper No. 57-A-86.

15. Caughey, T. K. and O'Kelly, M. E. J., "General Theory of Vibration of Damped Linear Dynamic Systems," Report, Dynamics Laboratory, California Institute of Technology, 1963.

16. O'Kelly, M. E. J., "Vibration of Viscously Damped Linear Dynamic Systems," Ph.D. Thesis, California Institute of Technology, 1964.

17. Clough, R. W., "Dynamic Effects of Earthquakes," Proceedings of the American Society of Civil Engineers, Vol. 86, No. ST4, April, 1960.

18. Iwan, W. D., "The Dynamic Response of Bilinear Hysteretic Systems," Ph.D. Thesis, California Institute of Technology, 1961.

19. Iwan, W. D., "An Electric Analog for Systems Containing Coulomb Damping," Experimental Mechanics, August, 1964.

20. Tanabashi, R., "Studies on the Nonlinear Vibrations of Structures Subjected to Destructive Earthquakes," Proceedings of the 1st World Conference on Earthquake Engineering, Berkeley, California, 1956.

21. Penzien, J., "Dynamic Response of Elasto-plastic Frames," Proceedings of the American Society of Civil Engineers, Vol. 86, No. ST7, July, 1960.

22. Veletsos, A. S., and Newmark, N. M., "Effect of Inelastic Behavior on the Response of Simple Systems to Earthquake Motions," Proceedings of the Second World Conference on Earthquake Engineering, Vol. II, Tokyo and Kyoto, Japan, 1960.

23. Jennings, P. C., "Response of Simple Yielding Structures to Earthquake Excitation," Ph.D. Thesis, California Institute of Technology, 1963.

24. Hanson, R. D., "Post-elastic Dynamic Response of Mild Steel Structures," Ph.D. Thesis, California Institute of Technology, 1965.

25. Berg, G. V., "The Analysis of Structural Response to Earthquake Forces," Ph.D. Thesis, University of Michigan, 1958.

26. Berg, G. V., and DaDeppo, D. A., "Dynamic Analysis of Elasto-plastic Structures," Proceedings of the American Society of Civil Engineers, Vol. 86, No. EM2, April, 1960.

27. Penzien, J., "Elasto-plastic Response of Idealized Multistory Structures Subjected to a Strong Motion Earthquake," Proceedings of the 2nd World Conference on Earthquake Engineering, Vol. II, Tokyo and Kyoto, Japan, 1960.

28. Berg, G. V., "Response of Multistory Structures to Earthquakes," Proceedings of the American Society of Civil Engineers, Vol. 87, No. EM2, April, 1961.

29. Bycroft, G. N., "Yield Displacements in Multistory Aseismic Design," Bulletin of the Seismological Society of America, Vol. 50, No. 3, July, 1960.

30. Adams, P. F., and Galambos, T. V., Discussion of "Comparison of Static and Dynamic Hysteresis Curves" by Hanson, R. D., Proceedings ASCE, Vol. 93, No. EM2, April, 1967.

31. Ruge, A. C., "The Determination of Earthquake Stresses in Elastic Structures by Means of Models," Bulletin of the Seismological Society of America, Vol. 24, No. 3, July, 1934.

32. Jacobsen, L. S., "Dynamic Behavior of Simplified Structures up to the Point of Collapse," Proceedings of the Symposium on Earthquake and Blast Effects on Structures, Los Angeles, California, 1952.

33. Osawa, Yutaka, "On the Damage to Buildings and Other Structures During the Earthquake of January 23, 1966, in the Vicinity of Matsushiro," Bulletin of the Earthquake Research Institute, Vol. 44, 1966, pp. 419-421.

34. Housner, G. W. and Jennings, P. C., "Generation of Artificial Earthquakes," Proceedings of the American Society of Civil Engineers, Vol. 90, No. EM1, February, 1964.

35. Martel, R. R., "The Effects of Earthquakes on Buildings with a Flexible First Story," Bulletin of the Seismological Society of America, Vol. 19, No. 3, September, 1929.

36. Biot, M. A., "Theory of Vibration of Buildings During Earthquakes," Zeitschrift für Augewandte Mathematik und Mechanik, Bd. 14, II, 4, 1934.

37. Jennings, P. C., "Periodic Response of a General Yielding Structure," Journal of the Engineering Mechanics Division, ASCE, Vol. 90, No. EM2, Proc. Paper 3871, April, 1964.

38. Non-linear Response Analysis of Tall Buildings to Strong Earthquake and its Application to Dynamic Design. SERAC Report No. 1-2, July, 1962, Faculty of Engineering, University of Tokyo, Tokyo, Japan.

39. Nigam, N. C., "Inelastic Interactions in the Dynamic Response of Structures,"Ph.D. Thesis, California Institute of Technology, 1967.

40. Hurty, W. C., and Rubinstein, M. F., Dynamics of Structures. Prentice Hall, 1965.

41. Husid, R., "Analisis de las Medidas de Períodos de Vibración de Edificios Nuevos," Revista del I.D.I.E.M., Vol. 4, Diciembre, 1965, No. 3.

42. Housner, G. W., and Brady, A. G., "Natural Periods of Vibration of Buildings," Journal of the Engineering Mechanics Division, ASCE, Vol. 89, No. EM4, Proc. Paper 3613, August, 1963.

43. Nielsen, N. N., "Dynamic Response of Multistory Buildings," Earthquake Engineering Research Laboratory, California Institute of Technology, Pasadena, California, June, 1964.

44. Todd, John, Editor, Survey of Numerical Analysis. McGraw-Hill Book Company, Inc., 1962, Chapter 9.

45. Hildebrand, F. B., Introduction to Numerical Analysis. McGraw-Hill Book Company, New York, 1956.

46. Cramer, H., Mathematical Methods of Statistics. Princeton University Press, Princeton, New Jersey, 1946.

47. Arias, A., and Husid, R., "Fórmula Empírica Para el Cálculo del Período Propio de Vibración de Edificios de Hormigón Armado con Muros de Rigidez," Primeras Jornadas Argentinas de Ingeniería Antisímica, San Juan, Argentina, April, 1962.

48. Rietz, H. L., Mathematical Statistics. The Carus Mathematical Monographs, Number three, 1927.

49. Bertero, V. V. and Iragorry, G. J., "Precast Chemically Prestressed Concrete Frame," Proceedings Second Pan American Symposium of Structures, Vol. 1, Paper No. 12, Lima, Perú, January, 1964.

50. Colaco, J. P., "Prediction of Steel Force Distribution in Reinforced Concrete Members from Bond-slip Characteristics," Doctoral dissertation, University of Illinois, 1965.

51. Sozen, M. A. and Nielsen, N. N., "Earthquake Resistance of Reinforced Concrete Frames," International Symposium on the Effects of Repeated Loading of Materials and Structures, Mexico City, September, 1966.

52. Yamada, M., and Nakaza, I., "Low Cycle Fatigue of Riveted and High Strength Bolted Joints in Steel Beams," International Symposium on the Effects of Repeated Loading of Materials and Structures, Mexico City, September, 1966.

53. Popov, E. P., "Low Cycle Fatigue of Steel Beam-to-column Connections," International Symposium on the Effects of Repeated Loading of Materials and Structures, Mexico City, September, 1966.

54. Loren, D. Lutes, "Stationary Random Response of Bilinear Hysteretic Systems," Ph.D. Thesis, California Institute of Technology, 1967.

55. Rosenblueth, E., and Bustamante, J. I., "Distribution of Structural Response to Earthquakes," Journal of the Engineering Mechanics Division, ASCE, Vol. 88, No. EM3, Part I, June, 1962.

56. Rosenblueth, Emilio, "Some Applications of Probability Theory in Asoismic Design," Proceedings of the 1st World Conference on Earthquake Engineering, Berkeley, California, June, 1956.

57. Rosenblueth, E., "Probabilistic Design to Resist Earthquakes," Proceedings of the American Society of Civil Engineers, Vol. 90, No. EM5, October, 1964.

58. Spitzer, F., Principles of Random Walk. D. Van Nostrand Company, Inc., 1964.

59. Wax, N., et al., Selected Papers on Noise and Stochastic Processes. Dover Publications, Inc., New York, 1954.

60. Schrödinger, E., and Kohlrausch, F., Physik. Zeits. 27, 306 (1926).

61. Housner, G. W., and Hudson, D. E., Applied Mechanics-Dynamics. D. Van Nostrand Company, Inc., Second edition, 1965.

# APPENDIX I

The following table contains all the cases considered in the study of elasto-plastic structures subjected to earthquake-like excitation. The data given include the yield angle, $\phi_y$, the angle of failure, $\phi_s$, the time of collapse, $t_o$, and the earthquake intensity.

TABLE I-1. Summary of Elasto-Plastic Response Calculations

| Case | $a_y/g$ | E | T (sec) | $\ell$ (ft) | $\phi_y$ (rad) | $\phi_s$ (rad) | $t_o$ (sec) | Earthquake |
|---|---|---|---|---|---|---|---|---|
| 1 | 0.1 | 1.7 | 1.0 | 10 | 0.0082 | 0.1082 | 53.53 | (1+2) |
| 2 | 0.1 | 1.7 | 1.0 | 10 | 0.0082 | 0.1082 | 38.30 | (3+4) |
| 3 | 0.1 | 1.7 | 1.0 | 10 | 0.0082 | 0.1082 | 44.84 | (5+6) |
| 4 | 0.1 | 1.7 | 1.0 | 10 | 0.0082 | 0.1082 | >60 | (7+8) |
| 5 | 0.05 | 4.5 | 1.0 | 10 | 0.0041 | 0.0541 | 0.81 | (1+2) |
| 6 | 0.05 | 4.5 | 1.0 | 10 | 0.0041 | 0.0541 | 2.70 | (3+4) |
| 7 | 0.05 | 4.5 | 1.0 | 10 | 0.0041 | 0.0541 | 1.47 | (5+6) |
| 8 | 0.05 | 4.5 | 1.0 | 10 | 0.0041 | 0.0541 | 3.02 | (7+8) |
| 9 | 0.1 | 2.3 | 2.0 | 10 | 0.0327 | 0.1327 | 59.53 | (1+2) |
| 10 | 0.1 | 2.3 | 2.0 | 10 | 0.0327 | 0.1327 | 31.20 | (3+4) |
| 11 | 0.1 | 2.3 | 2.0 | 10 | 0.0327 | 0.1327 | 26.32 | (5+6) |
| 12 | 0.1 | 2.3 | 2.0 | 10 | 0.0327 | 0.1327 | 39.05 | (7+8) |
| 13 | 0.1 | 2.3 | 1.5 | 10 | 0.0184 | 0.1184 | 40.00 | (1+2) |
| 14 | 0.1 | 2.3 | 1.5 | 10 | 0.0184 | 0.1184 | 36.52 | (3+4) |
| 15 | 0.1 | 2.3 | 1.5 | 10 | 0.0184 | 0.1184 | 21.55 | (5+6) |
| 16 | 0.1 | 2.3 | 1.5 | 10 | 0.0184 | 0.1184 | 29.25 | (7+8) |
| 17 | 0.1 | 2.3 | 0.5 | 10 | 0.00204 | 0.10204 | 37.20 | (1+2) |
| 18 | 0.1 | 2.3 | 0.5 | 10 | 0.00204 | 0.10204 | 34.78 | (3+4) |
| 19 | 0.1 | 2.3 | 0.5 | 10 | 0.00204 | 0.10204 | 29.62 | (5+6) |
| 20 | 0.1 | 2.3 | 0.5 | 10 | 0.00204 | 0.10204 | 25.15 | (7+8) |
| 21 | 0.05 | 2.3 | 1.5 | 10 | 0.0092 | 0.0592 | 7.50 | (1+2) |
| 22 | 0.05 | 2.3 | 1.5 | 10 | 0.0092 | 0.0592 | 9.77 | (3+4) |
| 23 | 0.05 | 2.3 | 1.5 | 10 | 0.0092 | 0.0592 | 10.73 | (5+6) |
| 24 | 0.05 | 2.3 | 1.5 | 10 | 0.0092 | 0.0592 | 10.47 | (7+8) |
| 25 | 0.05 | 2.3 | 2.0 | 10 | 0.01635 | 0.06635 | 26.25 | (1+2) |
| 26 | 0.05 | 2.3 | 2.0 | 10 | 0.01635 | 0.06635 | 10.22 | (3+4) |
| 27 | 0.05 | 2.3 | 2.0 | 10 | 0.01635 | 0.06635 | 11.88 | (5+6) |
| 28 | 0.05 | 2.3 | 2.0 | 10 | 0.01635 | 0.06635 | 9.55 | (7+8) |
| 29 | 0.05 | 2.3 | 0.5 | 10 | 0.00102 | 0.05102 | 6.68 | (1+2) |
| 30 | 0.05 | 2.3 | 0.5 | 10 | 0.00102 | 0.05102 | 9.87 | (3+4) |

| Case | $a_y/g$ | E | T (sec) | $\ell$ (ft) | $\phi_y$ (rad) | $\phi_s$ (rad) | $t_o$ (sec) | Earthquake |
|---|---|---|---|---|---|---|---|---|
| 31 | 0.05 | 2.3 | 0.5 | 10 | 0.00102 | 0.05102 | 6.12 | (5+6) |
| 32 | 0.05 | 2.3 | 0.5 | 10 | 0.00102 | 0.05102 | 5.87 | (7+8) |
| 33 | 0.05 | 3.45 | 0.5 | 10 | 0.00102 | 0.05102 | 2.57 | (1+2) |
| 34 | 0.05 | 3.45 | 0.5 | 10 | 0.00102 | 0.05102 | 7.25 | (3+4) |
| 35 | 0.05 | 3.45 | 0.5 | 10 | 0.00102 | 0.05102 | 3.70 | (5+6) |
| 36 | 0.05 | 3.45 | 0.5 | 10 | 0.00102 | 0.05102 | 2.95 | (7+8) |
| 37 | 0.05 | 3.45 | 2.0 | 10 | 0.01635 | 0.06635 | 3.07 | (1+2) |
| 38 | 0.05 | 3.45 | 2.0 | 10 | 0.01635 | 0.06635 | 2.49 | (3+4) |
| 39 | 0.05 | 3.45 | 2.0 | 10 | 0.01635 | 0.06635 | 6.07 | (5+6) |
| 40 | 0.05 | 3.45 | 2.0 | 10 | 0.01635 | 0.06635 | 5.33 | (7+8) |
| 41 | 0.05 | 3.45 | 1.5 | 10 | 0.0092 | 0.0592 | 2.90 | (1+2) |
| 42 | 0.05 | 3.45 | 1.5 | 10 | 0.0092 | 0.0592 | 2.22 | (3+4) |
| 43 | 0.05 | 3.45 | 1.5 | 10 | 0.0092 | 0.0592 | 7.35 | (5+6) |
| 44 | 0.05 | 3.45 | 1.5 | 10 | 0.0092 | 0.0592 | 5.25 | (7+8) |
| 45 | 0.1 | 3.45 | 1.5 | 10 | 0.0184 | 0.1184 | 15.85 | (1+2) |
| 46 | 0.1 | 3.45 | 1.5 | 10 | 0.0184 | 0.1184 | 12.78 | (3+4) |
| 47 | 0.1 | 3.45 | 1.5 | 10 | 0.0184 | 0.1184 | 10.19 | (5+6) |
| 48 | 0.1 | 3.45 | 1.5 | 10 | 0.0184 | 0.1184 | 14.50 | (7+8) |
| 49 | 0.1 | 3.45 | 2.0 | 10 | 0.0327 | 0.1327 | 18.76 | (1+2) |
| 50 | 0.1 | 3.45 | 2.0 | 10 | 0.0327 | 0.1327 | 15.82 | (3+4) |
| 51 | 0.1 | 3.45 | 2.0 | 10 | 0.0327 | 0.1327 | 12.23 | (5+6) |
| 52 | 0.1 | 3.45 | 2.0 | 10 | 0.0327 | 0.1327 | 12.03 | (7+8) |
| 53 | 0.1 | 3.45 | 0.5 | 10 | 0.00204 | 0.10204 | 13.36 | (1+2) |
| 54 | 0.1 | 3.45 | 0.5 | 10 | 0.00204 | 0.10204 | 19.58 | (3+4) |
| 55 | 0.1 | 3.45 | 0.5 | 10 | 0.00204 | 0.10204 | 9.58 | (5+6) |
| 56 | 0.1 | 3.45 | 0.5 | 10 | 0.00204 | 0.10204 | 10.44 | (7+8) |
| 57 | 0.30 | 6.9 | 1.0 | 10 | 0.0246 | 0.3246 | 35.5 | (7+8) |
| 58 | 0.05 | 1.15 | 1.0 | 10 | 0.0041 | 0.0541 | 35.5 | (7+8) |
| 59 | 0.1 | 2.3 | 1.0 | 10 | 0.0082 | 0.1082 | 35.5 | (7+8) |
| 60 | 0.1 | 3.45 | 1.0 | 10 | 0.0082 | 0.1082 | 13.05 | (1+2) |
| 61 | 0.1 | 3.45 | 1.0 | 10 | 0.0082 | 0.1082 | 9.82 | (3+4) |
| 62 | 0.1 | 3.45 | 1.0 | 10 | 0.0082 | 0.1082 | 12.12 | (5+6) |
| 63 | 0.1 | 3.45 | 1.0 | 10 | 0.0082 | 0.1082 | 17.18 | (7+8) |

| Case | $a_y/g$ | E | T (sec) | $\ell$ (ft) | $\phi_y$ (rad) | $\phi_s$ (rad) | $t_o$ (sec) | Earthquake |
|---|---|---|---|---|---|---|---|---|
| 64 | 0.05 | 3.45 | 1.0 | 10 | 0.0041 | 0.0541 | 2.56 | (1+2) |
| 65 | 0.05 | 3.45 | 1.0 | 10 | 0.0041 | 0.0541 | 3.52 | (3+4) |
| 66 | 0.05 | 3.45 | 1.0 | 10 | 0.0041 | 0.0541 | 4.72 | (5+6) |
| 67 | 0.05 | 3.45 | 1.0 | 10 | 0.0041 | 0.0541 | 13.15 | (7+8) |
| 68 | 0.05 | 2.3 | 1.0 | 10 | 0.0041 | 0.0541 | 4.23 | (1+2) |
| 69 | 0.05 | 2.3 | 1.0 | 10 | 0.0041 | 0.0541 | 4.28 | (3+4) |
| 70 | 0.05 | 2.3 | 1.0 | 10 | 0.0041 | 0.0541 | 10.13 | (5+6) |
| 71 | 0.05 | 2.3 | 1.0 | 10 | 0.0041 | 0.0541 | 13.97 | (7+8) |
| 72 | 0.1 | 2.3 | 1.0 | 10 | 0.0082 | 0.1082 | 33.6 | (1+2) |
| 73 | 0.1 | 2.3 | 1.0 | 10 | 0.0082 | 0.1082 | 24.6 | (3+4) |
| 74 | 0.1 | 2.3 | 1.0 | 10 | 0.0082 | 0.1082 | 33.0 | (5+6) |
| 75 | 0.1 | 2.3 | 1.0 | 10 | 0.0082 | 0.1082 | 35.5 | (7+8) |
| 76 | 0.05 | 2.3 | 1.0 | 20 | 0.00204 | 0.05204 | 37.87 | (1+2) |
| 77 | 0.05 | 2.3 | 1.0 | 20 | 0.00204 | 0.05204 | 11.52 | (3+4) |
| 78 | 0.05 | 2.3 | 1.0 | 20 | 0.00204 | 0.05204 | 14.70 | (5+6) |
| 79 | 0.05 | 2.3 | 1.0 | 20 | 0.00204 | 0.05204 | 30.50 | (7+8) |
| 80 | 0.05 | 2.3 | 1.0 | 15 | 0.00274 | 0.05274 | 17.50 | (1+2) |
| 81 | 0.05 | 2.3 | 1.0 | 15 | 0.00274 | 0.05274 | 9.67 | (3+4) |
| 82 | 0.05 | 2.3 | 1.0 | 15 | 0.00274 | 0.05274 | 12.53 | (5+6) |
| 83 | 0.05 | 2.3 | 1.0 | 15 | 0.00274 | 0.05274 | 21.86 | (7+8) |
| 84 | 0.05 | 2.3 | 1.0 | 25 | 0.00162 | 0.05162 | 33.38 | (1+2) |
| 85 | 0.05 | 2.3 | 1.0 | 25 | 0.00162 | 0.05162 | 13.31 | (3+4) |
| 86 | 0.05 | 2.3 | 1.0 | 25 | 0.00162 | 0.05162 | 20.92 | (5+6) |
| 87 | 0.05 | 2.3 | 1.0 | 25 | 0.00162 | 0.05162 | 35.94 | (7+8) |
| 88 | 0.05 | 2.3 | 1.0 | 30 | 0.00136 | 0.05136 | 37.92 | (1+2) |
| 89 | 0.05 | 2.3 | 1.0 | 30 | 0.00136 | 0.05136 | 19.42 | (3+4) |
| 90 | 0.05 | 2.3 | 1.0 | 30 | 0.00136 | 0.05136 | 26.35 | (5+6) |
| 91 | 0.05 | 2.3 | 1.0 | 30 | 0.00136 | 0.05136 | 41.20 | (7+8) |
| 92 | 0.05 | 2.3 | 1.5 | 20 | 0.0046 | 0.0546 | 24.75 | (1+2) |
| 93 | 0.05 | 2.3 | 1.5 | 20 | 0.0046 | 0.0546 | 13.30 | (3+4) |
| 94 | 0.05 | 2.3 | 1.5 | 20 | 0.0046 | 0.0546 | 13.09 | (5+6) |
| 95 | 0.05 | 2.3 | 1.5 | 20 | 0.0046 | 0.0546 | 15.17 | (7+8) |
| 96 | 0.05 | 2.3 | 1.5 | 15 | 0.00618 | 0.05618 | 15.08 | (1+2) |

| Case | $a_y/g$ | E | T (sec) | $\ell$ (ft) | $\phi_y$ (rad) | $\phi_s$ (rad) | $t_o$ (sec) | Earthquake |
|---|---|---|---|---|---|---|---|---|
| 97 | 0.05 | 2.3 | 1.5 | 15 | 0.00618 | 0.05618 | 10.63 | (3+4) |
| 98 | 0.05 | 2.3 | 1.5 | 15 | 0.00618 | 0.05618 | 11.97 | (5+6) |
| 99 | 0.05 | 2.3 | 1.5 | 15 | 0.00618 | 0.05618 | 12.32 | (7+8) |
| 100 | 0.05 | 2.3 | 1.5 | 25 | 0.00367 | 0.05367 | 30.01 | (1+2) |
| 101 | 0.05 | 2.3 | 1.5 | 25 | 0.00367 | 0.05367 | 16.70 | (3+4) |
| 102 | 0.05 | 2.3 | 1.5 | 25 | 0.00367 | 0.05367 | 16.95 | (5+6) |
| 103 | 0.05 | 2.3 | 1.5 | 25 | 0.00367 | 0.05367 | 20.14 | (7+8) |
| 104 | 0.05 | 2.3 | 1.5 | 30 | 0.00304 | 0.05304 | 38.42 | (1+2) |
| 105 | 0.05 | 2.3 | 1.5 | 30 | 0.00304 | 0.05304 | 21.52 | (3+4) |
| 106 | 0.05 | 2.3 | 1.5 | 30 | 0.00304 | 0.05304 | 21.22 | (5+6) |
| 107 | 0.05 | 2.3 | 1.5 | 30 | 0.00304 | 0.05304 | 22.47 | (7+8) |
| 108 | 0.05 | 2.3 | 2.0 | 30 | 0.00544 | 0.05544 | 42.53 | (1+2) |
| 109 | 0.05 | 2.3 | 2.0 | 30 | 0.00544 | 0.05544 | 21.23 | (3+4) |
| 110 | 0.05 | 2.3 | 2.0 | 30 | 0.00544 | 0.05544 | 22.17 | (5+6) |
| 111 | 0.05 | 2.3 | 2.0 | 30 | 0.00544 | 0.05544 | 23.38 | (7+8) |
| 112 | 0.05 | 2.3 | 2.0 | 25 | 0.00655 | 0.05655 | 40.02 | (1+2) |
| 113 | 0.05 | 2.3 | 2.0 | 25 | 0.00655 | 0.05655 | 19.78 | (3+4) |
| 114 | 0.05 | 2.3 | 2.0 | 25 | 0.00655 | 0.05655 | 21.42 | (5+6) |
| 115 | 0.05 | 2.3 | 2.0 | 25 | 0.00655 | 0.05655 | 18.83 | (7+8) |
| 116 | 0.05 | 2.3 | 2.0 | 20 | 0.00815 | 0.05815 | 31.97 | (1+2) |
| 117 | 0.05 | 2.3 | 2.0 | 20 | 0.00815 | 0.05815 | 16.02 | (3+4) |
| 118 | 0.05 | 2.3 | 2.0 | 20 | 0.00815 | 0.05815 | 17.12 | (5+6) |
| 119 | 0.05 | 2.3 | 2.0 | 20 | 0.00815 | 0.05815 | 15.37 | (7+8) |
| 120 | 0.05 | 2.3 | 2.0 | 15 | 0.01095 | 0.06095 | 20.37 | (1+2) |
| 121 | 0.05 | 2.3 | 2.0 | 15 | 0.01095 | 0.06095 | 13.24 | (3+4) |
| 122 | 0.05 | 2.3 | 2.0 | 15 | 0.01095 | 0.06095 | 13.02 | (5+6) |
| 123 | 0.05 | 2.3 | 2.0 | 15 | 0.01095 | 0.06095 | 11.60 | (7+8) |
| 124 | 0.05 | 2.3 | 2.0 | 5 | 0.03262 | 0.08262 | 6.68 | (1+2) |
| 125 | 0.05 | 2.3 | 2.0 | 5 | 0.03262 | 0.08262 | 6.05 | (3+4) |
| 126 | 0.05 | 2.3 | 2.0 | 5 | 0.03262 | 0.08262 | 9.05 | (5+6) |
| 127 | 0.05 | 2.3 | 2.0 | 5 | 0.03262 | 0.08262 | 8.83 | (7+8) |
| 128 | 0.05 | 2.3 | 0.5 | 30 | 0.00034 | 0.05034 | 31.19 | (1+2) |
| 129 | 0.05 | 2.3 | 0.5 | 30 | 0.00034 | 0.05034 | 27.15 | (3+4) |
| 130 | 0.05 | 2.3 | 0.5 | 30 | 0.00034 | 0.05034 | 19.93 | (5+6) |

| Case | $a_y/g$ | E | T (sec) | $\ell$ (ft) | $\phi_y$ (rad) | $\phi_s$ (rad) | $t_o$ (sec) | Earthquake |
|---|---|---|---|---|---|---|---|---|
| 131 | 0.05 | 2.3 | 0.5 | 30 | 0.00034 | 0.05034 | 25.75 | (7+8) |
| 132 | 0.05 | 2.3 | 0.5 | 25 | 0.00041 | 0.05041 | 24.39 | (1+2) |
| 133 | 0.05 | 2.3 | 0.5 | 25 | 0.00041 | 0.05041 | 22.05 | (3+4) |
| 134 | 0.05 | 2.3 | 0.5 | 25 | 0.00041 | 0.05041 | 15.60 | (5+6) |
| 135 | 0.05 | 2.3 | 0.5 | 25 | 0.00041 | 0.05041 | 18.35 | (7+8) |
| 136 | 0.05 | 2.3 | 0.5 | 20 | 0.00051 | 0.05051 | 17.47 | (1+2) |
| 137 | 0.05 | 2.3 | 0.5 | 20 | 0.00051 | 0.05051 | 19.45 | (3+4) |
| 138 | 0.05 | 2.3 | 0.5 | 20 | 0.00051 | 0.05051 | 12.43 | (5+6) |
| 139 | 0.05 | 2.3 | 0.5 | 20 | 0.00051 | 0.05051 | 13.95 | (7+8) |
| 140 | 0.05 | 2.3 | 0.5 | 15 | 0.00068 | 0.05068 | 12.95 | (1+2) |
| 141 | 0.05 | 2.3 | 0.5 | 15 | 0.00068 | 0.05068 | 14.84 | (3+4) |
| 142 | 0.05 | 2.3 | 0.5 | 15 | 0.00068 | 0.05068 | 8.97 | (5+6) |
| 143 | 0.05 | 2.3 | 0.5 | 15 | 0.00068 | 0.05068 | 11.02 | (7+8) |
| 144 | 0.05 | 2.3 | 0.5 | 5 | 0.00204 | 0.05204 | 2.48 | (1+2) |
| 145 | 0.05 | 2.3 | 0.5 | 5 | 0.00204 | 0.05204 | 4.27 | (3+4) |
| 146 | 0.05 | 2.3 | 0.5 | 5 | 0.00204 | 0.05204 | 3.27 | (5+6) |
| 147 | 0.05 | 2.3 | 0.5 | 5 | 0.00204 | 0.05204 | 1.77 | (7+8) |
| 148 | 0.05 | 2.3 | 1.0 | 5 | 0.00816 | 0.05816 | 2.52 | (1+2) |
| 149 | 0.05 | 2.3 | 1.0 | 5 | 0.00816 | 0.05816 | 2.82 | (3+4) |
| 150 | 0.05 | 2.3 | 1.0 | 5 | 0.00816 | 0.05816 | 5.42 | (5+6) |
| 151 | 0.05 | 2.3 | 1.0 | 5 | 0.00816 | 0.05816 | 10.92 | (7+8) |
| 152 | 0.05 | 2.3 | 1.5 | 5 | 0.01836 | 0.06836 | 3.05 | (1+2) |
| 153 | 0.05 | 2.3 | 1.5 | 5 | 0.01836 | 0.06836 | 3.00 | (3+4) |
| 154 | 0.05 | 2.3 | 1.5 | 5 | 0.01836 | 0.06836 | 7.49 | (5+6) |
| 155 | 0.05 | 2.3 | 1.5 | 5 | 0.01836 | 0.06836 | 4.66 | (7+8) |
| 156 | 0.05 | 3.16 | 0.5 | 10 | 0.00102 | 0.05102 | 2.90 | (1+2) |
| 157 | 0.05 | 3.16 | 0.5 | 10 | 0.00102 | 0.05102 | 7.85 | (3+4) |
| 158 | 0.05 | 3.16 | 0.5 | 10 | 0.00102 | 0.05102 | 4.67 | (5+6) |
| 159 | 0.05 | 3.16 | 0.5 | 10 | 0.00102 | 0.05102 | 3.32 | (7+8) |
| 160 | 0.05 | 3.16 | 0.5 | 10 | 0.00102 | 0.05102 | 3.26 | El Centro |
| 161 | 0.05 | 3.16 | 0.5 | 10 | 0.00102 | 0.05102 | 32.8 | Taft |
| 162 | 0.05 | 3.16 | 0.5 | 10 | 0.00102 | 0.05102 | 11.8 | Olympia |

| Case | $a_y/g$ | E | T (sec) | $\ell$ (ft) | $\varphi_y$ (rad) | $\phi_s$ (rad) | $t_o$ (sec) | Earthquake |
|---|---|---|---|---|---|---|---|---|
| 163 | 0.05 | 3.16 | 1.0 | 10 | 0.00410 | 0.05410 | 2.67 | (1+2) |
| 164 | 0.05 | 3.16 | 1.0 | 10 | 0.00410 | 0.05410 | 3.69 | (3+4) |
| 165 | 0.05 | 3.16 | 1.0 | 10 | 0.00410 | 0.05410 | 6.02 | (5+6) |
| 166 | 0.05 | 3.16 | 1.0 | 10 | 0.00410 | 0.05410 | 24.80 | (7+8) |
| 167 | 0.05 | 3.16 | 1.0 | 10 | 0.00410 | 0.05410 | 4.44 | El Centro |
| 168 | 0.05 | 3.16 | 1.0 | 10 | 0.00410 | 0.05410 | 13.8 | Taft |
| 169 | 0.05 | 3.16 | 1.0 | 10 | 0.00410 | 0.05410 | 11.9 | Olympia |

# APPENDIX II

1) Total correlation coefficients

The expression of the coefficient of total correlation between two variables is the following[46,48]:

$$r_{xy} = \frac{\sum xy - N\bar{x}\bar{y}}{\left\{\left(\sum x^2 - N\bar{x}^2\right)\left(\sum y^2 - N\bar{y}^2\right)\right\}^{\frac{1}{2}}}$$

where $x$ and $y$ are the variables, $N$ is the total number of cases, and $\bar{x}$ and $\bar{y}$ are average values of the variables.

2) Partial correlation coefficients

In the study under consideration four variables are available and two different types of partial correlation coefficients are computed[48]:

2a) The correlation coefficient between two of the variables keeping constant one of the remaining variables. The expression of this coefficient is

$$r_{xy.z} = \frac{r_{xy} - r_{xz}r_{yz}}{\left\{(1 - r_{xz}^2)(1 - r_{yz}^2)\right\}^{\frac{1}{2}}}$$

where $r_{uv}$ is the total correlation coefficient between the variables u and v.

2b) The correlation coefficient between two of the variables keeping constant the remaining two variables. This coefficient is given by:

$$r_{xy.zv} = \frac{r_{xy.z} - r_{xv.z}r_{yv.z}}{\sqrt{(1 - r^2_{xv.z})(1 - r^2_{yv.z})}}$$

where $r_{xy.z}$ is the partial correlation coefficient between the variables $x$ and $y$, keeping constant the variable $z$.

3) Multiple correlation coefficients

With four variables, two types of multiple correlation coefficients appear[48]: the first has two independent variables and the second type has three independent variables.

3a) The multiple correlation coefficient with one dependent and two independent variables has the equation:

$$R_{u(xy)} = \left\{1 - (1 - r^2_{ux})(1 - r^2_{uy.x})\right\}^{\frac{1}{2}}$$

where $r_{ux}$ and $r_{uy.x}$ were defined in 1) and 2a).

3b) The multiple correlation coefficient with one dependent and three independent variables is given by:

$$R_{u(xyz)} = \left\{1 - (1 - r^2_{ux})(1 - r^2_{uy.x})(1 - r^2_{uz.xy})\right\}^{\frac{1}{2}}$$